A
EXPERIMENTAL VERIFICATION OF EFFECTIVENESS OF SURFACE STRESS IMPROVEMENT TO MITIGATE PWSCC

This appendix presents results of experiments, either performed by the vendors or by an independent lab commissioned by EPRI, which investigated the effect of peening on the residual stress state and on the growth of SCC flaws. Section A.1 outlines the stress profiles experimentally measured by the peening vendors as well as other parameters indicating the near-surface condition. Peening was performed on flat plates of nickel based alloys and stainless steel by Toshiba, Hitachi-GE and MIC, and the results can be found in Section A.1.1. Since an important candidate location for peening is the dissimilar metal weld, stress measurements in the longitudinal and transverse directions were made by Toshiba and MHI on peened welded plates made from different combinations of nickel based alloys and stainless steels. These specimens include an Alloy 132 weld trough in Alloy 600 plate material and Alloy 600 and Type 304 stainless steel joined by an Alloy 132 dissimilar metal weld both treated with ULP and dissimilar metal (DM) weld of Alloy 132 joining Alloy 600 and Type 316 stainless steel treated with WJP by MHI. Details of these experiments are in Section A.1.2. The response of the alloys in their actual geometries is also important, so BMN mock ups were also peened by the ULP and WJP vendors, and the results are located in Sections A.1.3 to A.1.6.

Near surface properties were measured to ensure minimal adverse effects of peening on treated components. Surface roughness measurements were performed by Toshiba, MIC, and MHI on peened flat plates of Alloy 600, while Hitachi-GE compared surface roughness measurements of water jet peened plates to plates that were either shot peened or simply heavily ground. The surface roughness results are located in Section A.1.7. Hardness was used to assess the cold work done on and near a peened surface by all four peening vendors, and the details are provided in Section A.1.8.

MHI performed a series of "stuck nozzle tests" where a particular location was peened for much longer than the prescribed, optimized treatment time, the results of which are detailed in Section A.1.9.

In Section A.2, experiments used to determine the effect of peening on SCC are discussed. All four vendors performed experiments to determine if peening is effective at reducing initiation of SCC in samples with no pre-existing flaws, which are elaborated in Section A.2.1. With regard to samples with pre-existing flaws, tests were performed to investigate if peening could affect the flaws either during the peening application or during operation following peening. Discussion of these experiments is located in Sections A.2.2.1 and A.2.2.2 respectively.

Independent testing of SCC initiation in samples without pre-existing flaws was performed by AREVA on U-bends treated with ULP by Toshiba, ALP by MIC, or WJP by either Hitachi-GE or Mitsubishi. Details on the procedure and results are in Section A.3.

Section A.4 details experimental data related to the potential for peening to cause unacceptable side effects other than changes to flaw initiation and growth, which is covered in previous sections. Experiments investigating the effect of peening on UT inspectability and the vibrations to which peened and adjacent components are subjected, both performed by Hitachi-GE, are presented.

A.1 Experimentally Measured Stress Results

A.1.1 Stress Measurements on Flat Plate Specimens

Residual stress results were reported in EPRI Report MRP-162 [66] for water jet peening (WJP) by Ormond and MHI, underwater laser peening (ULP) by Toshiba, and air laser peening (ALP) by MIC. Figure A-1 below is taken from that report and shows that the ALP process generated the deepest levels of compressive residual stress. These stress profiles were measured by x-ray diffraction (XRD) with material removal by electropolishing. It should be understood that the ALP results shown in the figure are for ALP with an ablative layer, and are not fully representative of the results expected without an ablative layer, which are discussed in Section A.1.1.3 below.

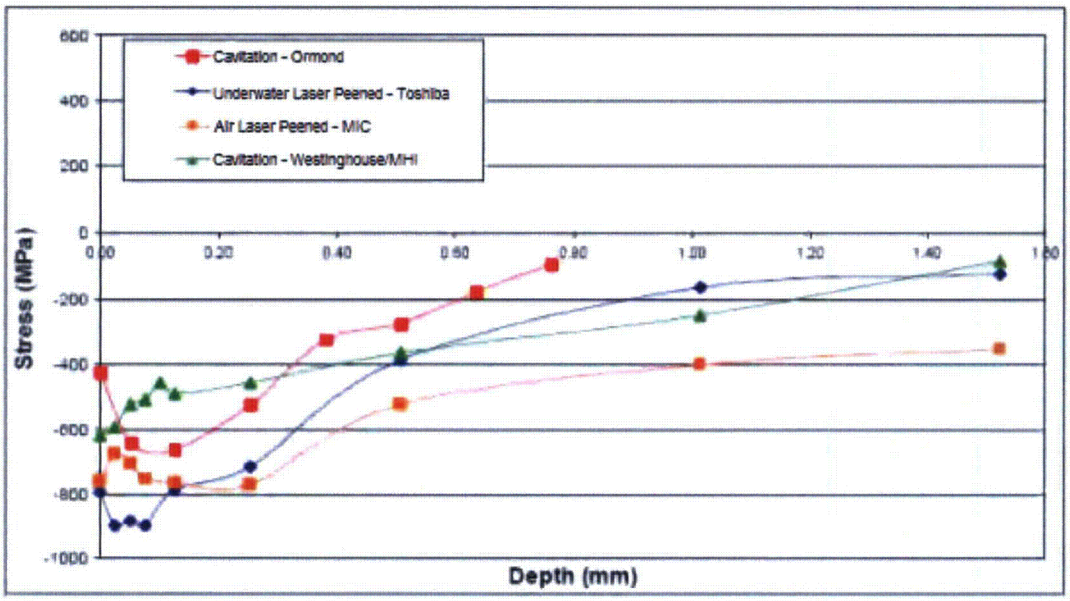

Figure A-1
Comparison of cavitation (water jet), laser, and air laser peening on Alloy 600 flat plate specimens with selected parameters for each process (Figure 4-31 from MRP-162 [66])

A.1.1.1 Flat Plates treated with ULP

In order to confirm applicability of the ULP process to PWR materials, underwater laser peening was performed on Alloy 600 and Alloy 132 samples by Toshiba. The residual stress depth profile was measured for the specimens after underwater laser peening. Figure A-2 shows the typical

results on Alloy 600 and Alloy 132. The underwater laser peening introduced compressive residual stresses up to a depth of around 1 mm from the surface.

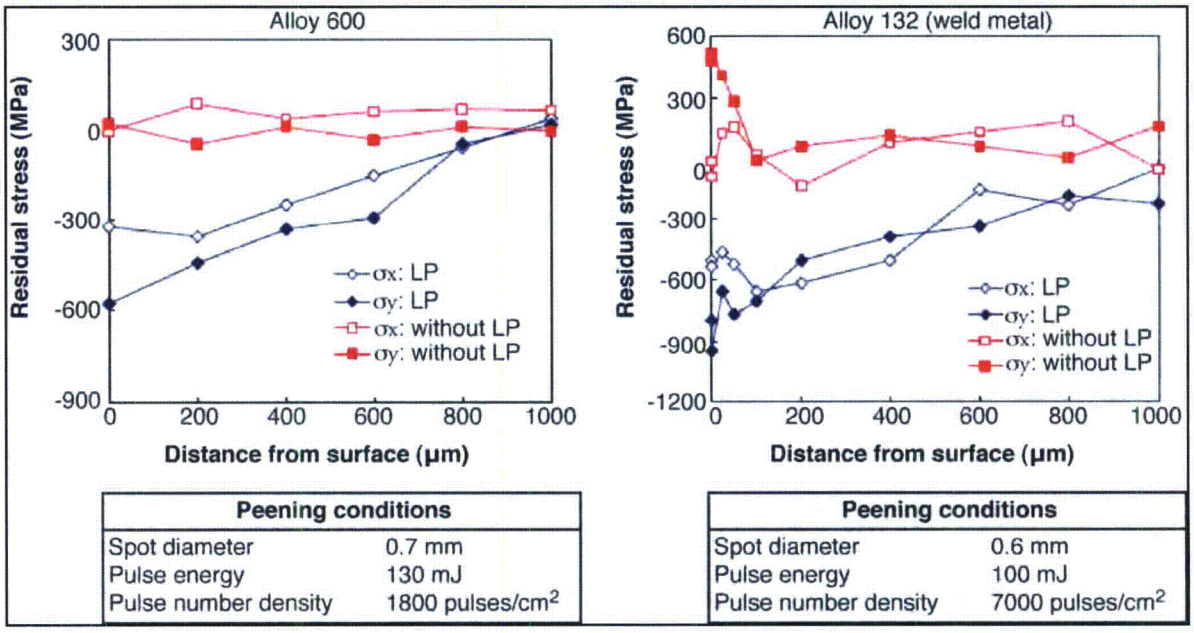

Figure A-2
Residual stress depth profile of Alloy 600 and Alloy 132 plane specimens, by Toshiba

Toshiba also provided results in Figure A-3 where a plate made from 20% cold worked 304 stainless steel was treated with underwater laser peening and residual stress profiles were determined along the surface. The results demonstrated that the ULP process is effective with stainless steel that has been 20% cold worked. The post-peening stress profile was compared to that for a flat plate of the same material that had not been peened. The tensile residual stress values on the surface outside the peened area did not exceed values measured in the unpeened plate, indicating that the ULP peening process does not cause elevated tensile stresses in adjacent areas.

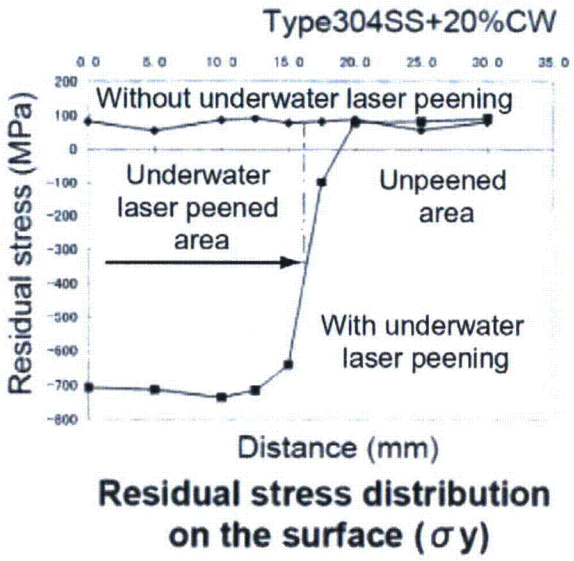

Figure A-3
Residual stress profiles on the surface and at depth for 304 stainless steel plate specimen treated with ULP by Toshiba

A.1.1.2 Flat Plates treated with WJP

Figure A-4 shows a typical WJP test setup at the Reactor Preventative Maintenance Center in Rinkai Works of Hitachi-GE Nuclear Energy (HGNE) Japan. The facility enables control of the same parameters that are to be applied by the WJP tooling for on-site application. Tests were performed to demonstrate the effectiveness of the process, including the effect on the materials.

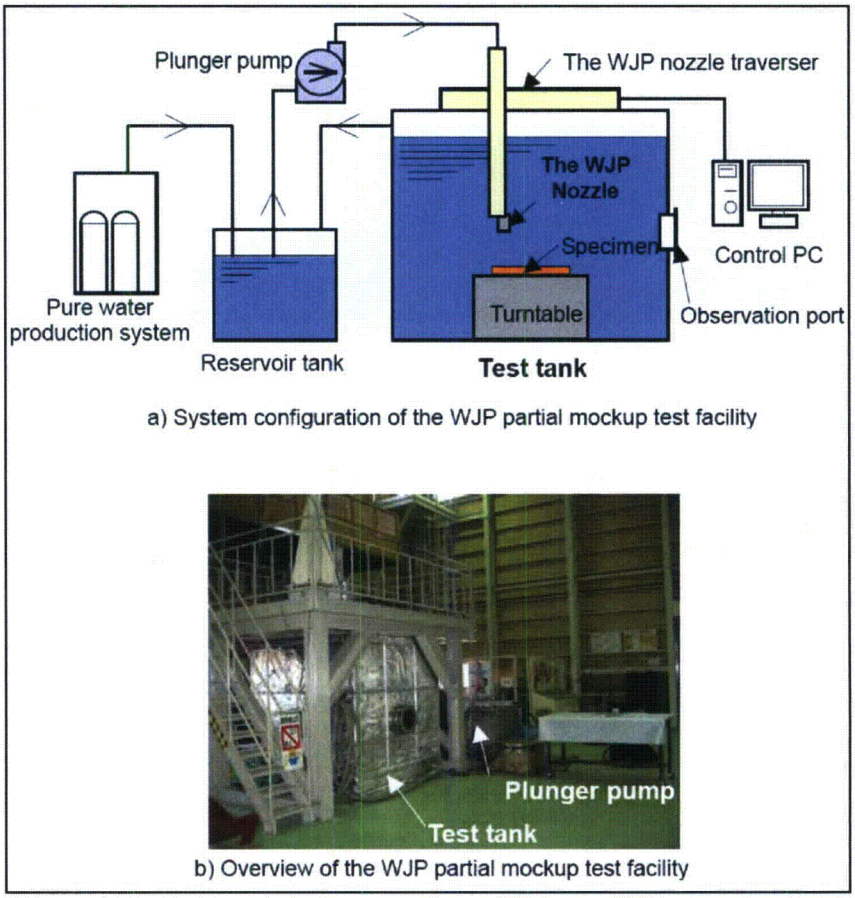

Figure A-4
The WJP partial mockup test facility, by Hitachi-GE

Figure A-5 to Figure A-8 show some examples of stress levels achieved after WJP treatment on flat plates of Alloy 600/182, Type 304/316L SS performed at this facility. As demonstrated, a wide and deep compressive residual stress was achieved on all specimens. As also evident from the results shown on these figures, the tensile stresses at the edges of the peened zones do not exceed those in unpeened plates, indicating that the WJP process does not result in elevated tensile stresses in adjacent areas.

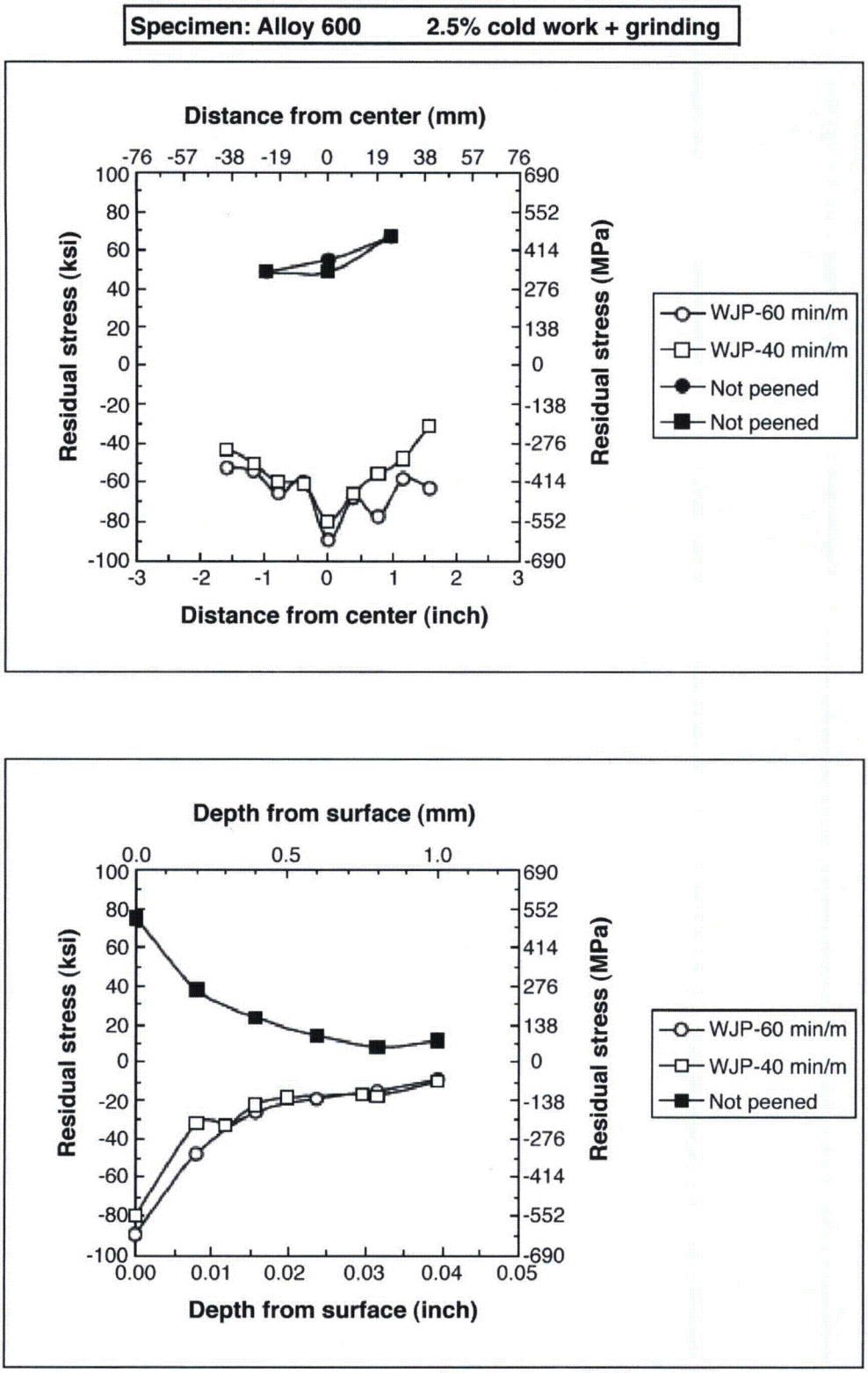

Figure A-5
Stress improvement with WJP (Alloy 600), by Hitachi-GE

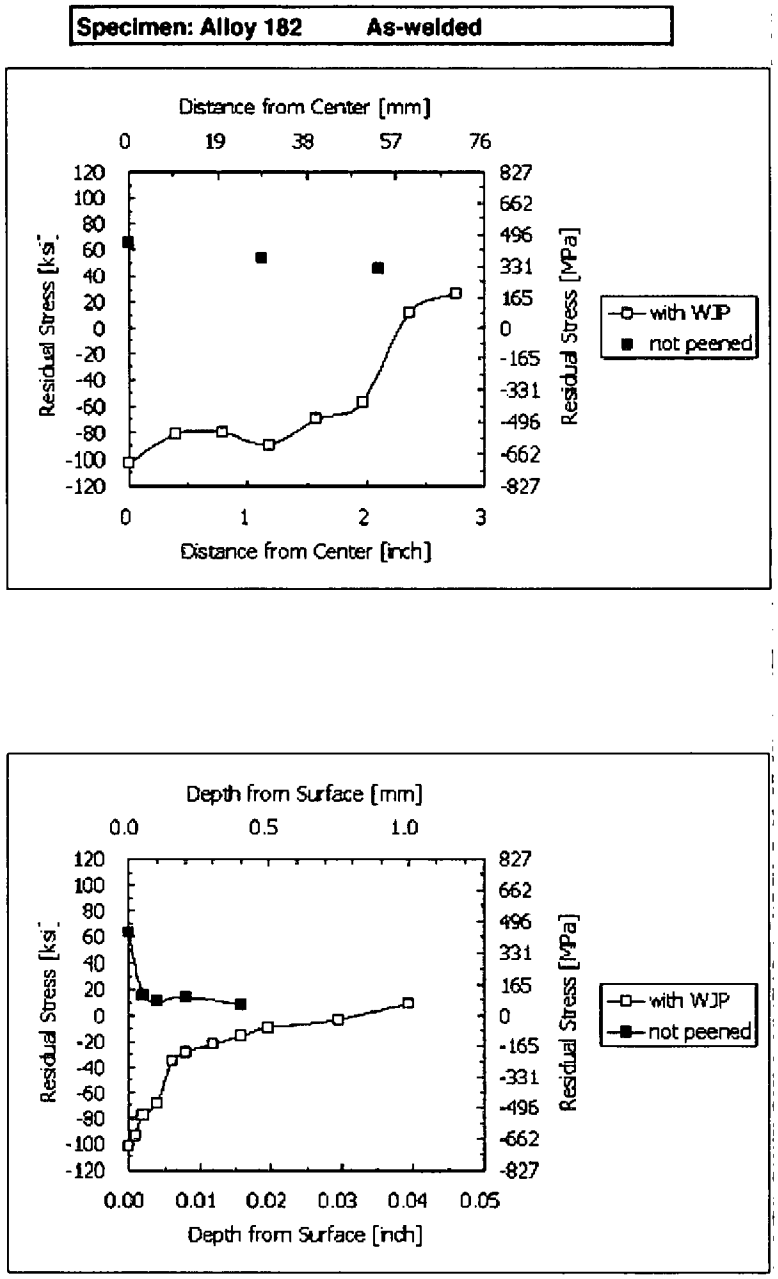

Figure A-6
Stress improvement with WJP (Alloy 182), by Hitachi-GE

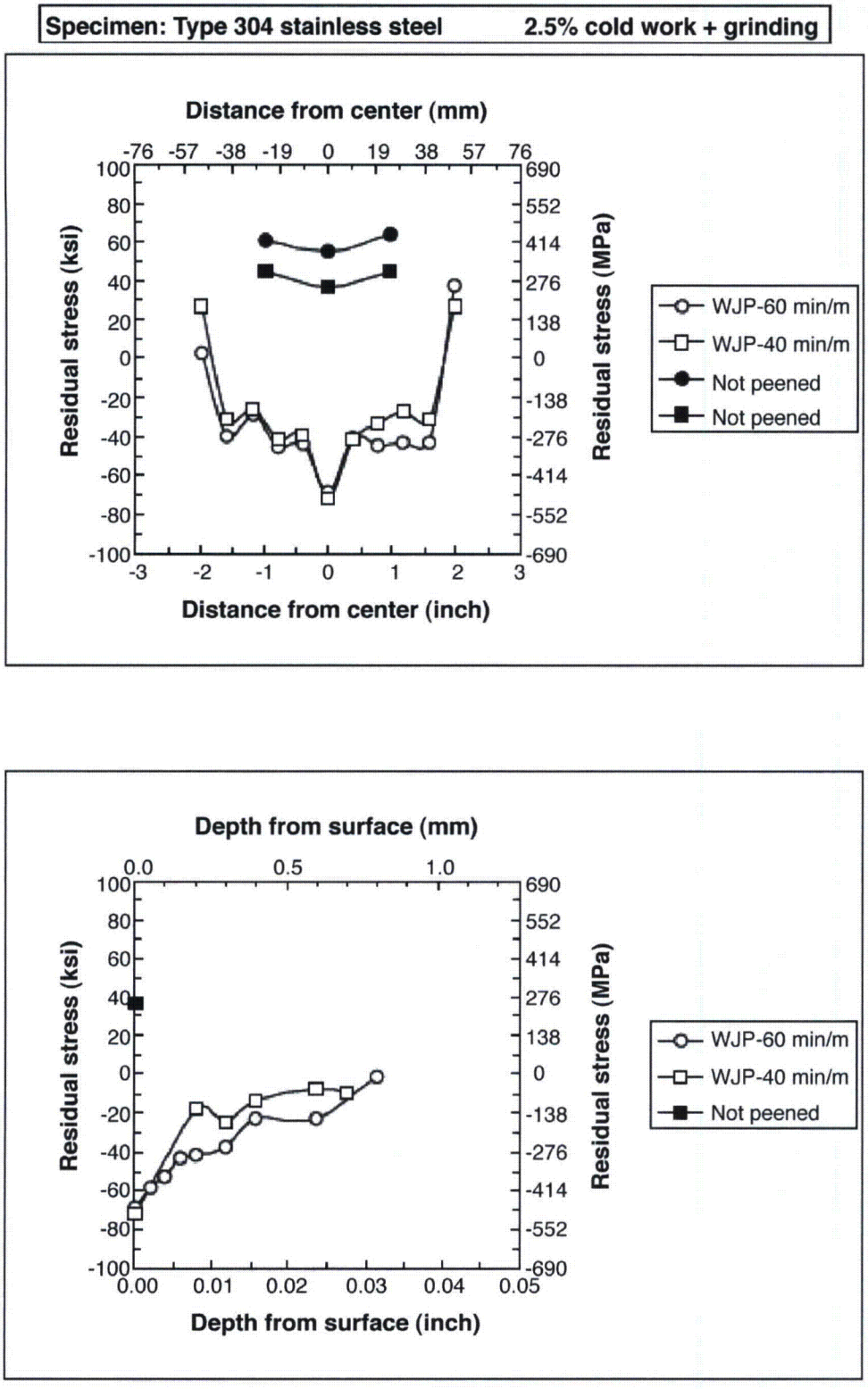

Figure A-7
Stress improvement with WJP (Type 304 SS), by Hitachi-GE

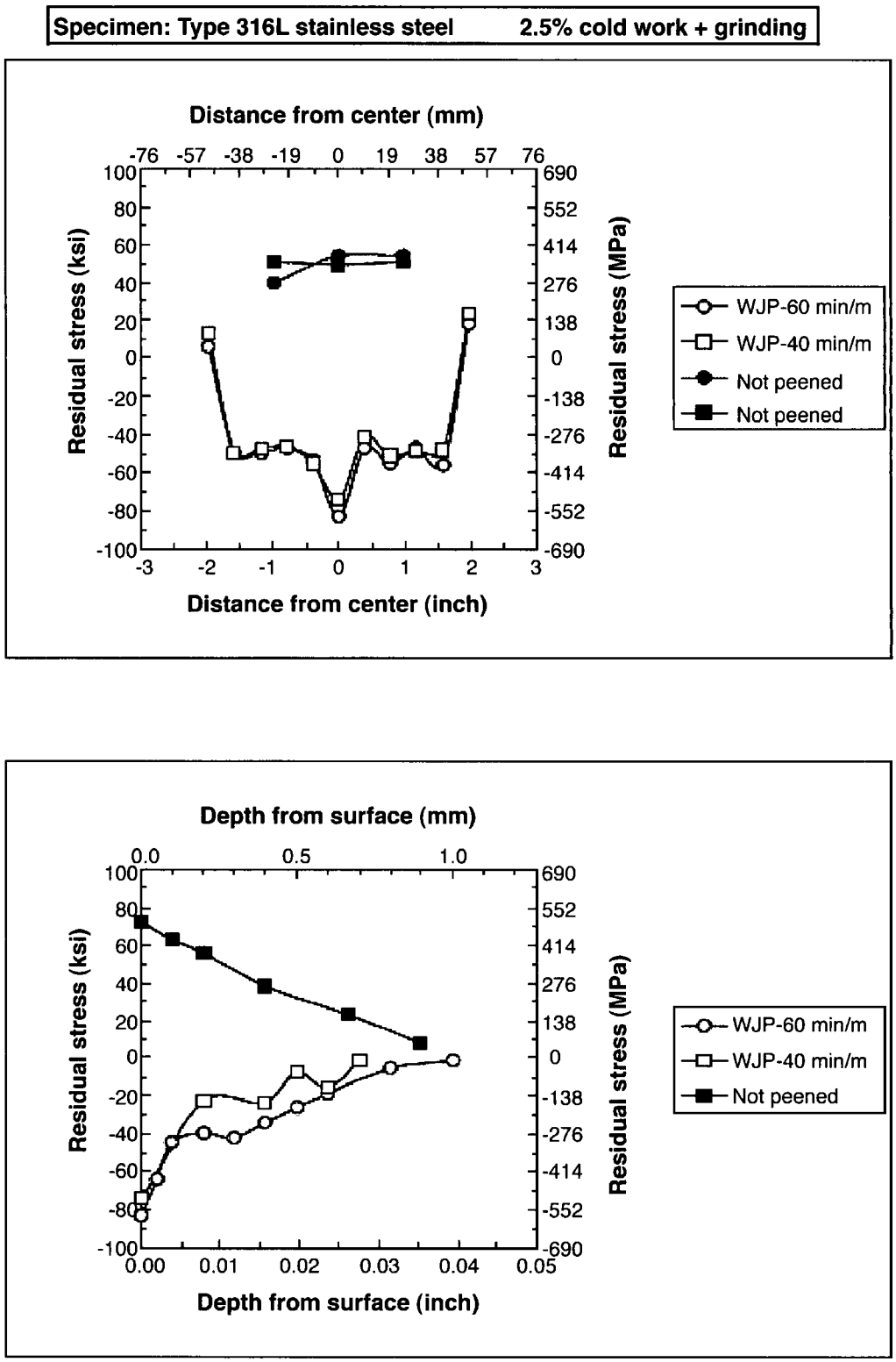

Figure A-8
Stress improvement with WJP (Type 316L SS), by Hitachi-GE

Hitachi-GE also performed some experiments to compare the residual stress induced on stainless steel and on nickel-based alloys by WJP with similar treatment parameters. Figure A-9 compares the level of compressive residual stress in 304 stainless steel, Alloy 600, and Alloy 182 on the basis of their proof stresses. The results suggest that for the same treatment conditions, more compressive residual stress is achieved in materials with a higher proof stress (i.e., the nickel based alloys), demonstrating that the compressive stress levels attained in stainless steel are conservative compared to those attained in nickel based alloys. This justifies the use of stainless steel in optimization tests by Hitachi-GE.

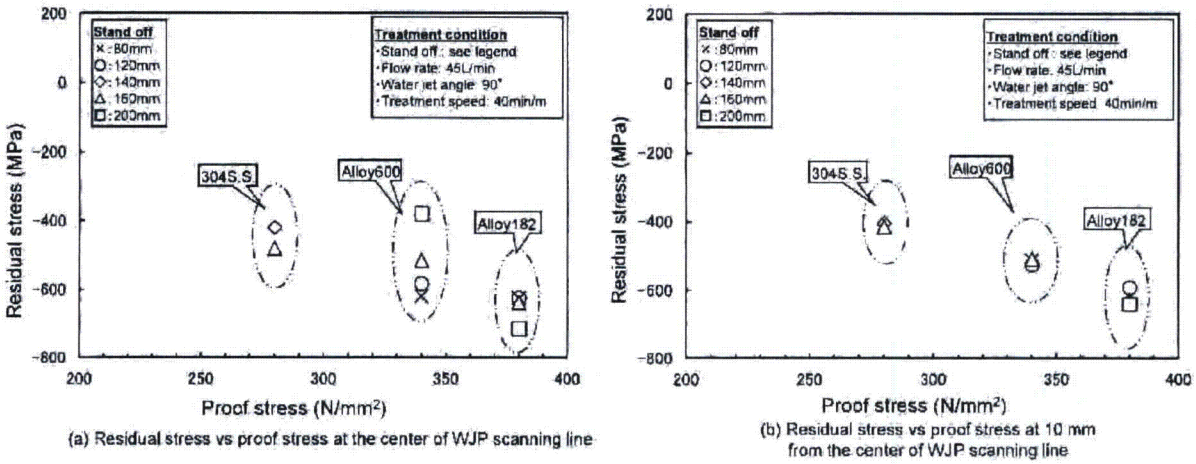

(a) Residual stress vs proof stress at the center of WJP scanning line

(b) Residual stress vs proof stress at 10 mm from the center of WJP scanning line

Figure A-9
Comparison of residual stress induced by WJP in stainless steel and nickel based alloys, provided by Hitachi-GE

To investigate the effect of peening on the surface residual stress profile both within and far from the peened area, Hitachi-GE peened a thin section of flat plate of 304 stainless steel and measured the surface residual stress at 5 mm intervals moving away from the WJP center line. The WJP center line does not correspond with the geometrical center of the plate so that the surface residual stress could be measured at a distance further away than the half width of the plate. In both the positive and negative y directions, the residual stress tended to neutral values near the plate edges.

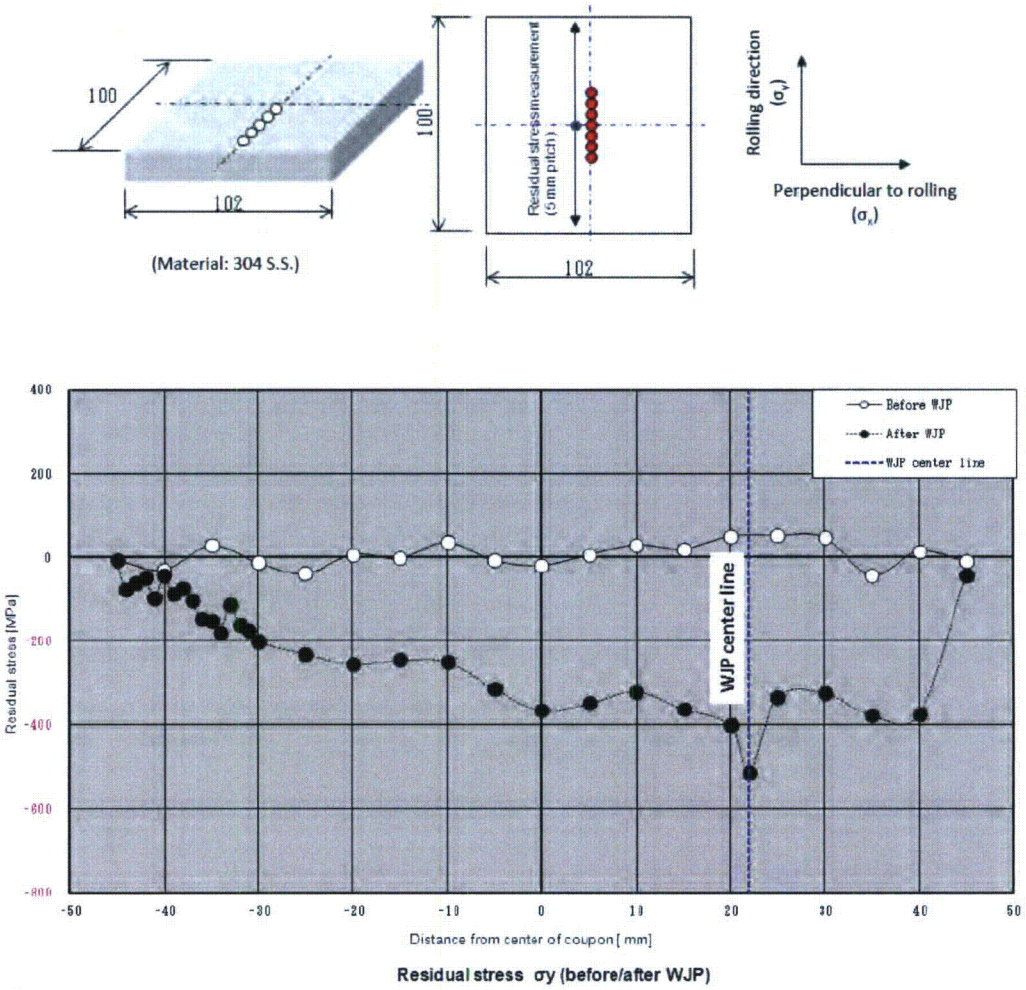

Figure A-10
Residual surface stress profile of a 304 stainless steel plate peened with WJP by Hitachi-GE

The effect of pre-existing flaws on the WJP-induced residual stress profile was assessed with the following experiments. Two specimens with the same dimensions were made from Type 304 Stainless Steel, and a different method of crack initiation was used on each specimen. Before cracking initiation, the specimens were thermally treated and machined. One specimen was pre-cracked with three point bending in potassium tetrathionate, which was used to create a single crack and evaluate the effect of WJP near a pre-existing crack. On the other specimen, multiple slits were created with electrical discharge machining (EDM) to examine the effect of WJP between pre-existing cracks. The target pre-crack depth was 10 mm. Once the flaws had been initiated, the surface was heavily ground in the direction perpendicular to the cracks. In order to establish pre-peening residual stress profile, residual stress measurements were made by XRD on the surface, at 100 μm below the surface, and at 200 μm below the surface. WJP was performed on the surface in the direction perpendicular to the cracks, and residual stress measurements by XRD were made at the same locations as before peening.

The residual stress measurements from the SCC cracked specimen and the EDM cracked specimen are shown in Figure A-11 and Figure A-12 respectively. In both specimens, all residual stress measurements were tensile before the surfaces were treated with WJP. Despite the presence of flaws, the WJP process was still able to induce compressive residual stress at and near the surface in both specimens. In the specimen cracked using three point bending in potassium tetrathionate, the residual stress values were of similar magnitudes close to the crack (less than 20 mm from the crack) and far from the crack (50 mm from the crack). In the specimen pre-cracked with EDM, compressive residual stress was induced in all regions between the cracks, but the stress became somewhat less compressive immediately adjacent to the flaw.

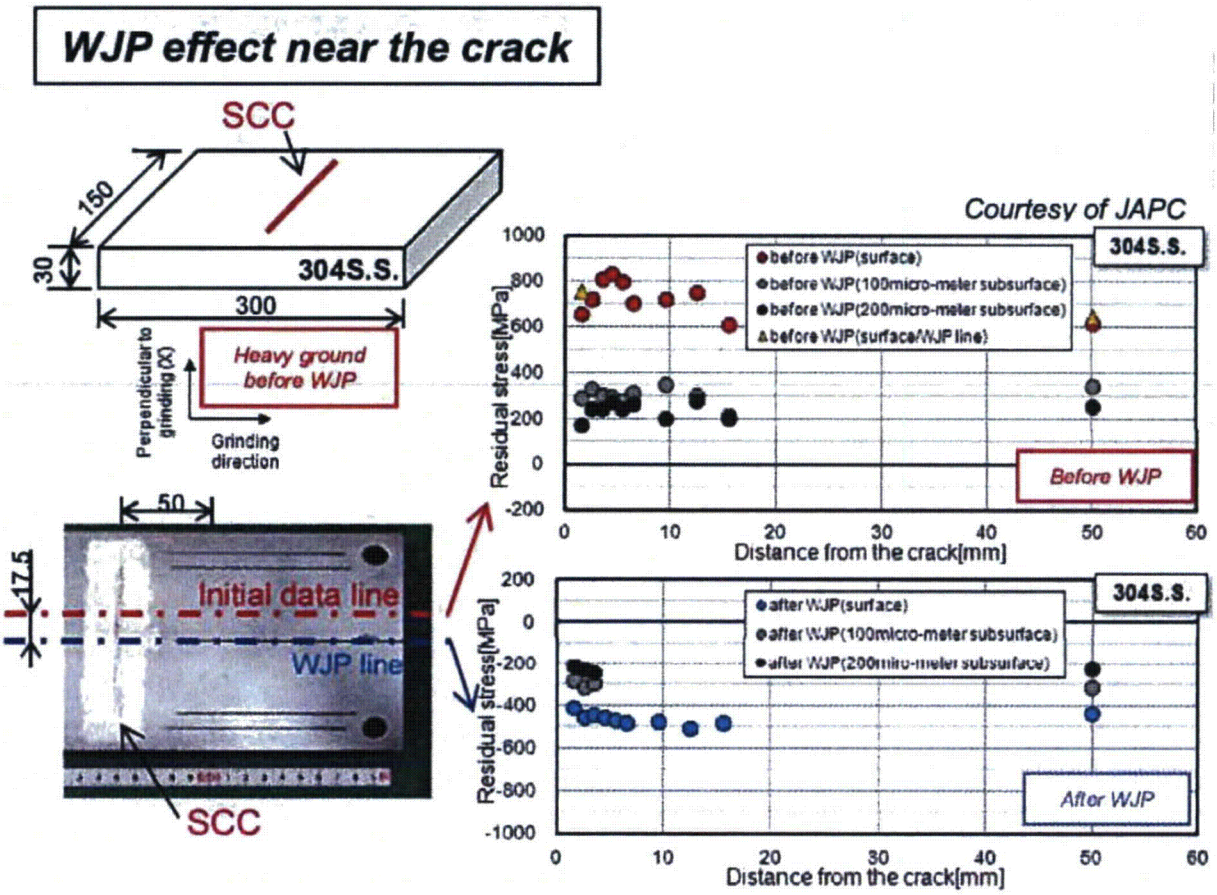

Figure A-11
Residual stress profiles before and after WJP in a specimen with a pre-existing flaw, provided by Hitachi-GE

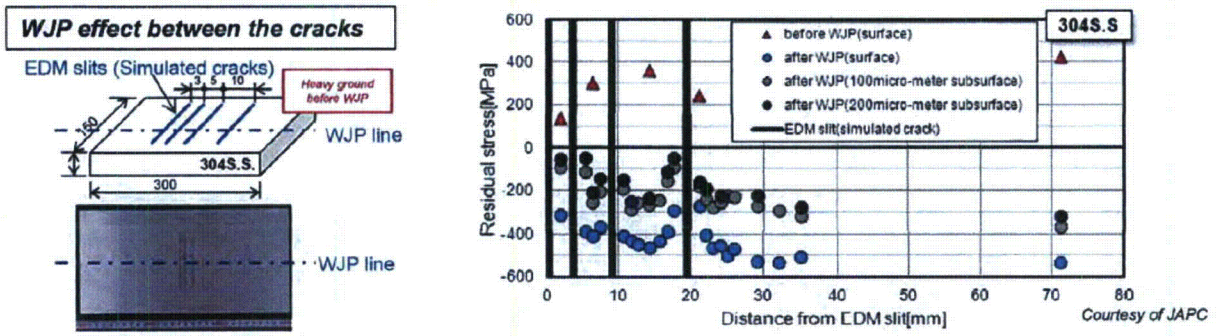

Figure A-12
Residual stress profiles before and after WJP in a specimen with multiple pre-existing cracks, provided by Hitachi-GE

A.1.1.3 Flat Plates treated with ALP

MIC assessed the effect of air laser peening (with an ablative layer) on the surface residual stress profile, both inside and outside the peened area. An area with a width of 12 mm on an Alloy 600 specimen was peened and the surface stress was measured every 2 mm from the center of the peened area to a point 20 mm from the center of the peened area. The measured stress values are shown in Figure A-13. The grey line in the figure shows the limit of the peened area. Within the peened area, the surface residual stresses are highly compressive. (Note that these are for ALP with an ablative tape, so they are not fully representative of data for the ALP process planned for use in nuclear plant applications which would not use an ablative layer). The region just adjacent to the peened area also has compressive residual stresses.

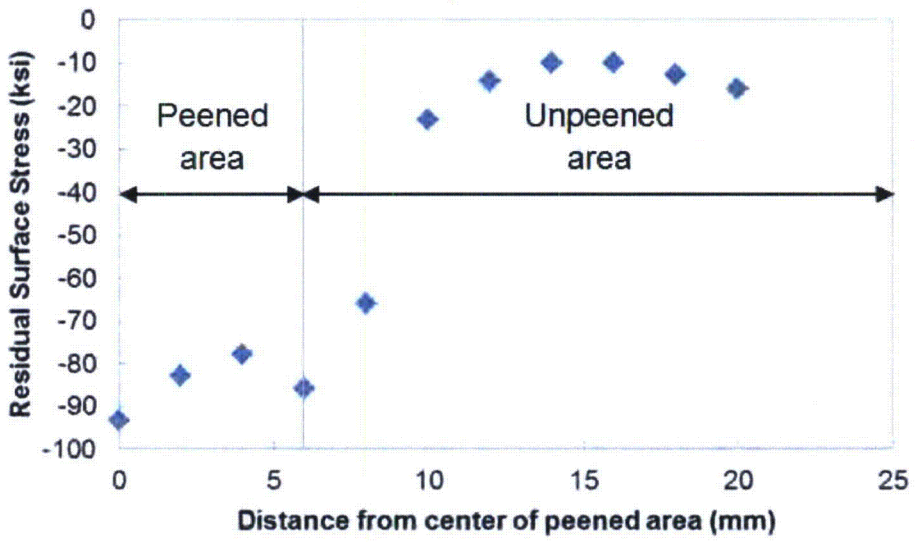

Figure A-13
Surface stress measurements performed on an Alloy 600 specimen treated with ALP to assess edge effects

The following results address the effect of presence or absence of the ablative layer in Alloy 600 plates treated with ALP. They were previously published in MRP-162 [66] and are reproduced here for convenience.

Residual stress as a function of depth of Alloy 600 flat plates is shown in Figure A-14 for various air laser peening treatments performed by MIC. These measurements were performed to select the best parameters for the air laser peening process for PWR Alloy 600 components. For the air laser peening process, the investigated parameters were the irradiance, the short pulse duration, the number of peening layers, the presence or absence of an ablative layer, and the type of ablative layer if one was used. As shown in Figure A-14, the absence of an ablative layer for this process results in a high surface tensile stress, but the stress becomes neutral around 0.025 mm (or 0.001 inch) and compressive at higher depths. As mentioned in MRP-162, air laser peening with large spot and longer duration creates a large heat input, which is difficult to cool down. When there is no ablative layer, this high heat input results in melting the surface. When the brittle re-solidified surface layer shrinks after melting, this results in high surface tensile stress in a very thin layer of surface material corresponding to the melted surface. Air laser peening the surface with an additional peening layer at a low irradiance with no ablative layer (after the specimen was previously peened at a high irradiance with no ablative layer) did not modify the high surface tensile stress.

The specimens treated with the presence of an ablative layer (using two layers of tape or coating) all showed highly compressive stresses at the treated surface, as the ablative layer protects the surface from thermal effects. Using the coating for the ablative layer creates slightly more compressive stresses at the surface compared to using the tape (all other parameters being similar). All specimens treated with air laser peening (regardless of the selected parameters) showed very deep compressive stresses, deeper than 1.5 mm (depth at which the stress measurement was stopped).

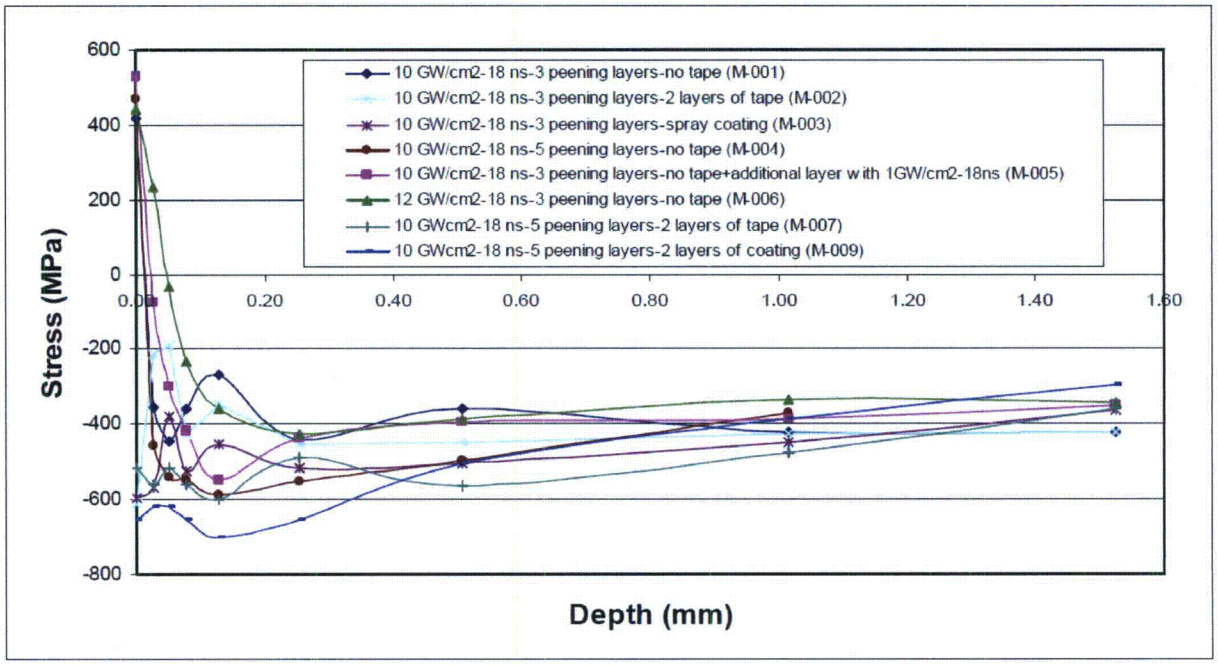

Figure A-14
Residual stress as a function of depth for Alloy 600 flat plates with various air laser peening treatments for parameters selection (treated by MIC).

Parameters for some additional tests of air laser peening treatment on Alloy 600 were selected as 10 GW/cm^2 irradiance, 18 ns pulse width, 5 layers of peening, and with either two layers of tape or polymer spray coating as the ablative layer. Four new flat plates were treated with these selected parameters to confirm the results of these parameters by stress measurement and to measure the stress in both in- plane directions. The residual stress as a function of depth for these Alloy 600 flat plates air laser peened with the selected parameters is shown in Figure A-15. All specimens air laser peened with the selected parameters show both high compressive stress at the surface as well as a depth of compressive stress higher than 1.5 mm (depth at which the stress measurement was stopped). Using the coating for the ablative layer creates slightly more compressive stresses at the surface compared to the tape, as observed previously. The effect of the peening treatment direction is not significant in this case. As mentioned in Section 2.4.1, the intention for nuclear power plant applications of ALP is to peen without the ablative layer due to time and cost considerations, so these results are of interest but are not fully representative of the planned nuclear plant process.

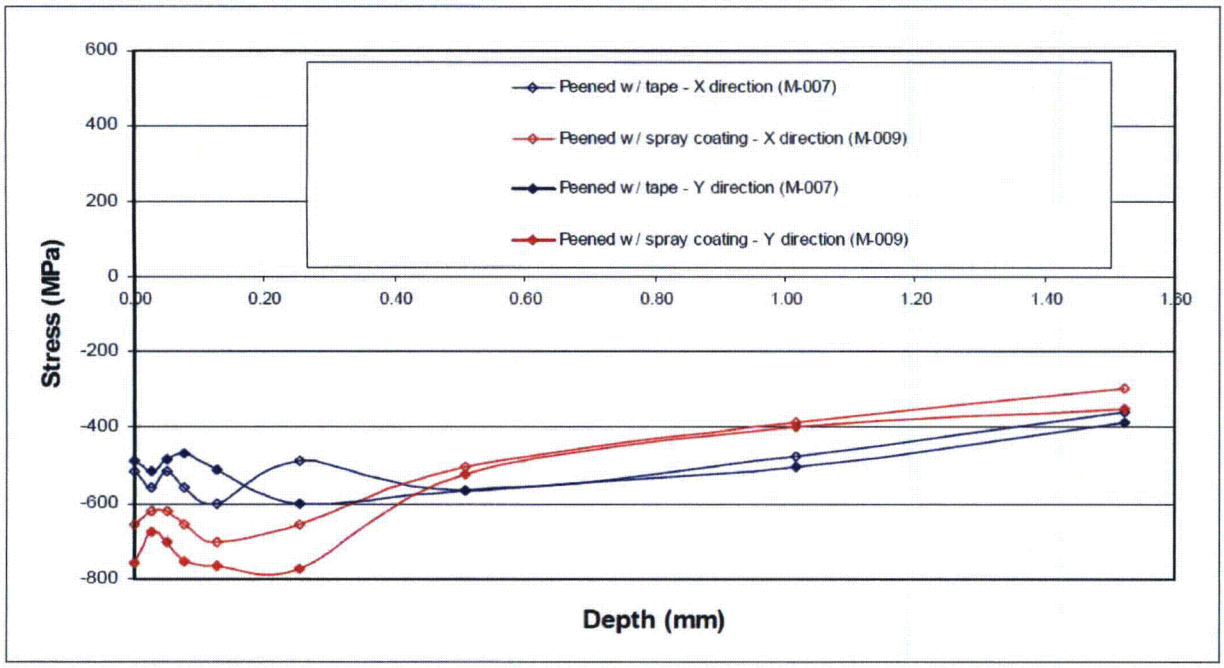

Figure A-15
Residual stress as a function of depth for Alloy 600 flat plates air laser peened with selected parameters: 10 GW/cm^2 irradiance, 18 ns pulse width, 5 layers of peening, and either two layers of tape or polymer spray coating as the ablative layer (treated by MIC).

A.1.2 Stress Analyses of Welded Plates

A.1.2.1 Welded Plates treated with ULP

Stress measurements were conducted at the surface and with depth on the welded plate specimens. The stress measurement results for the untreated specimens and underwater laser peened specimens by Toshiba are discussed. Specimens treated with WJP have been omitted as the process was applied by a vendor not under consideration in the present report. This was previously published in MRP-162 [66], and it is reproduced here for convenience.

The weld specimens consisted of 0.5 inch (13 mm) thick Alloy 600 plate material with a typical single V-groove joint configuration. The plates were welded using the shielded metal arc welding (SMAW) process with a NiCrFe-3 (182) filler material. The welded specimens were restrained during the welding process and were further strained at the centerline of the weld root and face, by placing a spacer plate between two weld specimens, thereby creating a 4-point bending condition as shown in Figure A-16. A typical side view of the welded plates showing side A and side B with respectively the root and face exposed to the surface is shown in Figure A-17. The specimen surfaces (weld area) were manually ground flush to facilitate consistent surface treatment and stress analyses on the surfaces. It is not expected that a utility will need to measure the surface stresses before and after surface treatment to verify the stress improvement. To allow comparison of the stress profile between untreated and treated surfaces, only part of the weld specimen surface was surface treated on both side A and side B of the specimen: a one by two inches area (25 mm by 51 mm) centered on the weld in the longitudinal direction (with

respect to the specimen and not the weld) and on one half of the transverse direction, as shown in Figure A-16.

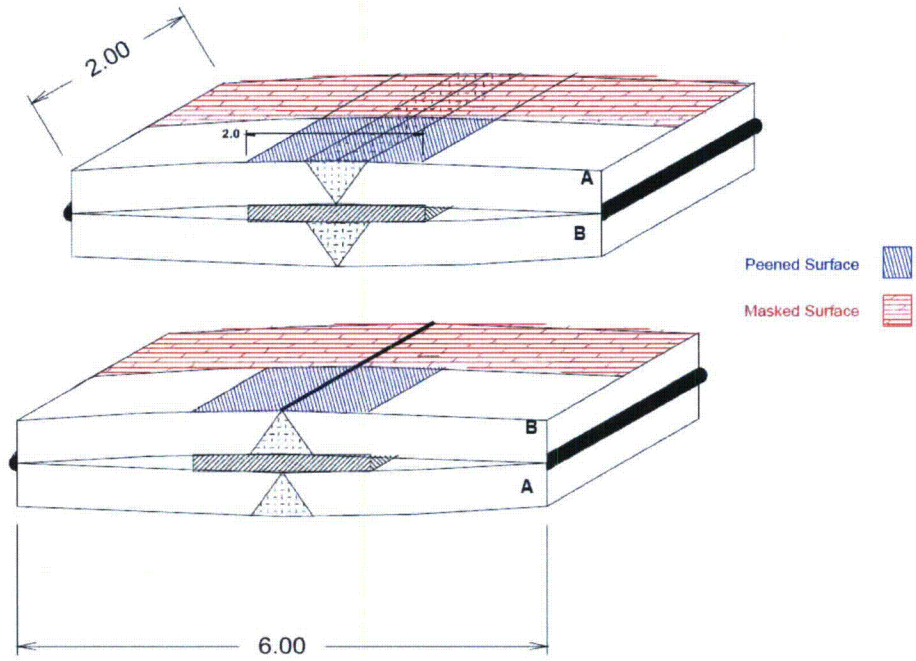

Figure A-16
Welded specimen with a one inch by two inches peened surface on side A (top, face of weld) and side B (bottom, weld root). The masked surface is used for the cavitation (water jet) peened specimens only. Dimensions are shown in inches.

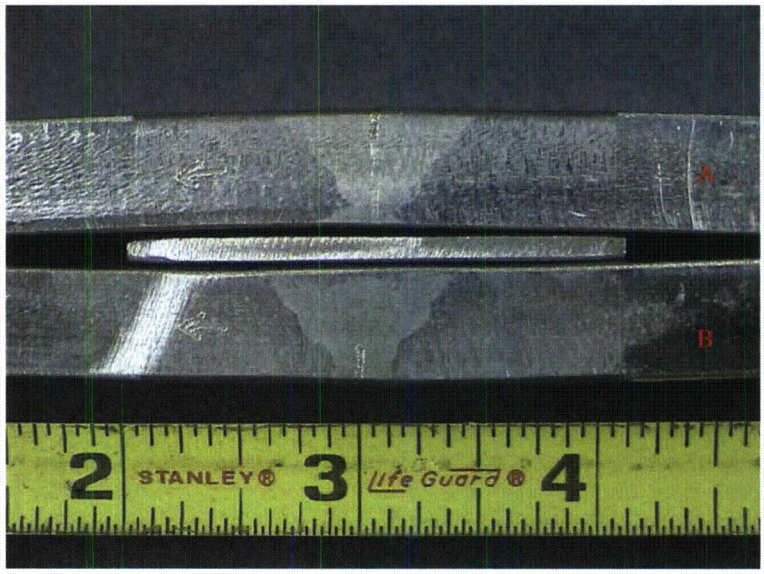

Figure A-17
Typical side view of the welded plates showing side A (face of weld) and side B (weld root) exposed to the surface

Surface XRD measurements were performed along the longitudinal centerline of side A (with respect to the specimen and not the weld) and side B before surface conditioning. Measurements were taken at the weld center line and at 5 mm increments up to 25 mm from the weld centerline. Stress measurements with depth in untreated specimens were performed at four locations on side A and B, as indicated in Figure A-18 (showing the side A of an untreated specimen). Stress measurements with depth in peened specimens were measured in similar locations, as seen in Figure A-19 (sides A and B) to allow for comparison of peened and untreated surfaces. For side A, locations 1 and 2 correspond to the weld centerline and locations 3 and 4 to the weld fusion line (15 mm from the weld center line). For side B, locations 1 and 2 correspond to the weld centerline and locations 3 and 4 to locations 1 mm from the weld center line. Locations 1, 2, 3, and 4 were determined by etching the cross section (Figure A-17). Stress measurements with depth at these four locations were performed in the longitudinal and transverse directions (with respect to the specimen and not the weld). Depth stress measurements were typically continued until the stress profile returned to the base line condition (1 to 1.5 mm).

Stresses (applied and residual) in the longitudinal direction (0°) as a function of distance from the weld center line for untreated welded plates A and B are shown respectively in Figure A-20 and Figure A-22. The surface stresses are either tensile or compressive varying with the distance from the weld center and the specimen number. The stress in the longitudinal directions is expected to be tensile at the face of the weld, due to the face of the weld cooling last and also due to the bending configuration of the plate. The welded plate surfaces were ground to facilitate surface treatment of the surfaces and stress analyses. As a result, the XRD surface stress results are probably not reliable, because the metal surface was smeared by the grinding step, i.e., the XRD surface stress measurements are affected by the cold work induced by the surface preparation.

Stress in the transverse direction (90°) as a function of distance from the weld center line for untreated welded plates A and B are shown respectively in Figure A-21 and Figure A-23. The surface stresses are either neutral or compressive varying with the specimen number. As discussed for the longitudinal specimens, these XRD surface stress results are probably not reliable because the metal surface was smeared by the grinding step (to facilitate surface treatment application).

Stress was measured with depth on weld specimen 9A at four locations: locations 1 and 2 correspond to the weld centerline and locations 3 and 4 to the weld fusion line (15 mm from the weld center line), as shown in Figure A-18. The stress results with depth at each location are shown in Figure A-24 for the longitudinal (0°) direction and Figure A-25 for the transverse direction (90°). The results in Figure A-24 and Figure A-25 show fairly consistent stress profiles for the locations at the weld centerline (1 and 2) and the locations at the weld fusion line (3 and 4), except at the surface for the reason mentioned earlier. One can note in Figure A-24 that the longitudinal stress is more tensile in the HAZ (locations 3 and 4) than at the center of the weld (locations 1 and 2) as expected, except for the surface stress for the reason mentioned earlier. Treated specimens were peened in designated areas to allow comparison between untreated and treated surfaces (comparison between locations 1 and 2 and locations 3 and 4), as shown in Figure A-19.

Stress in the longitudinal and the transverse directions as a function of depth for Alloy 600 welded plate specimen 4A and 4B underwater laser peened with selected parameters (by

Toshiba) are respectively shown in Figure A-26 and Figure A-27. The stress with depth for the peened surface in both the longitudinal and transverse directions is more compressive than the one for the unpeened surface at the center of the weld on the face side (locations 1 and 2 for side A) and at the fusion line on the face side (locations 3 and 4 for side A). The longitudinal stress with depth for the peened surface is more compressive than the one for the unpeened surface at the center of the weld on the toe side (locations 1 and 2 for side B) and 1 mm away from the center of the weld on the toe side (locations 3 and 4 for side B). The transverse stress with depth for the peened surface is more compressive than the one for the unpeened surface up to about 0.3 mm depth at the center of the weld on the toe side (locations 1 and 2 for side B) and up to about 0.6 mm depth at 1 mm from the center of the weld on the toe side (locations 3 and 4 for side B). For this last graph, the important thing is that peening the surface resulted in creating a highly compressive stress in the surface layers of the treated surface, which would correspond to the surface exposed to the coolant.

Residual stress in the longitudinal and the transverse directions as a function of depth for Alloy 600 welded plate specimen 8A and 8B underwater laser peened with selected parameters (by Toshiba) are respectively shown in Figure A-28 and Figure A-29. The stress with depth for the peened surface in both the longitudinal and transverse directions is more compressive than the one for the unpeened surface at the center of the weld on the face side (locations 1 and 2 for side A) and at the fusion line on the face side (locations 3 and 4 for side A). The stress with depth for the peened surface in both longitudinal and transverse directions is more compressive than the one for the unpeened surface at the center of the weld on the toe side (locations 1 and 2 for side B) and 1 mm away from the center of the weld on the toe side (locations 3 and 4 for side B).

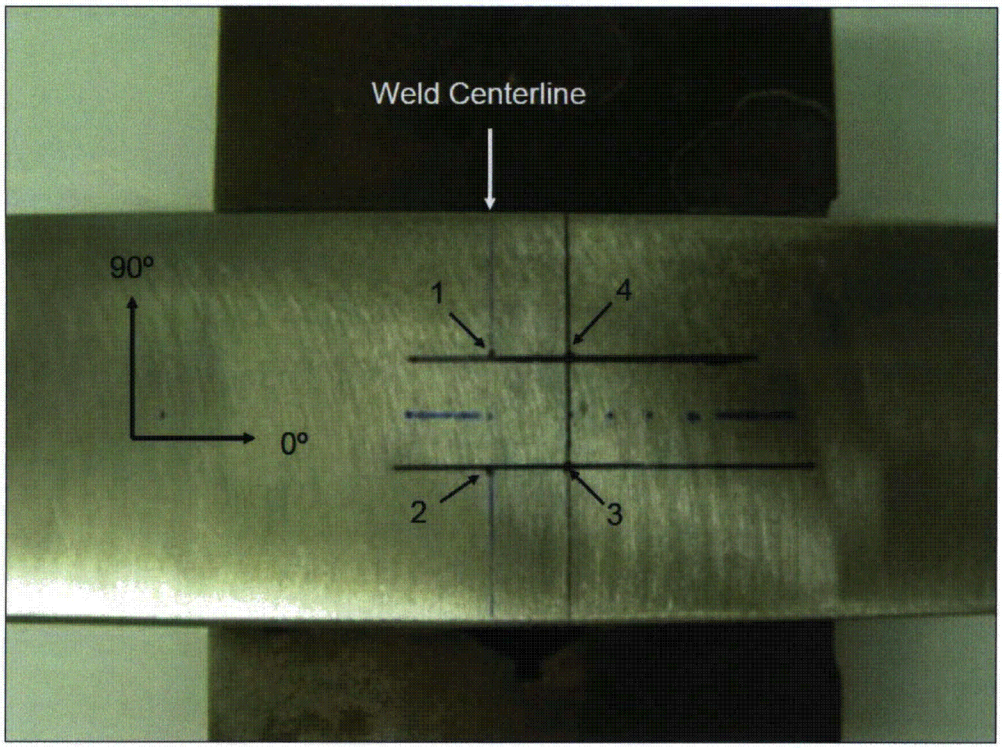

Figure A-18
Stress measurements with depth for weld specimens were evaluated at 4 locations. The locations in this case (side A) are associated with the weld centerline (locations 1 and 2) and the weld fusion line (locations 3 and 4)

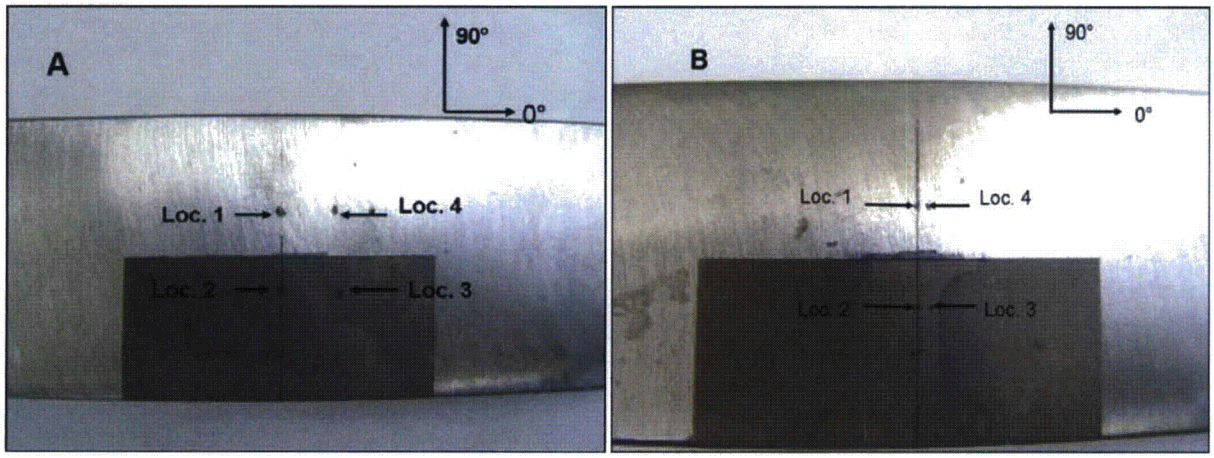

Figure A-19
Surface treated specimens with typical stress measurements with depth locations 1, 2, 3, and 4 on side A (left) and side B (right). Locations 2 and 3 are within the peened area and the corresponding locations 1 and 4 are in the untreated area (underwater laser peened specimen shown)

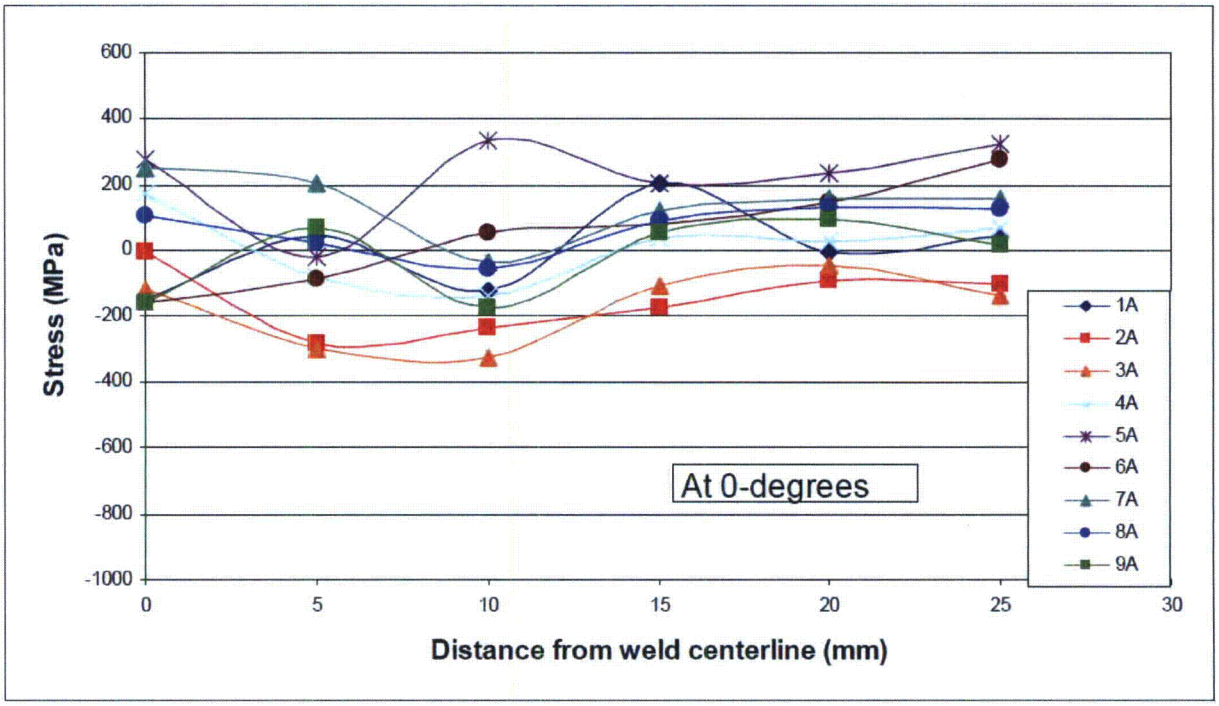

Figure A-20
Stress in the longitudinal direction (0°) as a function of distance from the weld center line for untreated welded plates A

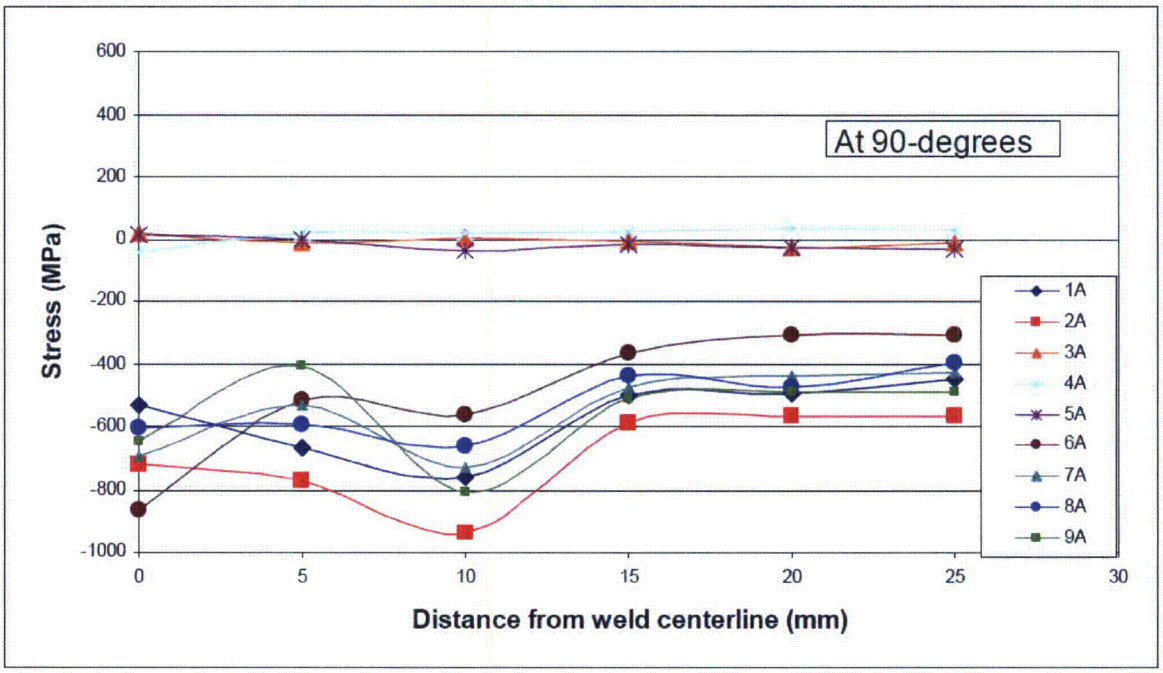

Figure A-21
Stress in the transverse direction (90°) as a function of distance from the weld center line for untreated welded plates A

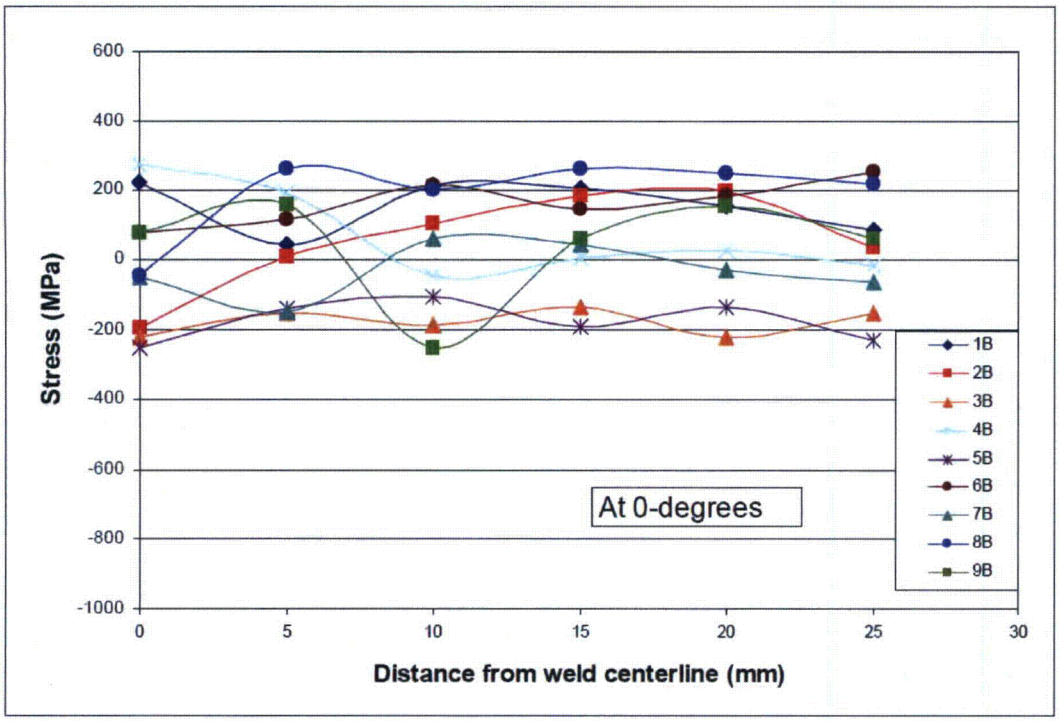

Figure A-22
Stress in the longitudinal direction (0°) as a function of distance from the weld center line for untreated welded plates B

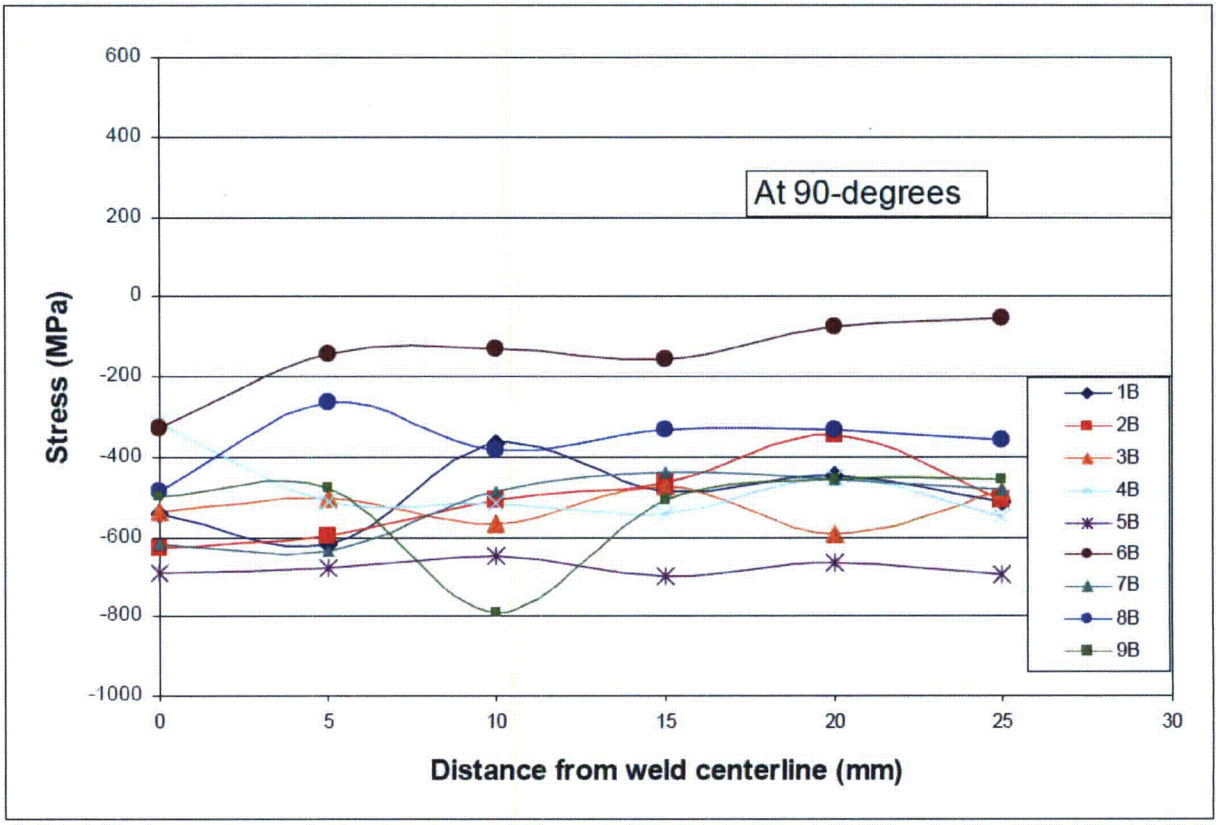

Figure A-23
Stress in the transverse direction (90°) as a function of distance from the weld center line for untreated welded plates B

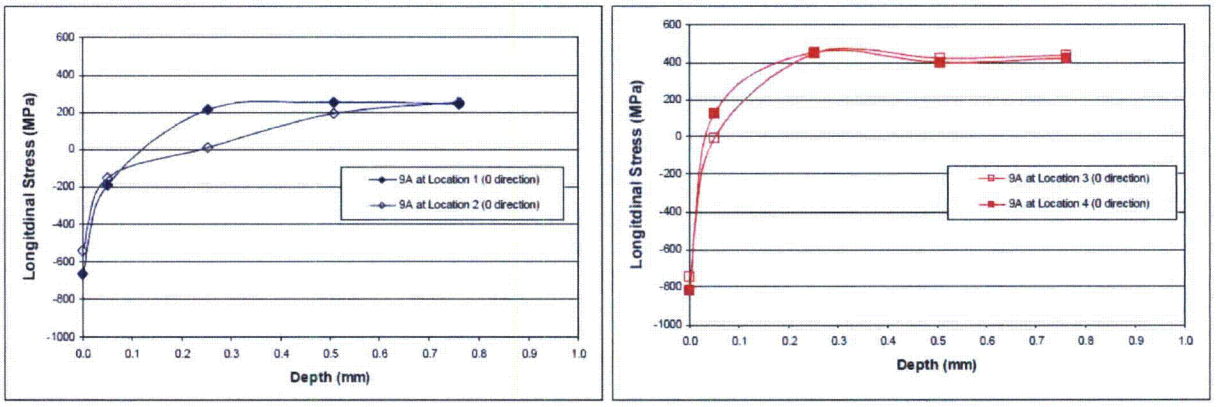

Figure A-24
Comparison of longitudinal stress (0°) as a function of depth between locations 1, 2, 3, and 4 for untreated welded plate 9A (reference)

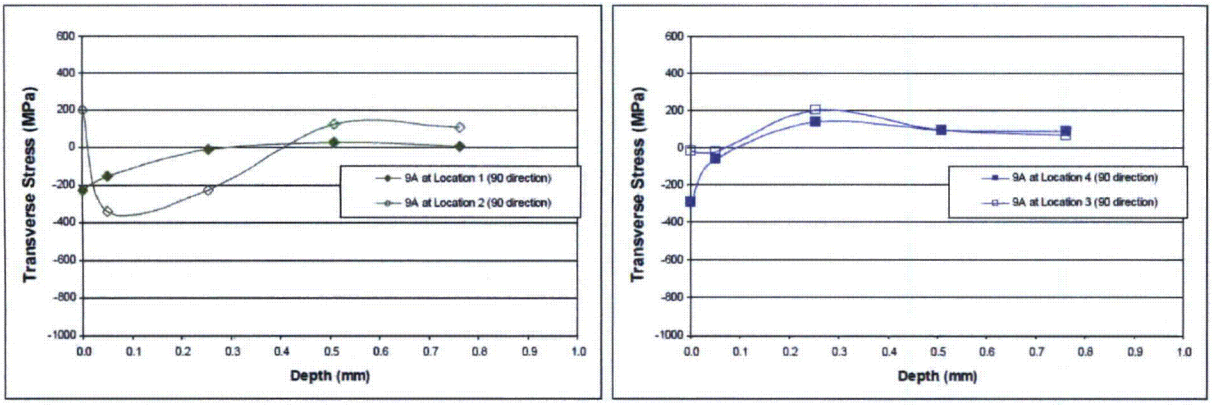

Figure A-25
Comparison of transverse stress (90°) as a function of depth between locations 1, 2, 3, and 4 for untreated welded plate 9A (reference)

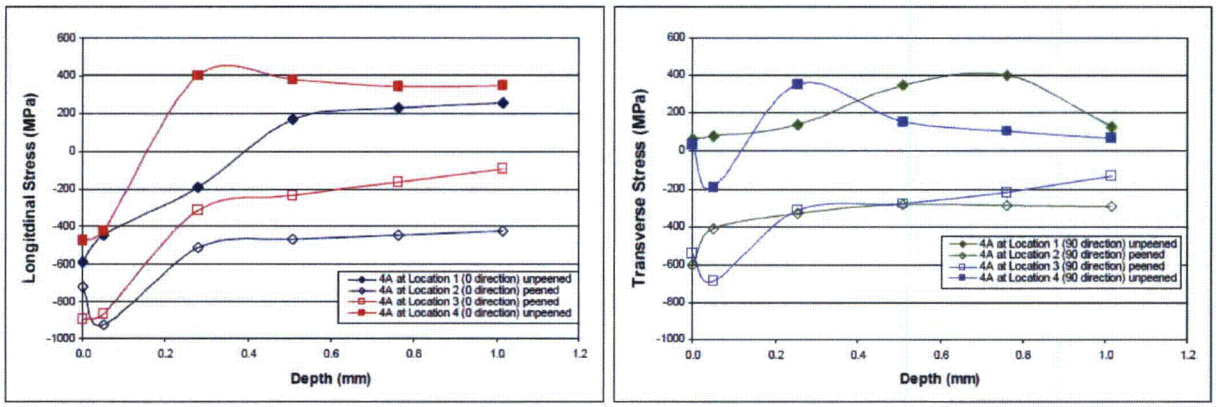

Figure A-26
Stress as a function of depth for welded plate specimen 4A underwater laser peened with selected parameters 2.3 GW/cm^2 irradiance, 8 ns pulse width, 4500 pulses/cm^2 coverage and no ablative layer (treated by Toshiba)

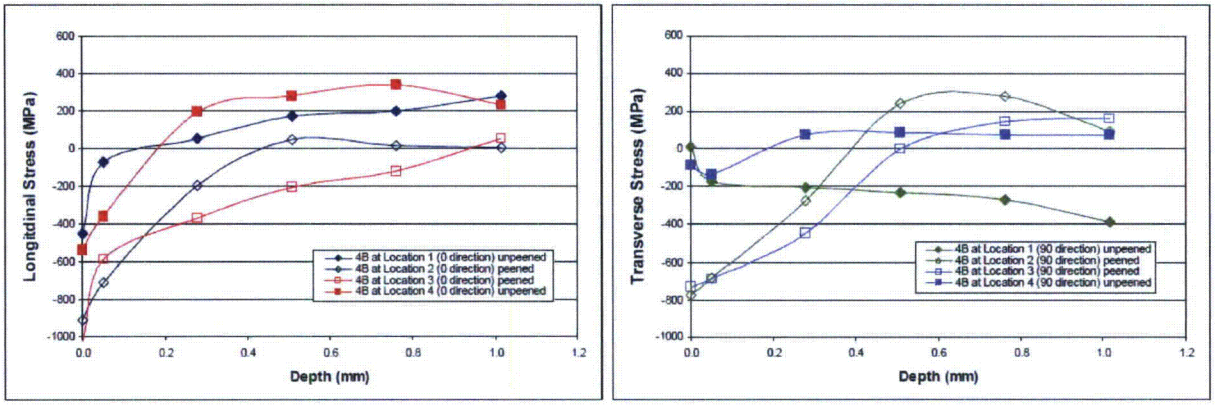

Figure A-27
Stress as a function of depth for welded plate specimen 4B underwater laser peened with selected parameters 2.3 GW/cm^2 irradiance, 8 ns pulse width, 4500 pulses/cm^2 coverage and no ablative layer (treated by Toshiba)

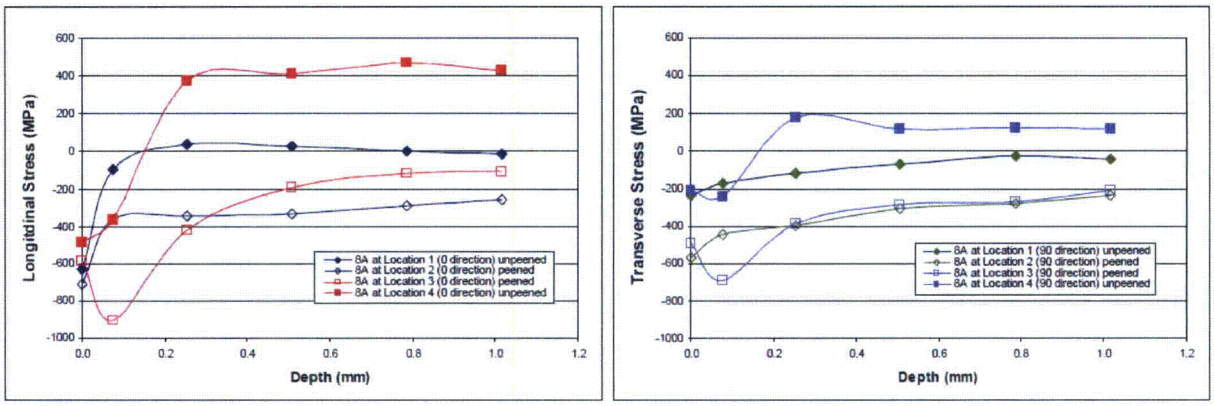

Figure A-28
Stress as a function of depth for welded plate specimen 8A underwater laser peened with selected parameters 2.3 GW/cm^2 irradiance, 8 ns pulse width, 4500 pulses/cm^2 coverage and no ablative layer (treated by Toshiba)

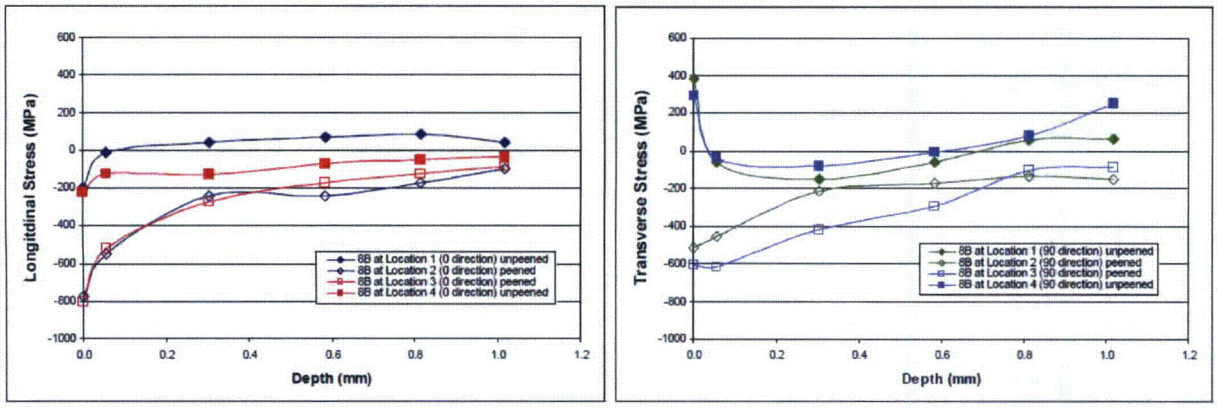

Figure A-29
Stress as a function of depth for welded plate specimen 8B underwater laser peened with selected parameters 2.3 GW/cm^2 irradiance, 8 ns pulse width, 4500 pulses/cm^2 coverage and no ablative layer (treated by Toshiba)

Toshiba constructed two welded plates of Alloy 600 and Type 304 stainless steel joined by Alloy 182 with a thickness of 38 mm. A small area of one of the plates, including the weld joint and both alloys, was peened as depicted in Figure A-30 and Figure A-31, and the residual stress profile as a function of depth was measured in both directions at the same locations on both plates. In both alloys, compressive stress profiles were induced in the peened specimen to a depth of at least 1 mm in both directions.

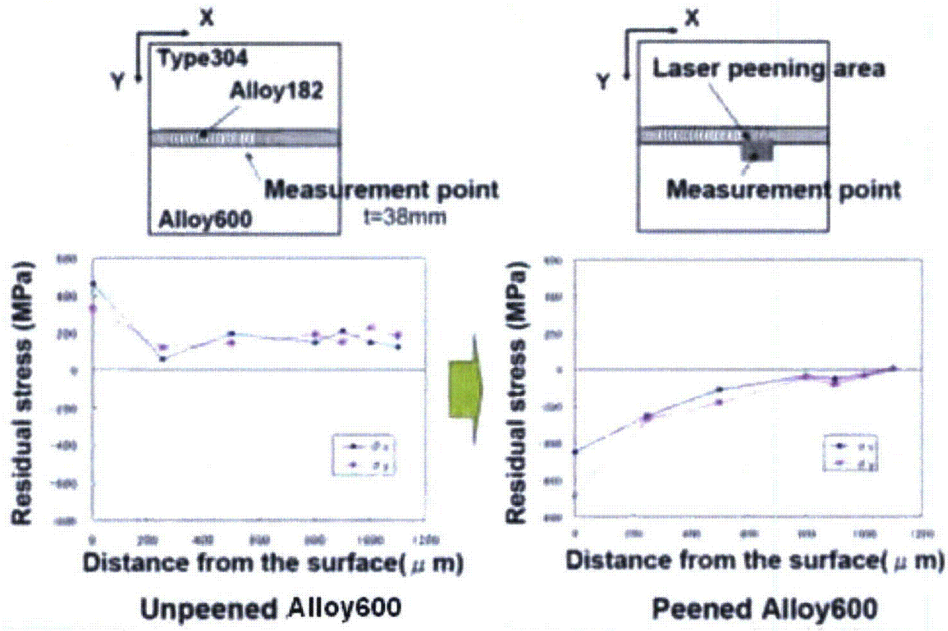

Figure A-30
Results of residual stress improvement on the Alloy 600 side of a welded plate

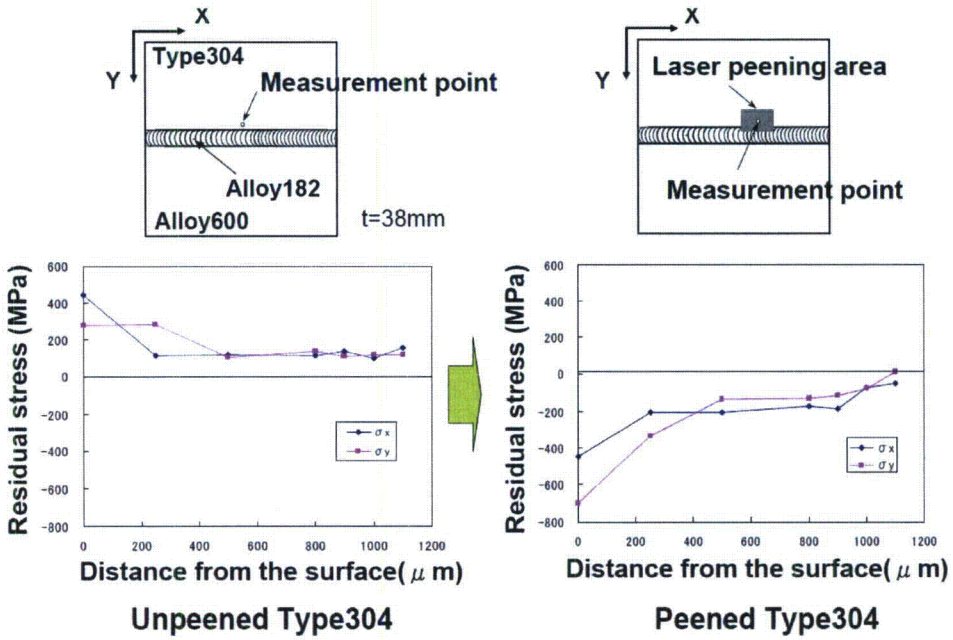

Figure A-31
Results of residual stress improvement on the Type 304 stainless steel side of a welded plate

A.1.2.2 Welded Plates treated with WJP

Mitsubishi also performed stress measurements on welded plates. The objective of this series of tests was to develop an appropriate set of parameters under which the large-radius surface configuration of the WJP process can be operated. After the samples were treated, residual stress measurements were taken using the x-ray diffraction method. The x-ray diffraction method is used to measure the residual stress at various depths after electro-chemical polishing of the coupons. Surface inspections to verify the integrity of the post-treated material were completed using visual and dye-penetrant testing.

These tests were performed on coupons manufactured from a plate of Alloy 600 material that was welded to a plate of 316 stainless steel using ENiCrFe-1 (Alloy 132) weld metal. The coupons were submerged in a pressurized test chamber to simulate the effect of being under several meters of water. Figure A-32 is a schematic of the test chamber and the coupons used for the tests where the nozzle is positioned perpendicular (90°) to the coupon. The test coupons are much thinner than the actual components on the reactor vessel. This feature makes the results of the testing conservative. Thinner coupons are more likely to deform due to the WJP process which reduces the effectiveness of the residual stress mitigation. Thus, the effects of the WJP process on actual reactor components will be the same or greater than those shown in the testing, meaning that the results of these tests lead to conservative values for the process parameters. The tests are conducted by passing the WJP nozzle over the weld of the coupon. During treatment, the nozzle passes over the entire welded region on the test coupons at a constant rate to ensure constant coverage. Figure A-33 gives details of the path of the WJP treatment and the locations where residual stress measurements were taken for each coupon.

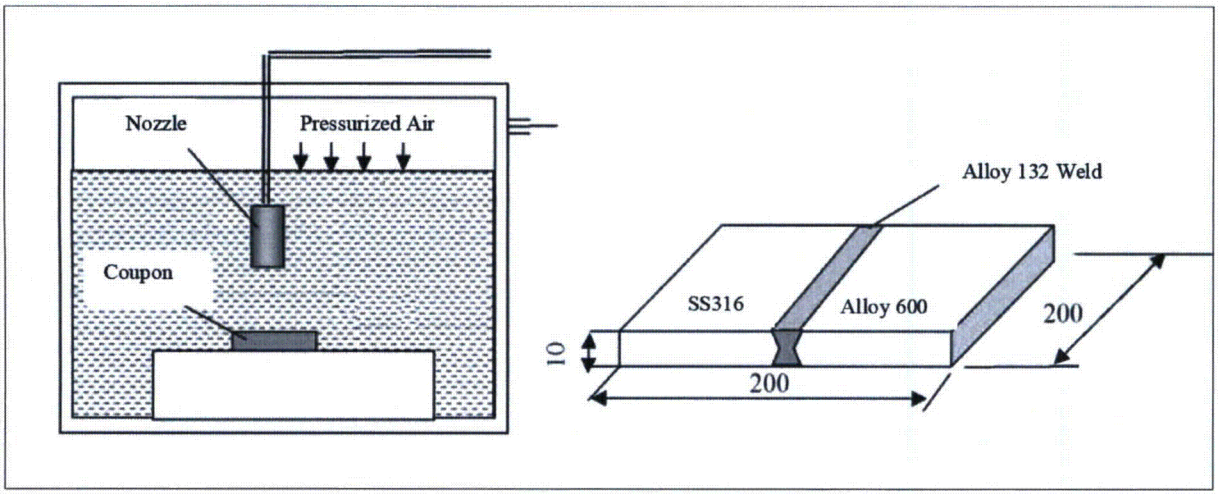

Figure A-32
Test configuration for large diameter applications, provided by Mitsubishi

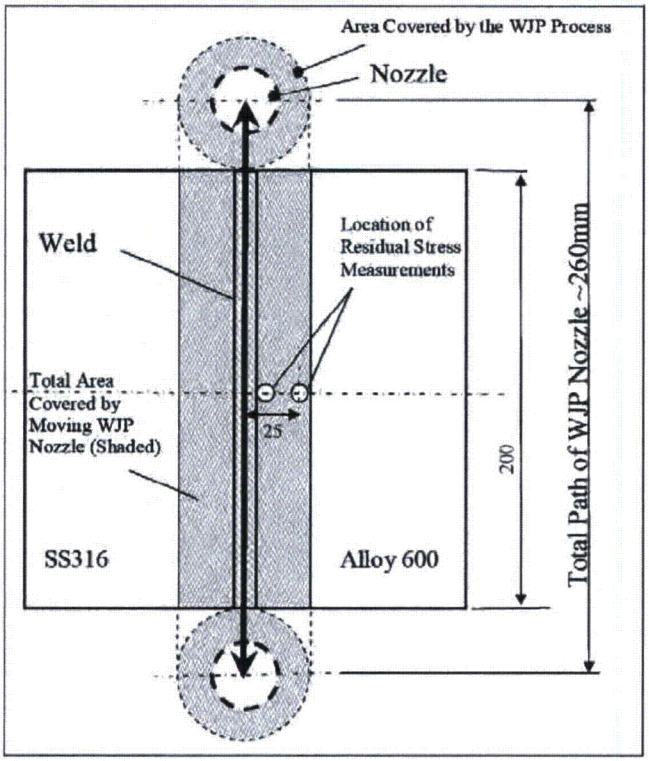

Figure A-33
WJP process parameter testing for flat or large radius applications, provided by Mitsubishi

As shown in Figure A-33, the residual stress measurements were conducted at two locations for each coupon, the boundary between the weld and base metal, and 25 mm from the weld center near the edge of the affected zone, both on the alloy 600 side of the weld. Also, measurements were taken at various depths: 0 mm (surface), 0.2 mm, 0.5 mm, 0.8 mm, 1.0 mm, and 1.3 mm.

Testing at various depths was conducted by removing material using electro-chemical etching. Residual stress measurements were not made in the weld metal plate due to the high level of difficulty of using the x-ray diffraction to measure stresses within the weld microstructure. The mechanical properties of the weld metal and the Alloy 600 plate are similar enough to generate comparable response to the WJP process and the results for the base plate next to the weld can be taken as representative of the weld itself. At each location, residual stress measurements were taken in two-directions: along the weld (equivalent to hoop stress for a large pipe circumferential weld), and perpendicular to the weld direction (equivalent to axial stress).

Table A-1 and Table A-2 contain the results of residual stress measurements for each of the tested parameter sets and for the untreated, or initial, material state. It can be seen from Table A-1 that for the untreated condition, the surface stress state is tensile to deeper than 1 mm below the surface both next to the weld and at 25 mm from the weld center. By contrast, the results for the treated surfaces for all sets of test conditions are all compressive to at least 1 mm. The residual stress profiles achieved by WJP are compressive to a depth of 1.0 mm, as shown in Figure A-34 and Figure A-35.

Table A-1
Test Data at two different locations on an unpeened welded plate, provided by Mitsubishi

Coupon Config.	Measurement Location		Residual Stress (MPa) X-ray Diffraction	
	Location	Depth (mm)	Axial	Hoop
Welded Plates	At Weld	0.00	862	538
		0.20	252	300
		0.50	275	199
		0.79	184	335
		1.04	104	172
		1.32	169	144
	25mm from Weld	0.00	548	375
		0.19	331	211
		0.50	208	217
		0.77	297	248
		1.02	12	99
		1.27	156	75

Table A-2
Test Data at two different locations on a peened welded plate, provided by Mitsubishi

Coupon Config.	Measurement Location		Residual Stress (MPa) X-ray Diffraction	
	Location	Depth (mm)	Axial	Hoop
Welded Plates	At Weld	0.00	-414	-293
		0.24	-271	-
		0.51	-114	-173
		0.78	-81	-161
		1.01	-121	-193
		1.32	-66	-209
	25mm from Weld	0.00	-411	-267
		0.23	-322	-338
		0.51	-257	-197
		0.78	-165	-197
		0.99	-200	-219
		1.29	5	-27

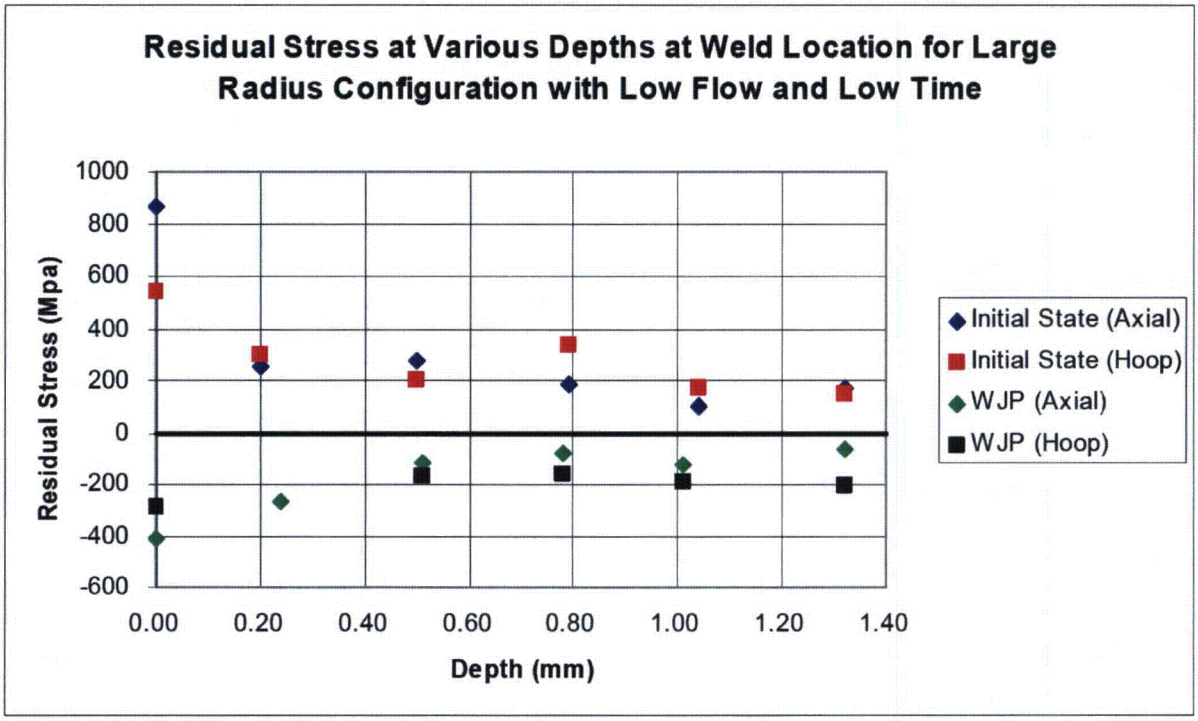

Figure A-34
Results of residual stress improvement treatment of welded plate at weld location, provided by Mitsubishi

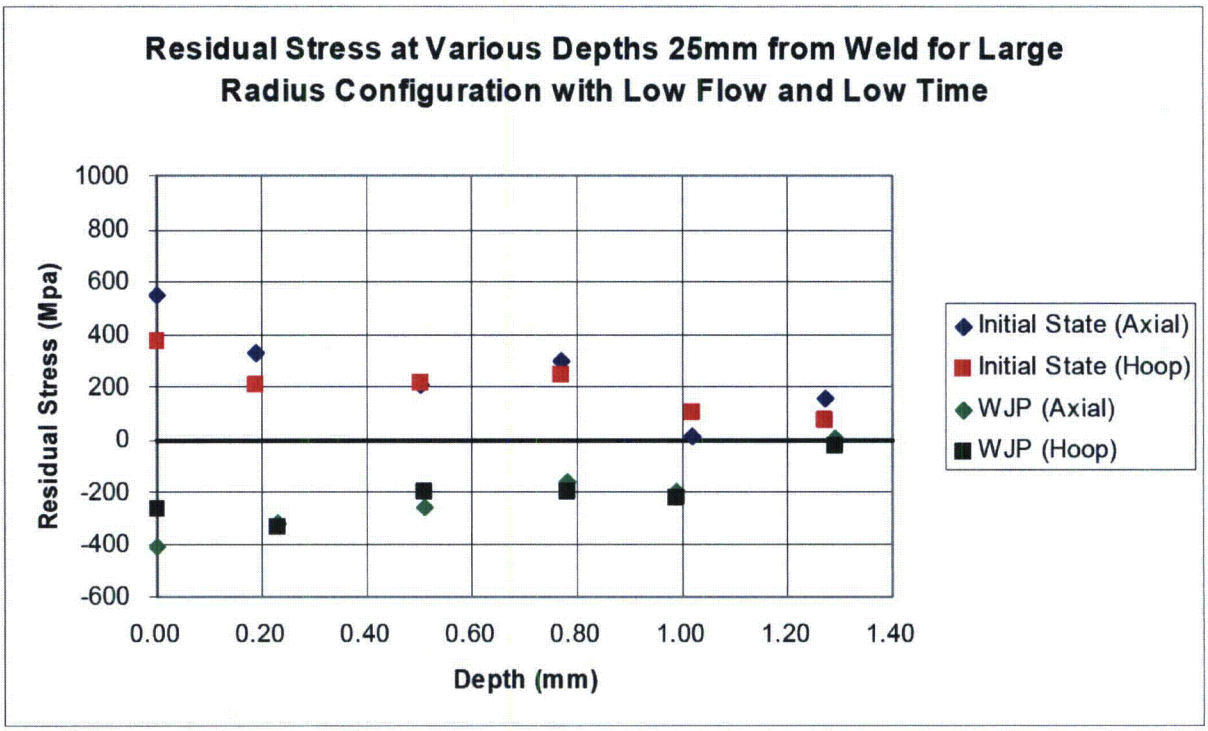

Figure A-35
Results of residual stress improvement effect of welded plate 25 mm from weld center, provided by Mitsubishi

The effectiveness of WJP near a crack in welded plates was investigated in conjunction with the experiments described in Section A.1.1.2 on the effect of WJP near or between cracks on flat plates. A plate of Alloy 600 with a trough of Alloy 182 weld metal in the middle was used for this experiment, and it had the same dimensions as the Type 304 stainless steel specimens used in the flat plate experiments. A crack was initiated using three point bending in potassium tetrathionate in the Alloy 182 weld metal. The experimental procedure used was the same as the one used in the flat plate experiments. Before cracking, the specimen was subjected to thermal treatment and machining. After cracking, the surface was heavily ground in the direction perpendicular to the cracks after cracking, pre-WJP residual stress was measured with XRD at three depths (on the surface, 100 μm below the surface, and 200 μm below the surface), WJP was applied perpendicular to the flaws, and post-WJP residual stress was measured with XRD at the same depths. A schematic and a photo of the specimen are depicted in Figure A-36.

Before WJP was applied to the surface, all residual stress measurements from before applying WJP were tensile. The residual stress values at the surface were significantly more tensile than those measured below the surface such that the stress variation with respect to depth was much larger than the variation with respect to distance from the crack. After WJP, the residual stress values were compressive in both the Alloy 182 weld metal and the Alloy 600 base metal. The magnitude of compressive residual stress at the surface was much larger than the residual stress magnitude below the surface. The residual stress measurements are shown in Figure A-36.

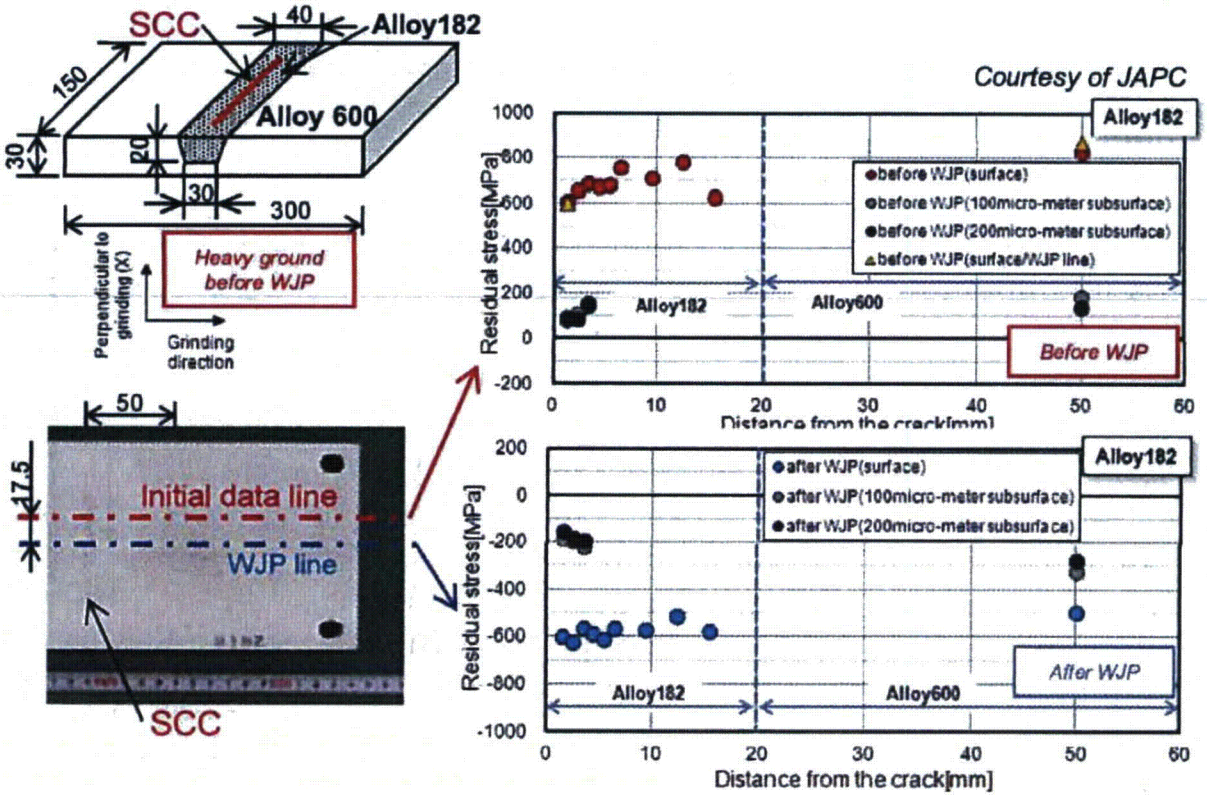

Figure A-36
Residual stress profiles before and after WJP in a welded plate with a pre-existing crack, provided by Hitachi-GE

A.1.3 Stress Analyses of Underwater Laser Peened BMN-size Pipes and Mock-ups

A.1.3.1 BMN Size Pipes

This section was previously published in MRP-162 [66] and is reproduced here for convenience. The objective of this task was to confirm that the treatment can be effective in a cylindrical geometry specifically representative of BMNs. This is an important step before the treatment of the BMN mock-up for two reasons: (1) the delivery systems need to be developed or verified for treatment of the BMN-size pipe ID surface and (2) because of the simple specimen geometry, the ID stress resulting from the peening treatment on the pipe can be calculated by accounting for the stress relieved by sectioning of the pipe for ID access (this is not possible on the ID of the mock-up, due to the complicated geometry). A secondary objective of this task was to investigate the effects of successive treatments on the inside and outside surfaces of the pipes. BMN-size pipe specimens were fabricated from Alloy 600 tubing material. Specimens approximately matched the thickness and ID of an average BMN (pipe shown in Figure A-37).

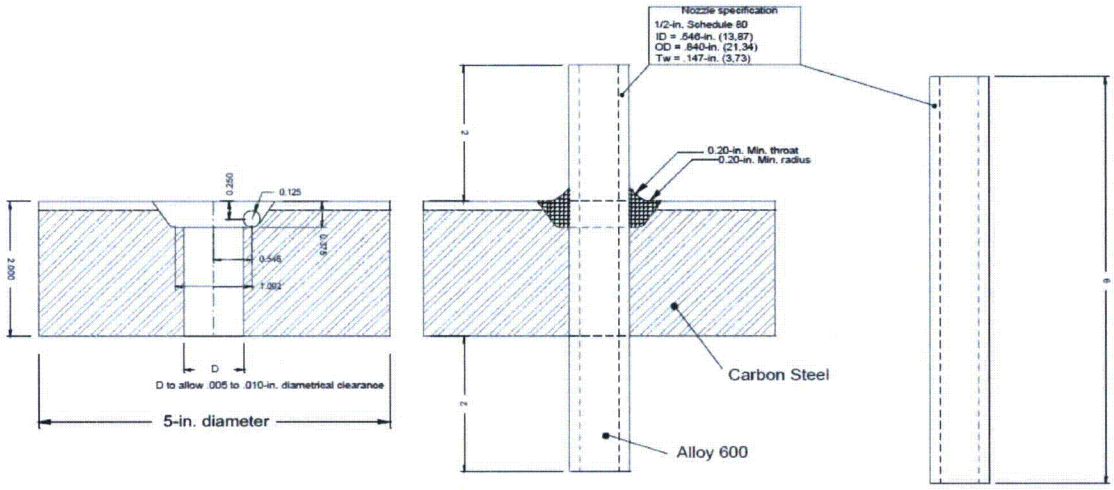

Figure A-37
Drawing of mock-up fabrication with materials and dimensions indicated (in inches)

Peening was applied around the ID and the OD surfaces of the pipe for a two inches height (51 mm) centered on the pipe axially. As an example, underwater laser peening of the BMN-size pipe is shown in Figure A-38.

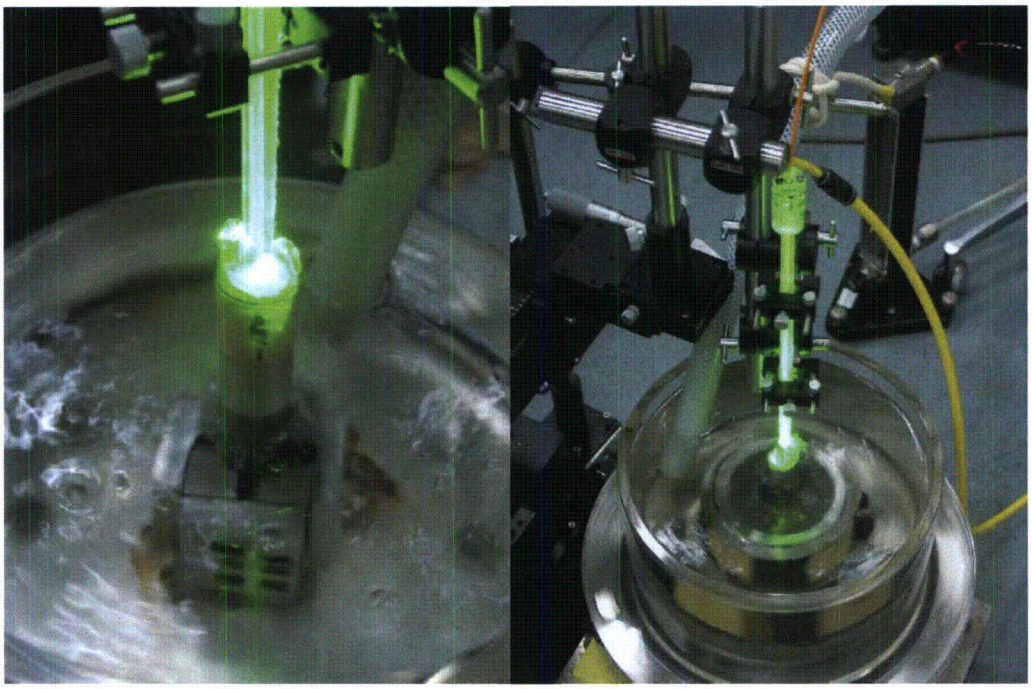

Figure A-38
Underwater laser peening of BMN-size pipe specimen (left) and BMN mock-up (right) (provided by Toshiba)

To measure the stress on the ID, the BMN-size pipe was sectioned in two along the longitudinal direction. Figure A-39 shows the stress measurements locations for the pipe specimens.

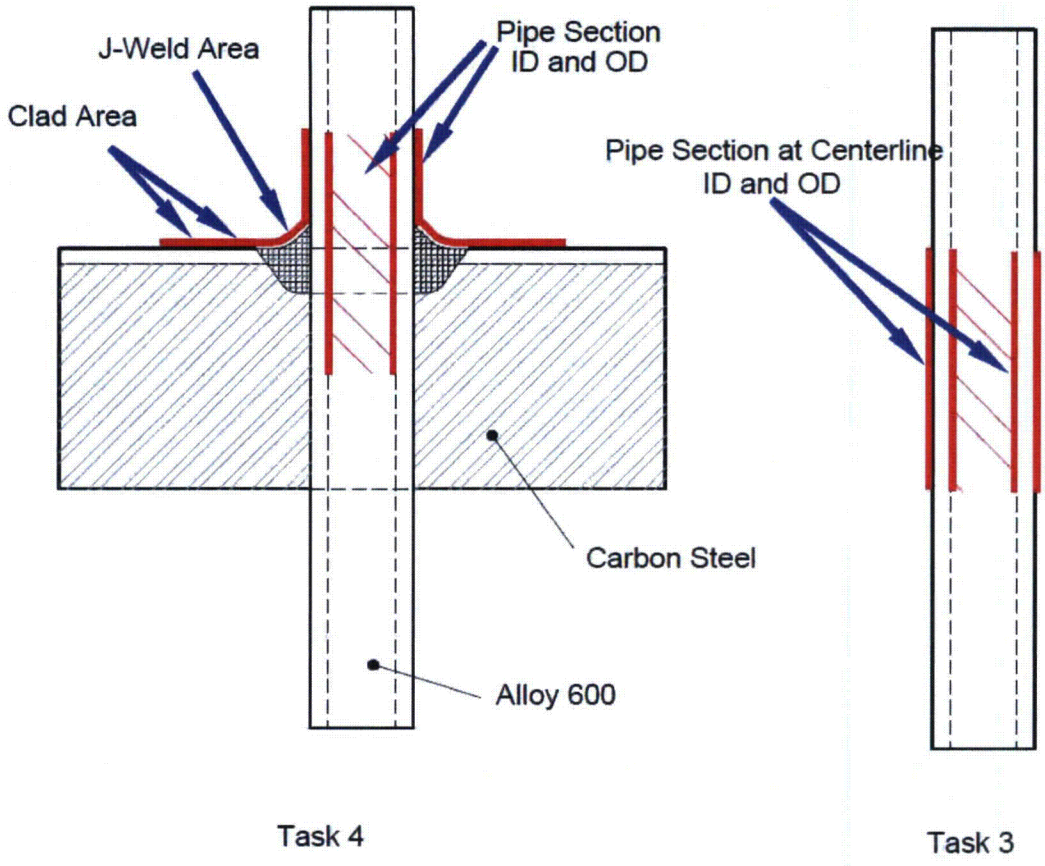

Figure A-39
Treated surfaces (in red) and XRD stress measurement locations (in blue) for underwater laser peened BMN-size pipes (Task 3 specimens) and BMN mock-ups (Task 4 specimens)

To investigate the effects of peening order on the residual stresses in BMN-size pipes, the underwater laser peened pipes were treated progressively and OD surface stresses were measured by XRD in the following order:

1. XRD on the outer surface for four azimuthal locations centered longitudinally on the pipes,
2. Treatment on the outer surface,
3. XRD measurements at the same locations,
4. Treatment on the inner surface, and
5. XRD measurements at the same locations.

OD surface residual stress measurement results before surface treatment (as received) for two Alloy 600 BMN-size pipes are shown in Figure A-40 and Figure A-41. The OD hoop and axial

surface residual stress of the as received specimens is compressive around the pipes (around -200 MPa for the hoop stress and around -400 MPa for the axial stress).

OD surface residual stress measurement results after underwater laser peening of the OD only and after laser peening of both the OD and ID for two Alloy 600 BMN-size pipes are also shown in Figure A-40 and Figure A-41. Laser peening on the OD increases the OD compressive residual stress magnitude in both directions compared to the as received condition (from -200 to -600 MPa for the hoop stress and from -400 to close to -1000 MPa for the axial stress). Laser peening of the ID (after peening of the OD) reduces the OD compressive residual stress magnitude compared to OD peening only (from -600 to -450 MPa for the hoop stress and from -1000 to -700 MPa for the axial stress), but increases it compared to as received condition (from -200 to -450 MPa for the hoop stress and from -400 to close to -700 MPa for the axial stress). The residual stress on the outer surface was significantly reduced by laser peening on the inside surface. This can be attributed to the relatively thin wall thickness of the specimens (3.75 mm). The compressive residual stress created on one side of the pipe affects the other side of the pipe, as the treatment induced compressive stress depth is around 1 mm and as the redistribution of the stress to satisfy equilibrium occurs.

Axial and hoop residual stress for Alloy 600 pipe material treated by ULP on both the OD and ID surfaces are shown in Figure A-42 and Figure A-43. Figure A-42 shows the stress measured from the OD, while Figure A-43 shows the stress measured from the ID. After OD and ID treatment, high compressive hoop and axial residual surface stress are achieved on both the OD and ID surfaces (but more compressive on the OD surface). The depth of the compressive residual stress is between 0.6 mm and 1 mm on OD side and between 1 mm and 1.3 mm on the ID side. The surface treated last (ID) shows deeper compressive stress due to the peening order.

As a side note, there is good agreement on the OD surface residual stress measurement results after OD and ID treatment between Figure A-40, Figure A-41, and Figure A-42.

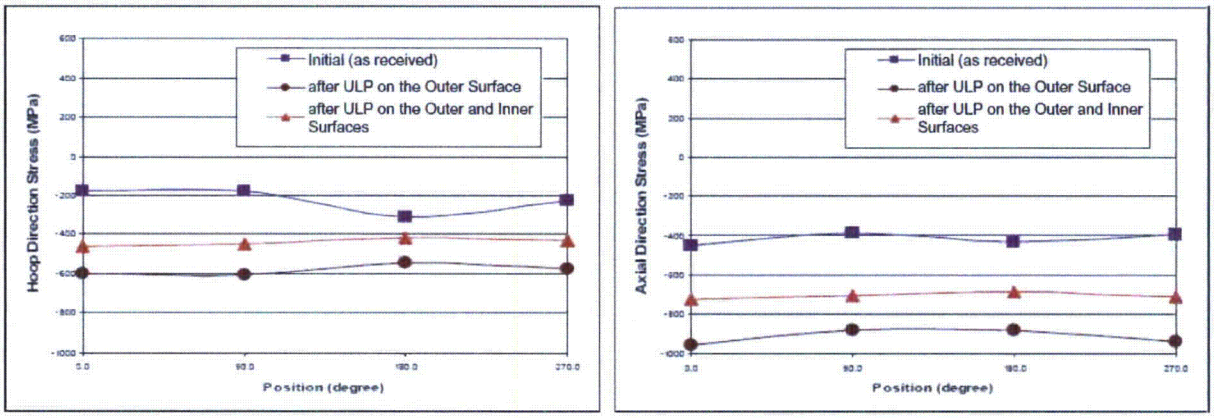

Figure A-40
OD surface residual stress measurement results for pipe specimen No. 1 before surface treatment (as received), after underwater laser peening of OD only, and after underwater laser peening of both OD and ID (treated and measured by Toshiba)

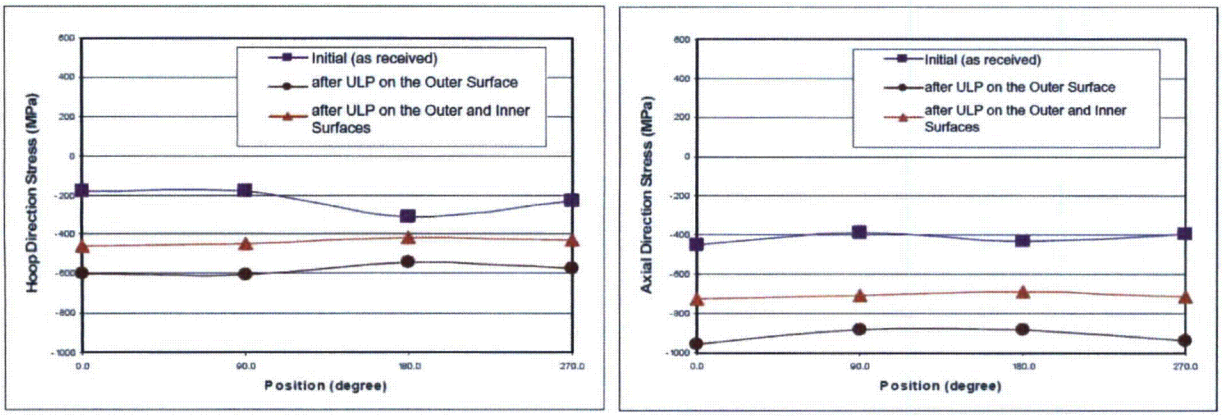

Figure A-41
OD surface residual stress measurement results for pipe specimen No. 2 before surface treatment (as received), after underwater laser peening of OD only, and after underwater laser peening of both OD and ID (treated and measured by Toshiba)

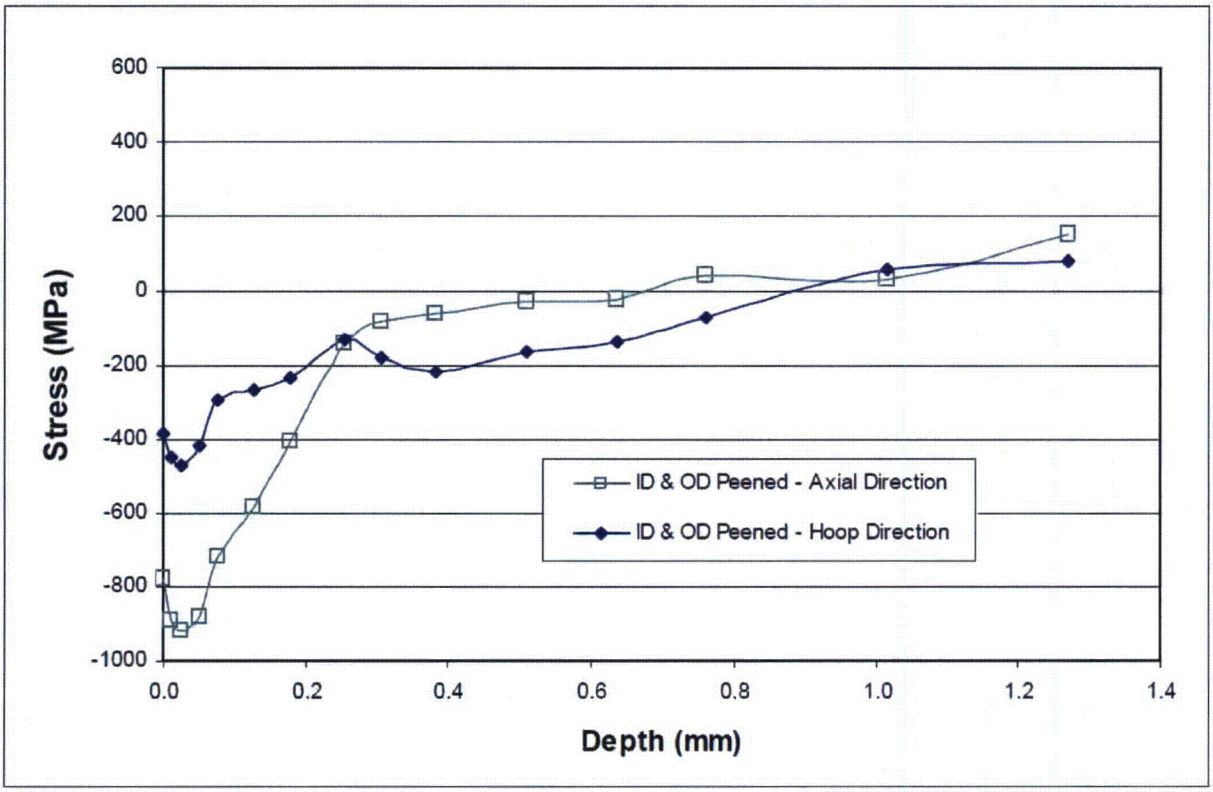

Figure A-42
Axial and hoop residual stress with depth measured from the OD of underwater laser peened Alloy 600 BMN-size pipes after OD and ID treatment (by Toshiba)

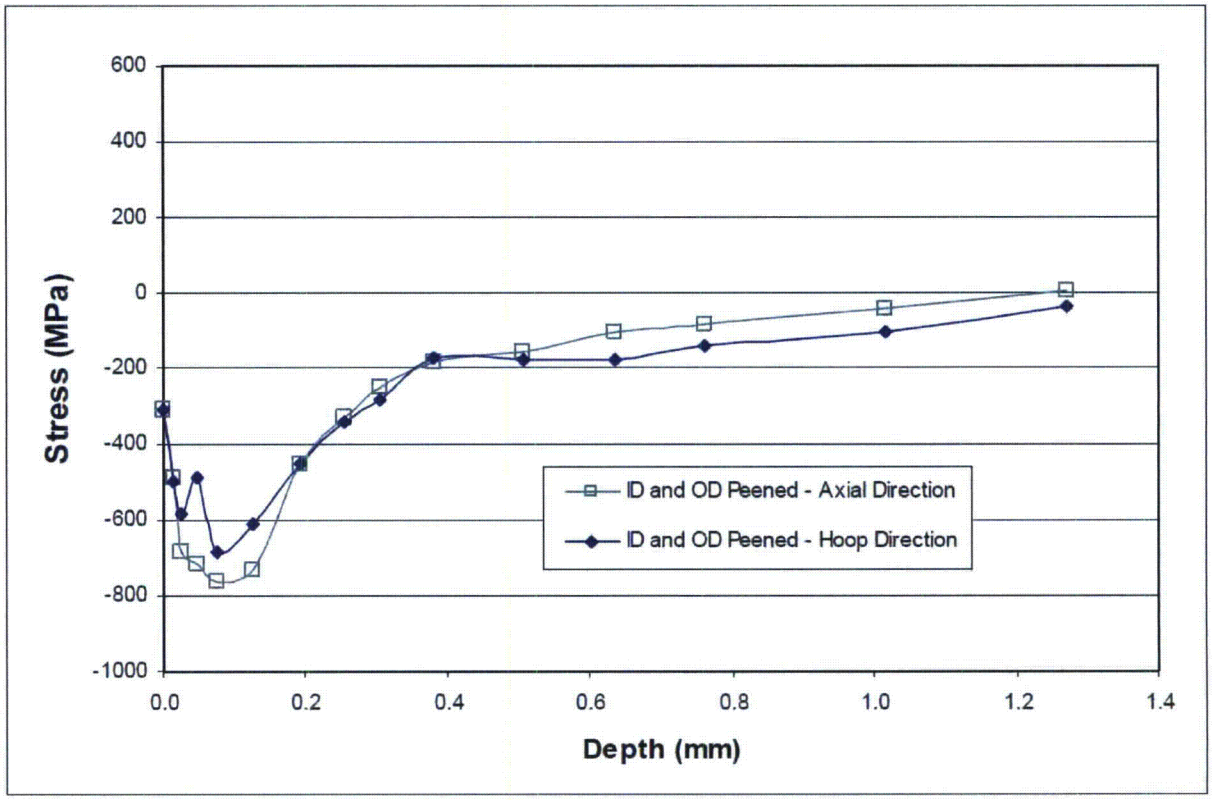

Figure A-43
Axial and hoop residual stress with depth measured from the ID of underwater laser peened Alloy 600 BMN-size pipes after OD and ID treatment (by Toshiba)

A.1.3.2 BMN Mock ups

The objective of this task was to verify that the treatment can be effective in a BMN mock-up configuration. This was previously published in MRP-162 [66], and it is reproduced here for convenience.

The specimens consisted of a generic J-groove mock-up configuration, as shown in Figure A-37. The mock-up was modeled from an instrumentation nozzle at the centerline of the vessel. This location allowed the weld preparation to be symmetrical and welding to be more consistent between the mock-ups designated for various surface treatments.

The base plate of the mock-up consisted of a 5 inch (13 mm) diameter carbon steel round stock bored out to accept a ½ inch Schedule 80 Alloy 600 pipe with a 0.005 to 0.010 inch (0.1 to 0.3 mm) diametrical clearance. The carbon steel hub surface was overlaid with ER309L weld material to simulate cladding. The overlay was ground flat to an overall thickness of 0.125 inches (3.2 mm).

The bore was prepared with the J-groove geometry shown in Figure A-37. The surface of the groove was buttered with a NiCrFe-3 (182) weld material prior to insertion of the pipe material. The 6 inch (152 mm) long schedule 80 pipe was inserted to allow 2 inches (51 mm) to extend above the J-groove. The pipe was manually welded with the shielded metal arc welding process

with NiCrFe-3 (182) weld material. The final weld was ground smooth (similar to preparation for dye-penetrant (PT) testing) and to blend with the pipe and overlay.

Peening was applied around the ID of the mock-up for a distance of at least two inches (51 mm). The two inch (51 mm) length for the ID was centered on the root of the J-groove weld. The OD of the mock-up was peened for a one inch (25 mm) height above the toe of the weld on the pipe side and for a one inch (25 mm) length from the toe of the weld on the carbon steel. Figure A-39 shows the area intended for surface treatment. As an example, underwater laser peening of the BMN mock-up is shown in Figure A-38.

The surface profile was measured on the OD and ID surfaces of the mock-up to a depth of 1.0 mm using XRD. The XRD "stress" measurement of the mock-up on the ID surface shows the difference from before to after surface treatment, but does not correspond to a true stress measurement result, as the mock-up had to be sectioned to access to the ID surface and no stress correction could be easily applied due to the complex geometry of the mock-up.

OD surface residual stress measurement results for the pipe and clad section of the mock-up and for the clad section and the weld area of the mock-up before underwater laser peening (ULP) are respectively shown in Figure A-44 and Figure A-45.

The OD hoop surface residual stress of the untreated mock-up is compressive around the pipe (between -76 and -49 MPa), compressive around the clad (between -575 and -417 MPa at 15 mm from the pipe and between -501 and -417 MPa at 20 mm from the pipe), and tensile around the weld (between 287 and 360 MPa).

Laser peening on the OD increased the OD compressive residual stress magnitude compared to the as received condition in the pipe and clad (at both 15 mm and 20 mm from the pipe). Specifically, the OD hoop surface residual stress of the mock-up after OD treatment only is between -531 and -450 MPa around the pipe, between -710 and -580 MPa around the clad at 15 mm from the pipe, and between -671 and -474 MPa around the clad at 20 mm from the pipe. No measurements were performed in the weld region after the OD treatment only.

Laser peening of the ID (after peening of the OD) increases the OD compressive residual stress magnitude compared to as received condition in the pipe and clad (at 15 mm, but not at 20 mm). Laser peening of the OD and then the ID modified the stress state from tensile to compressive in the weld region. The final OD hoop surface stress of the mock-up after both OD and ID treatment is between -500 and -467 MPa around the pipe, between -716 and -639 MPa around the clad at 15 mm from the pipe, between -699 and -335 MPa around the clad at 20 mm from the pipe, and between -338 and -91 MPa around the weld. In general, laser peening of the ID (after peening of the OD) resulted in OD compressive residual stress magnitudes close to the results for the OD treatment only. This can be attributed to the large "thickness" of the mock-up. The presence of one region of the weld with a relatively low OD residual stress of -91 MPa indicates that further optimization of the peening process would be desirable prior to use of the process on BMNs in domestic plants.

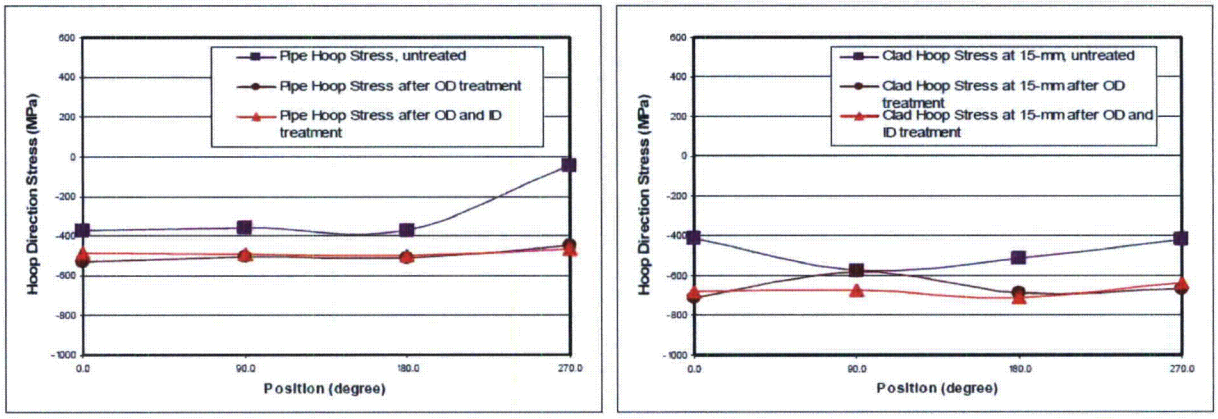

Figure A-44
OD surface residual stress measurements results for the pipe and clad section of the mock-up before underwater laser peening (ULP), after ULP on the OD, and after ULP on both the OD and ID (treated and measured by Toshiba)

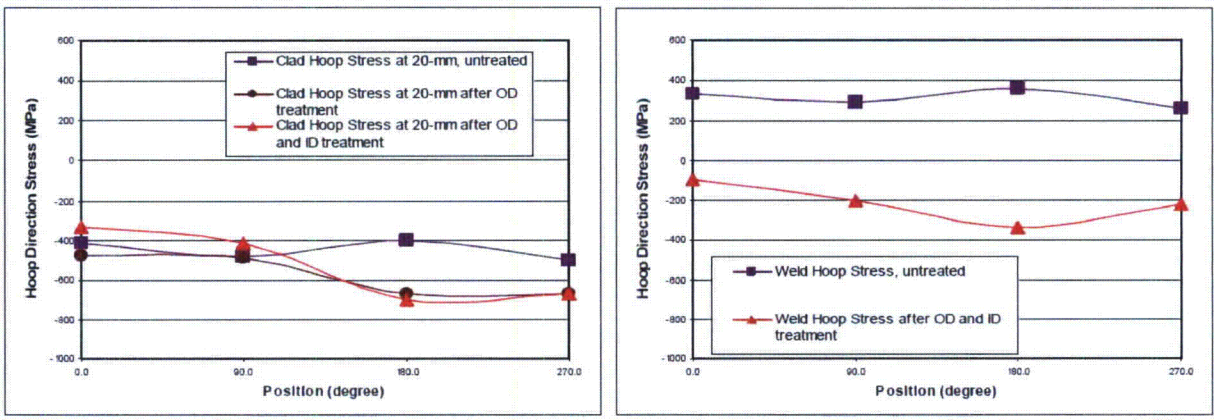

Figure A-45
OD surface residual stress measurements results for the clad section and the weld area of the mock-up before underwater laser peening (ULP), after ULP on the OD, and after ULP on both the OD and ID (treated and measured by Toshiba)

A.1.4 Reactor Mock up Experimentation performed by Hitachi-GE

Figure A-46 and Figure A-47 show the effect of water jet peening on the stresses of a small-diameter pipe ID such as that found in BMNs. To measure residual stress on the ID surface of the pipe with XRD, the specimen was divided into four sectors. Therefore, the measured data are more conservative compared to the surface of a non-divided pipe, due to the relaxation introduced by the cutting process. These test results demonstrate the capability of stress improvement by WJP.

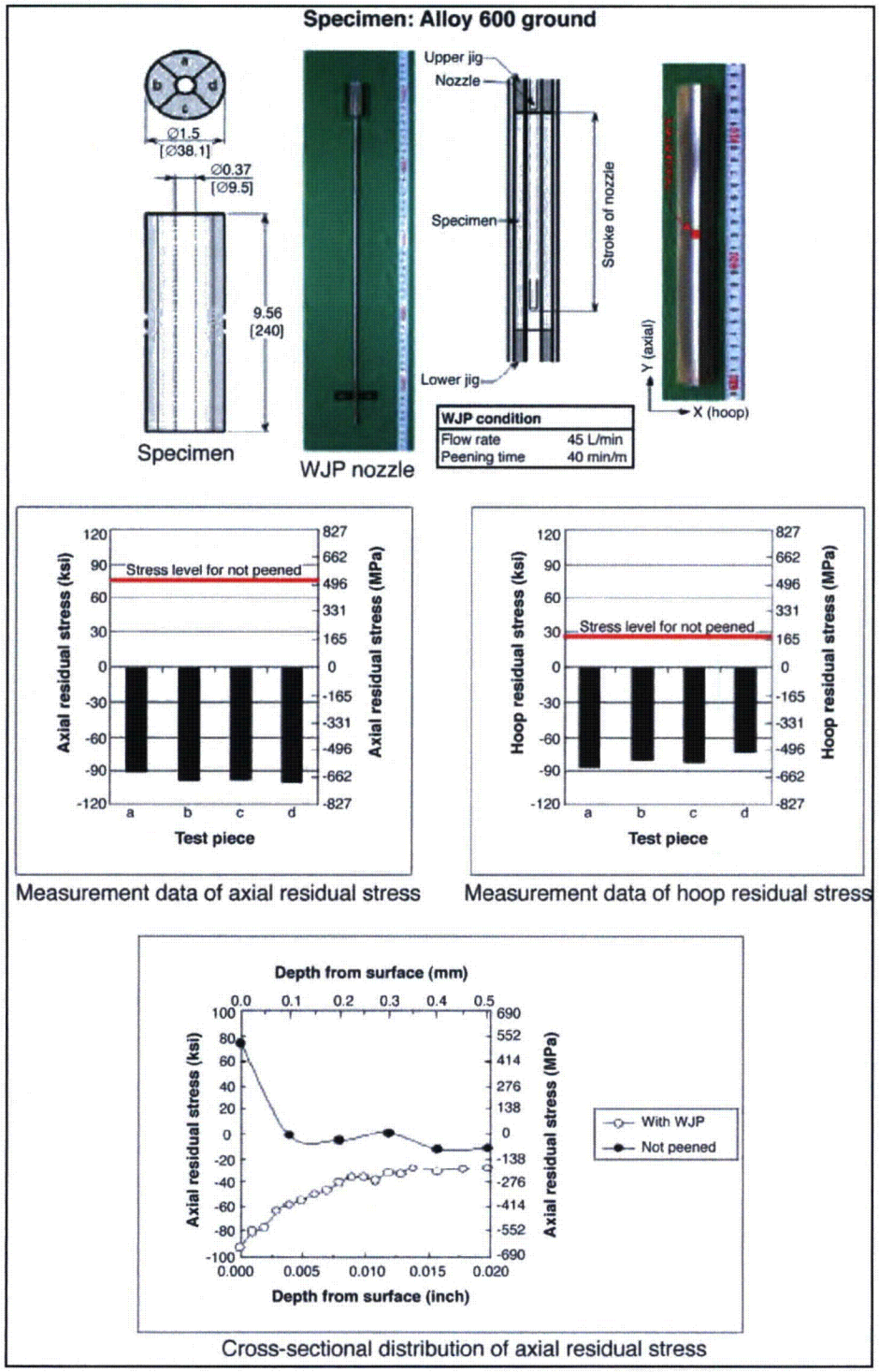

Figure A-46
Stress improvement with WJP (Alloy 600—Small Diameter Pipe ID(1/2)), by Hitachi-GE

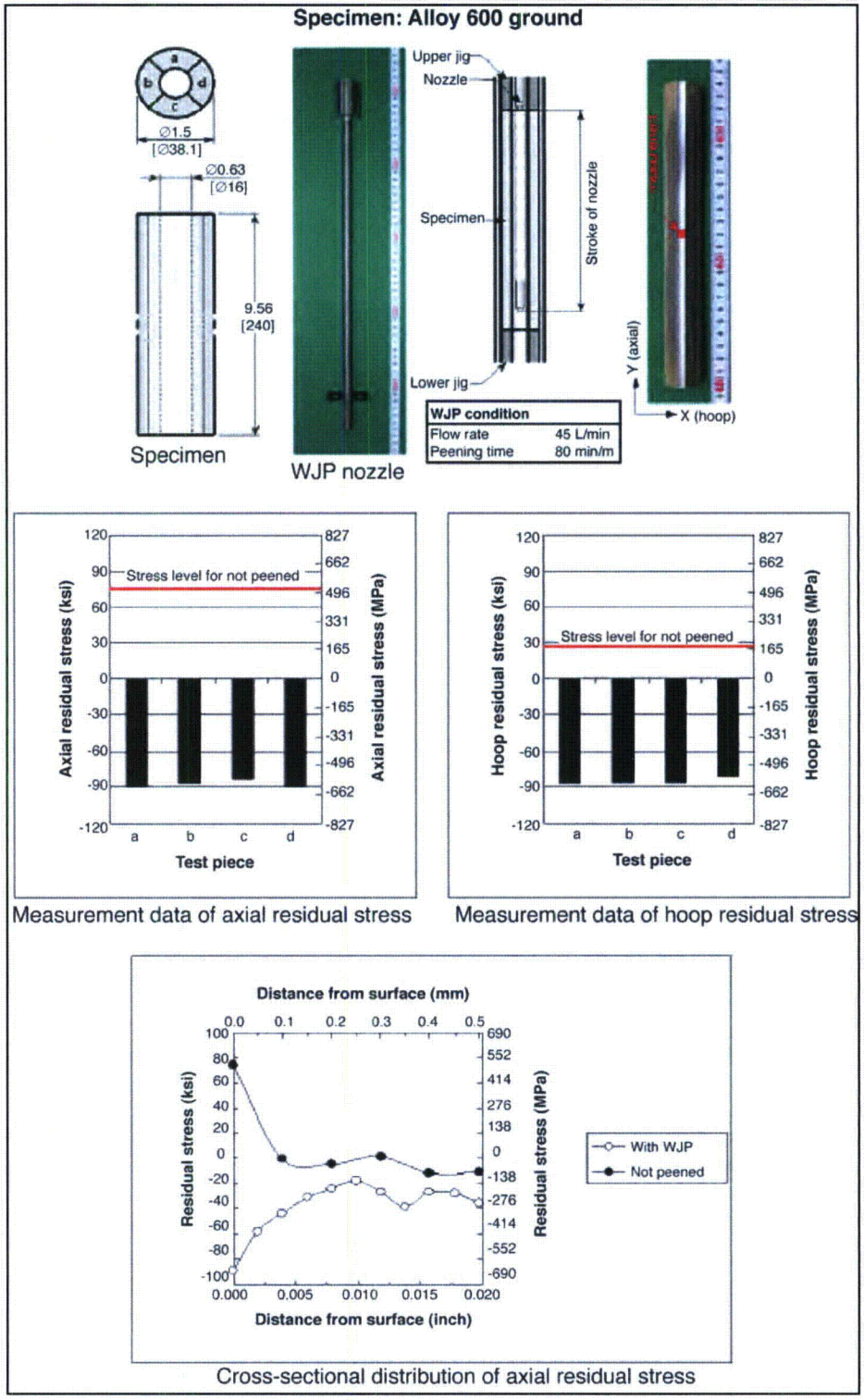

Figure A-47
Stress improvement with WJP (Alloy 600—Small Diameter Pipe ID(2/2)), by Hitachi-GE

Hitachi-GE also performed experiments to determine the applicability of water jet peening to variously shaped reactor internal parts. Since WJP utilizes water jet flow with numerous cavitations, the effective area is not limited to the area where the water jet directly hits but extends to adjacent areas where the water jet flow with effective cavitations reaches. Therefore, WJP can be applied not only to flat surfaces but also to the angular/round/3D shaped surfaces. The various geometric configurations that have been proven to be effectively mitigated by WJP are described in Figure A-48 through Figure A-51. The mockups were constructed from Type 304 stainless steel.

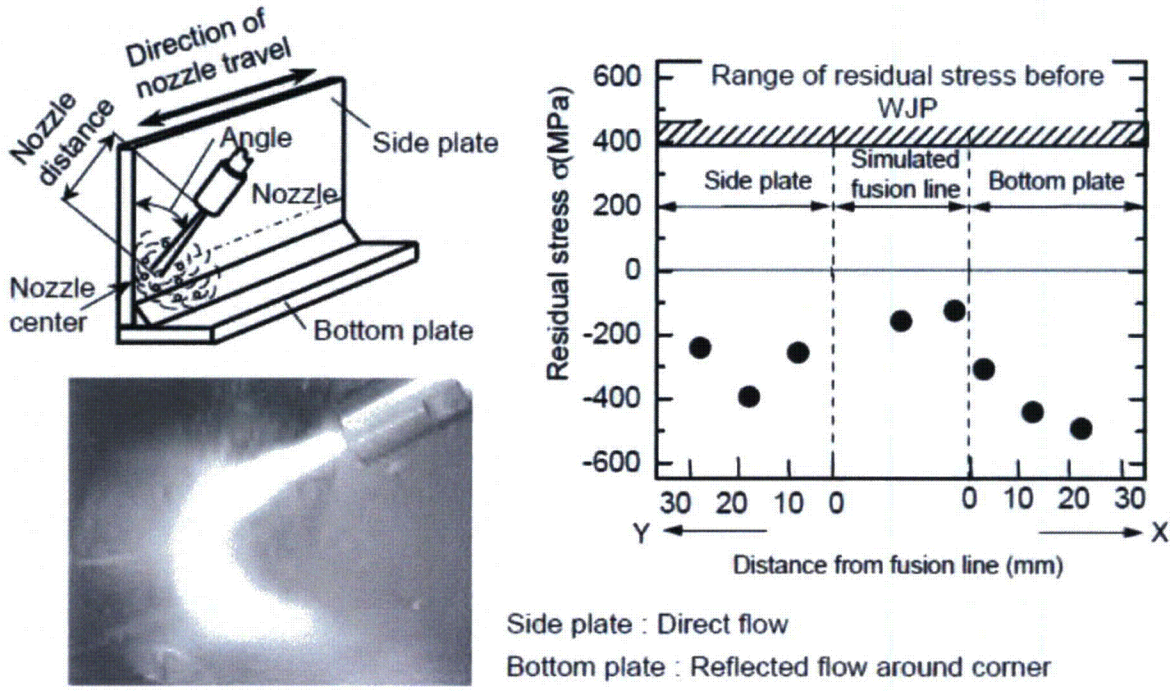

Figure A-48
WJP stress improvement effect at a corner location, provided by Hitachi-GE

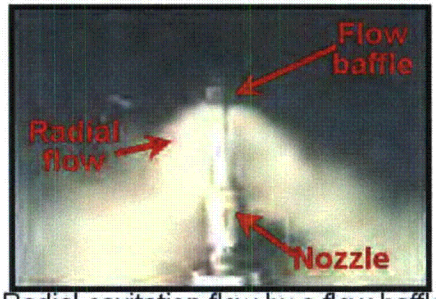

Radial cavitation flow by a flow baffle

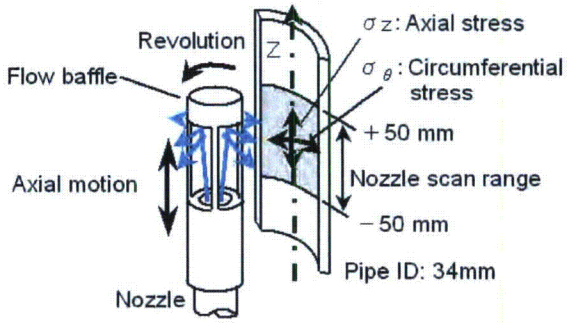

WJP procedure for small diameter pipe ID

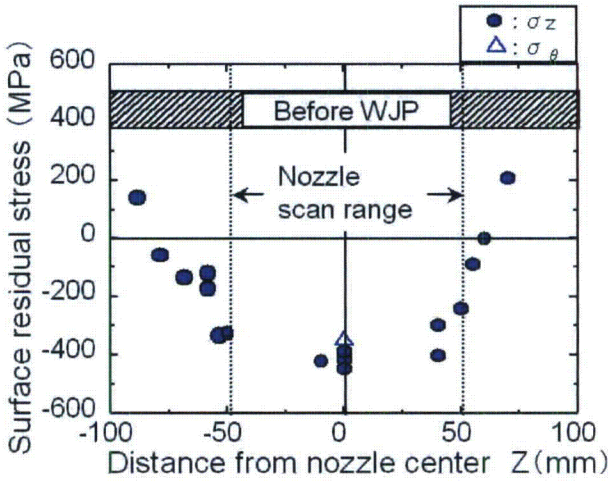

Stress distribution of pipe ID

Figure A-49
WJP stress improvement effect on pipe inner surface, provided by Hitachi-GE

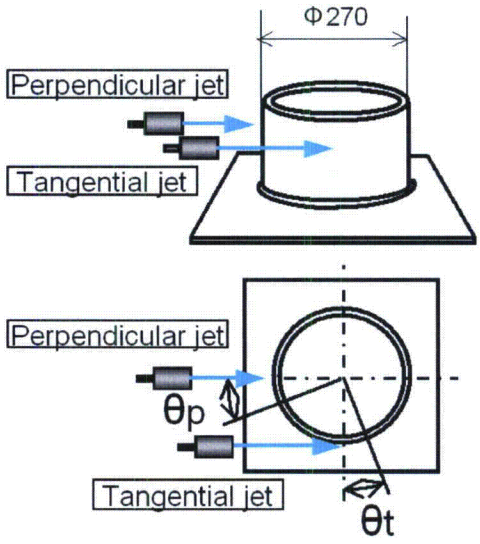

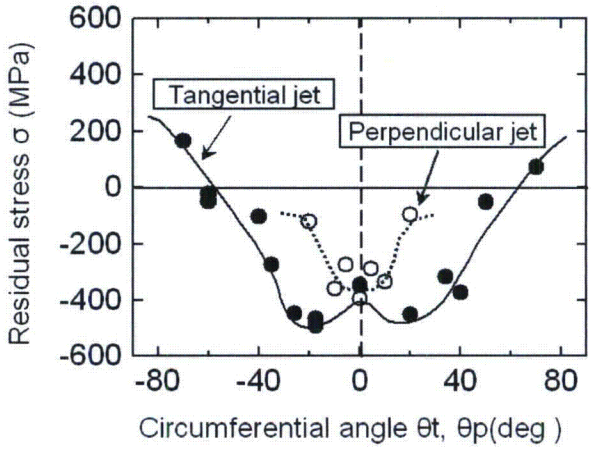

Residual stress distribution of outer diameter surface

Figure A-50
WJP stress improvement effect on pipe outer surface, provided by Hitachi-GE

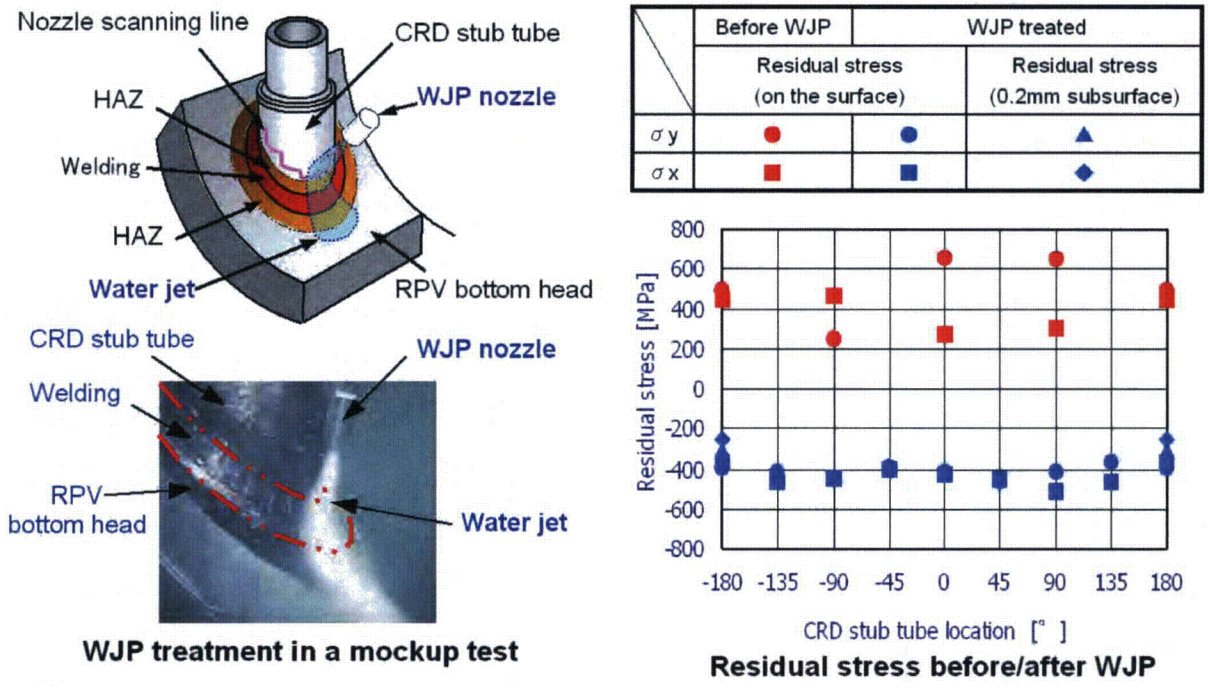

Figure A-51
WJP stress improvement effect on a BMN mockup, provided by Hitachi-GE

Figure A-48 shows WJP being applied to a test piece representing a corner and the resulting stress improvement. It should be noted that the residual stress was improved at the bottom plate, which was not directly jetted by the water. Figure A-49 shows another example of the effect on a pipe inner surface mitigation. In this process, WJP effectiveness was achieved in the nozzle scanned range. Figure A-50 shows the stress improvement effect as a result of WJP on a pipe outer surface. The test showed that residual stress improvement was achieved with the water jet nozzle pointed in both a perpendicular and tangential angle to the pipe outer surface. Figure A-51 shows the positive effect of WJP on a complex 3D shaped surface such as a BMN OD.

Since residual stress on surfaces of the operating reactor internal components cannot be measured, laboratory process and tooling qualification data are used to quantify the stress improvement that can be achieved on these components. HGNE measured the surface residual stress following WJP mitigation of an actual nuclear power plant component in Shika-2 (ABWR) of Hokuriku-EPCO, Japan during its construction. The result was a level of compression similar to that achieved in laboratory tests as shown in Figure A-52.

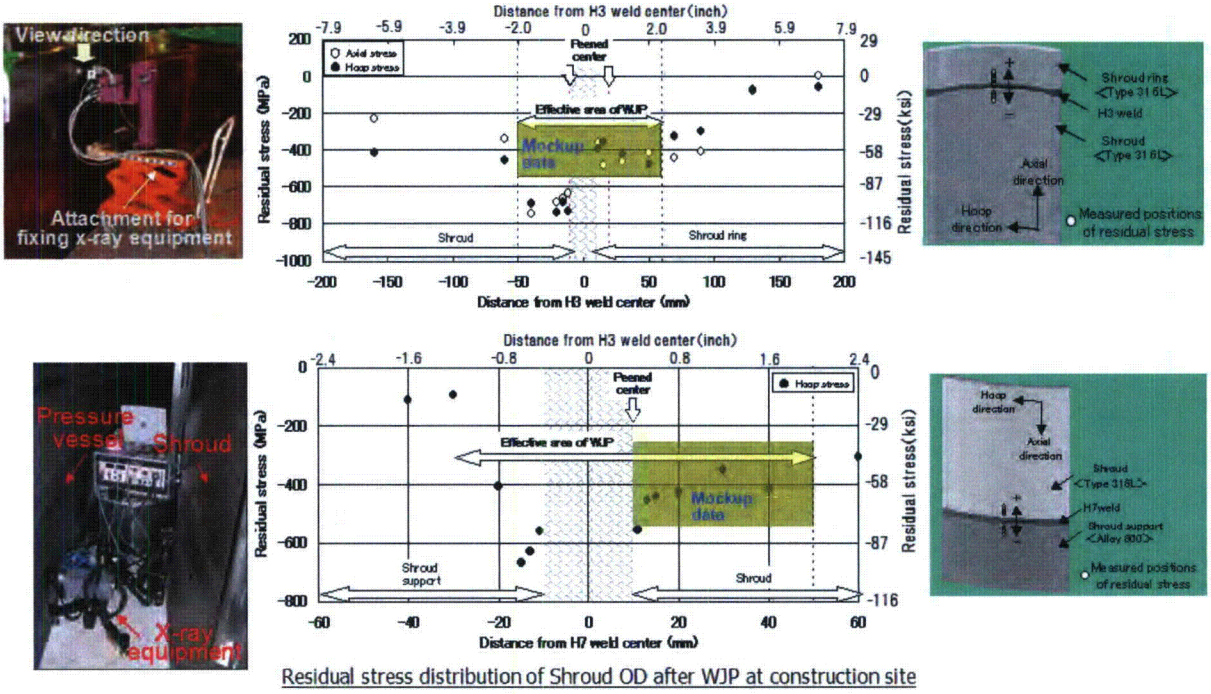

Residual stress distribution of Shroud OD after WJP at construction site

Figure A-52
Residual stress values on actual plant component compared with mockup residual stress measurements, provided by Hitachi-GE

A.1.5 Test Data on Peened ID BMN Mock-up performed by Mitsubishi

A.1.5.1 Description of BMN ID Mock-up Testing

Mitsubishi peened mock-ups for the BMN of a PWR, which were constructed so that the WJP process could be validated on a simulated component from a plant. The objective of these tests was to verify the effectiveness of WJP on a replica of actual components. The ID configuration was specially designed for the ID of the BMN components, therefore these tests provide confidence that results from the application of the WJP process in laboratory testing are indicative of the results obtained in the field. The mock-up specimens were fabricated from Alloy 600 tubing inserted into a plate and welded to simulate the penetration of the BMN through the shell of the reactor vessel. In total, four mock-up blocks were fabricated, two with a 16.0 mm ID hole in the tube and two with a 9.5 mm ID hole in the tube. The WJP process was applied using optimized parameter values as determined by Mitsubishi. Figure A-53 shows a schematic for the test blocks.

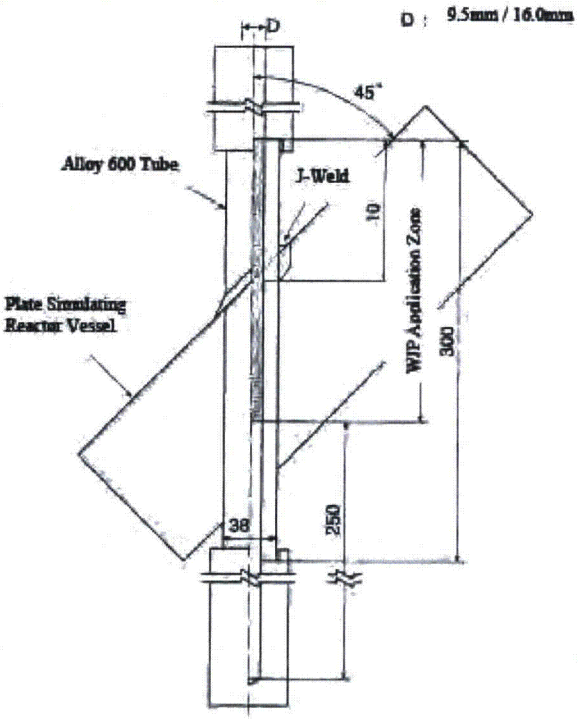

Figure A-53
Mock up Test Block Design, provided by Mitsubishi

The purpose of creating two sets of test blocks was so that one set could be maintained and examined in the as-fabricated condition and the other set subjected to the WJP application process. This allowed for a direct comparison between the samples. Unlike the previous laboratory testing, no artificial stress states were induced in the samples. The stresses created were due to the welding process as is the case for the real components within a reactor vessel. After application of the WJP process, all four samples, the two which were left in the as-welded condition as well as the two which underwent the WJP process, were examined by visual inspection and PT inspections to verify the material integrity. Examples of the test results are shown in subsequent sections. In addition, residual stress measurements were made using strain gauges and the x-ray diffraction method. X-ray diffraction measurements were made at depths of 0.1 mm, 0.2 mm, 0.3 mm, 0.4 mm, and 0.5 mm at three different locations on each tube as shown in Figure A-54. The results and conclusions from these tests are presented in Sections A.1.5.2 to A.1.5.3.

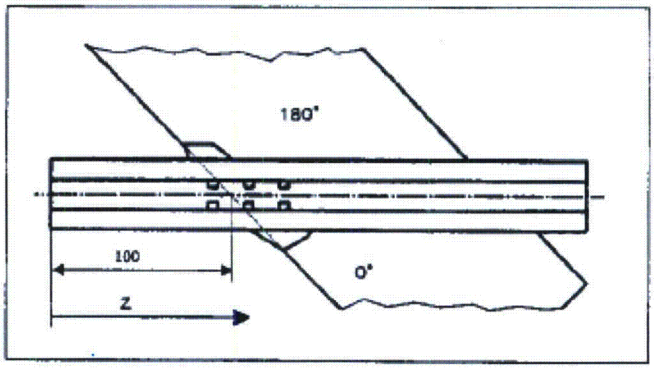

Figure A-54
Locations of Residual Stress Measurements, provided by Mitsubishi

A.1.5.2 Results of BMN ID Mock-up Testing

Table A-3 presents the data from the testing for the mock-up using the 9.5 mm ID tube in the state before the WJP treatment was applied. Figure A-55 and Figure A-56 show the resulting trends of residual stress against axial position and depth below the treated surface.

Table A-3
Residual Stress Measurements from Validation Test for ID Configuration – 9.5 mm ID before WJP, provided by Mitsubishi

Coupon Config.	Tube ID (mm)	WJP process	Measurement Location		Residual Stress (MPa)						
					Strain Gauge (A)		X-ray @ 0.5mm (B)			Residual (A+B)	
			Degrees	Axial (mm)	Axial	Hoop	Depth	Axial	Hoop	Axial	Hoop
Mock-up	9.5	Non-Peened (Initial Material State)	0°	90	202	378	0.00	-125	-29	77	349
							0.51	-52	30	150	408
				110	120	376	0.00	-50	30	70	406
							0.10	-46	28	74	404
							0.20	-52	33	68	409
							0.31	-67	30	53	406
							0.39	-71	25	49	401
							0.50	-87	18	33	394
				129	-28	43	0.00	103	146	75	189
							0.50	41	58	13	101
			180°	90	56	372	0.00	-107	-141	-51	231
							0.49	-88	-91	-32	281
				110	195	417	0.00	-64	-77	131	340
							0.11	-56	-69	139	348
							0.20	-48	-29	147	388
							0.30	-37	-31	158	386
							0.41	-32	-20	163	397
							0.52	-36	-22	159	395
				129	3	-2	0.00	-36	-32	-33	-34
							0.49	6	2	9	0

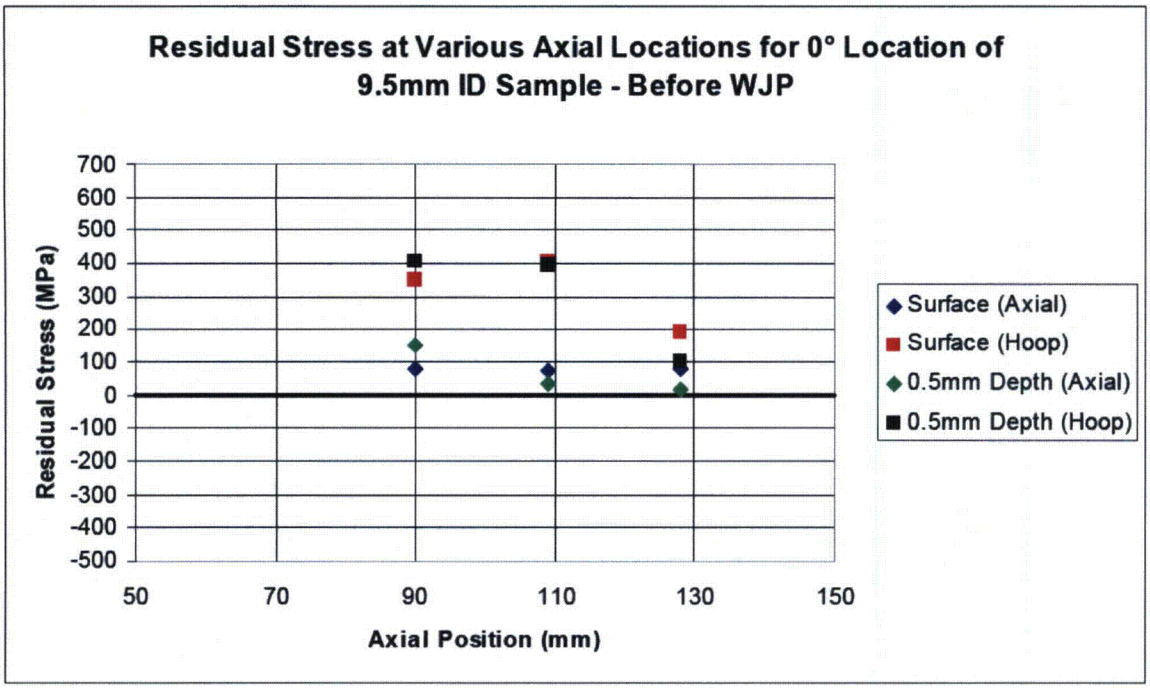

Figure A-55
Residual Stress at Axial Locations for 0° on 9.5 mm ID Sample – Before WJP, provided by Mitsubishi

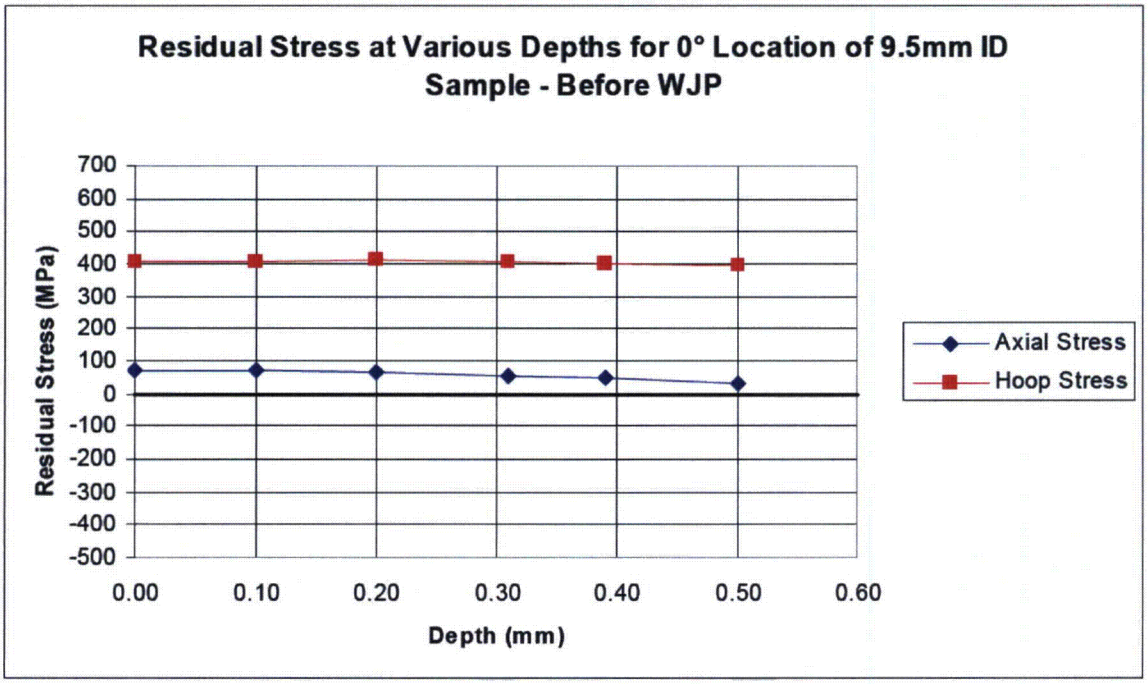

Figure A-56
Residual Stress at Various Depths for 0° Location on 9.5 mm Sample – Before WJP, provided by Mitsubishi

Table A-4 presents the data from the testing for the mock-up using the 9.5 mm ID tube after the WJP treatment has been applied. Figure A-57 and Figure A-58 show the resulting trends of residual stress against axial position and depth below the treated surface.

Table A-4
Data from Validation Test for ID Configuration – 9.5 mm ID, provided by Mitsubishi

Coupon Config.	Tube ID (mm)	WJP process	Measurement Location		Residual Stress (MPa)						
					Strain Gauge (A)		X-ray @ 0.5mm (B)			Residual (A+B)	
			Degrees	Axial (mm)	Axial	Hoop	Depth	Axial	Hoop	Axial	Hoop
Mock-up	9.5	Peened (Minimum WJP Effect)	0°	90	26	102	0.00	-449	-383	-423	-281
							0.51	-203	-213	-177	-111
				109	87	121	0.00	-434	-434	-347	-313
							0.10	-363	-341	-276	-220
							0.20	-211	-295	-124	-174
							0.31	-174	-235	-87	-114
							0.39	-194	-203	-107	-82
							0.50	-117	-140	-30	-19
				128	-49	112	0.00	-409	-327	-458	-215
							0.52	-137	-209	-186	-97
			180°	90	-128	131	0.00	-407	-389	-535	-258
							0.51	-129	-175	-257	-44
				110	108	180	0.00	-479	-449	-371	-269
							0.09	-362	-352	-254	-172
							0.19	-337	-311	-229	-131
							0.32	-261	-245	-153	-65
							0.42	-215	-225	-107	-45
							0.50	-201	-204	-93	-24
				129	-57	0	0.00	-362	-381	-419	-381
							0.51	-183	-202	-240	-202

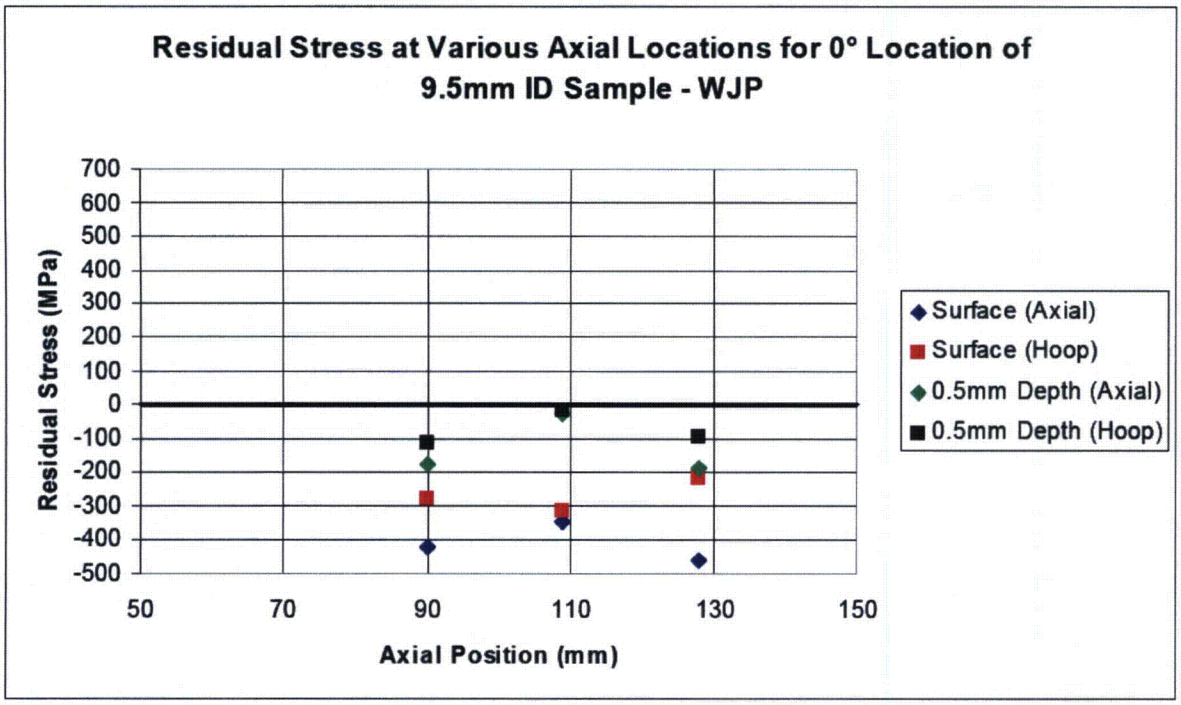

Figure A-57
Residual Stress at Axial Locations for 0° Location on 9.5 mm Sample – WJP, provided by Mitsubishi

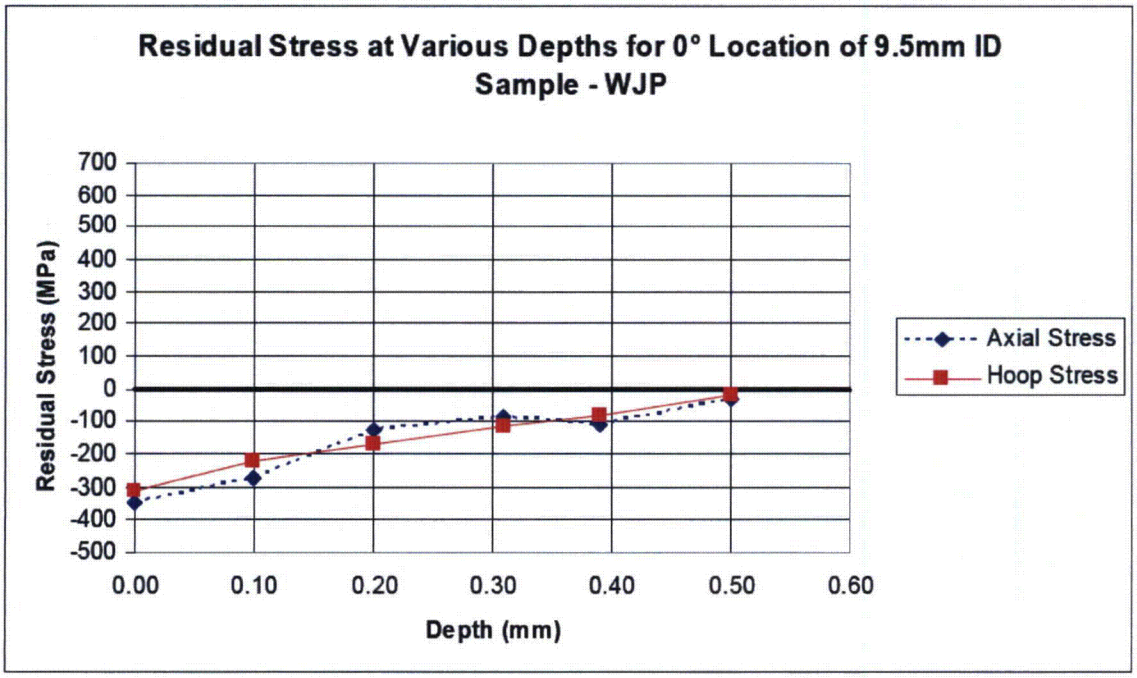

Figure A-58
Residual Stress at Various Depths for 0° Location on 9.5 mm Sample – WJP, provided by Mitsubishi

Table A-5 presents the data from the testing for the mock-up using the 16.0 mm ID tube in the state before the WJP treatment was applied. Residual stress levels and trends are similar to those for the 9.5 mm ID tube.

Table A-5
Data from Validation Test for ID Configuration – 16.0 mm before WJP, provided by Mitsubishi

Coupon Config.	Tube ID (mm)	WJP process	Measurement Location		Residual Stress (MPa)						
					Strain Gauge (A)		X-ray @ 0.5mm (B)			Residual (A+B)	
			Degrees	Axial (mm)	Axial	Hoop	Depth	Axial	Hoop	Axial	Hoop
Mock-up	16.0	Non-Peened (Initial Material State)	0°	90	284	435	0.00	58	-73	342	362
							0.51	-11	-64	273	371
				109	183	448	0.00	73	12	256	460
							0.10	59	19	242	467
							0.20	42	35	225	483
							0.31	26	56	209	504
							0.39	5	71	188	519
							0.50	-23	82	160	530
				128	103	276	0.00	55	5	158	281
							0.49	-77	-48	26	228
			180°	90	64	146	0.00	-50	-125	14	21
							0.51	-77	-63	-13	83
				110	110	478	0.00	-46	-32	64	446
							0.09	-40	-39	70	439
							0.20	-37	-42	73	436
							0.30	-41	-49	69	429
							0.41	-33	-53	77	425
							0.51	-25	-52	85	426
				129	126	196	0.00	85	111	211	307
							0.50	63	95	189	291

Table A-6 presents the data from the testing for the mock-up using the 16.0 mm ID tube after the WJP treatment has been applied. Residual stress levels and trends are similar to those observed in the testing of the 9.5 mm ID tube. The data from Table A-5 and Table A-6 are plotted in Figure A-59.

Table A-6
Data from Validation Test for ID Configuration – 16.0 mm ID, provided by Mitsubishi

Coupon Config.	Tube ID (mm)	WJP process	Measurement Location		Residual Stress (MPa)							
					Strain Gauge (A)		X-ray @ 0.5mm (B)			Residual (A+B)	
			Degrees	Axial (mm)	Axial	Hoop	Depth	Axial	Hoop	Axial	Hoop
Mock-up	16.0	Peened (Minimum WJP Effect)	0°	90	90	142	0.00	-443	-463	-353	-321
							0.51	-173	-204	-83	-62
				109	48	208	0.00	-412	-598	-364	-390
							0.10	-361	-454	-313	-246
							0.20	-312	-450	-264	-242
							0.31	-329	-394	-281	-186
							0.39	-218	-315	-170	-107
							0.50	-166	-228	-118	-20
				130	36	100	0.00	-352	-408	-316	-308
							0.49	-143	-143	-107	-43
			180°	89	31	188	0.00	-343	-465	-312	-277
							0.50	-143	-203	-112	-15
				110	93	102	0.00	-467	-506	-374	-404
							0.10	-398	-458	-305	-356
							0.20	-362	-440	-269	-338
							0.31	-302	-349	-209	-247
							0.39	-288	-208	-195	-106
							0.50	-224	-178	-131	-76
				129	67	83	0.00	-402	-401	-335	-318
							0.49	-143	-163	-76	-80

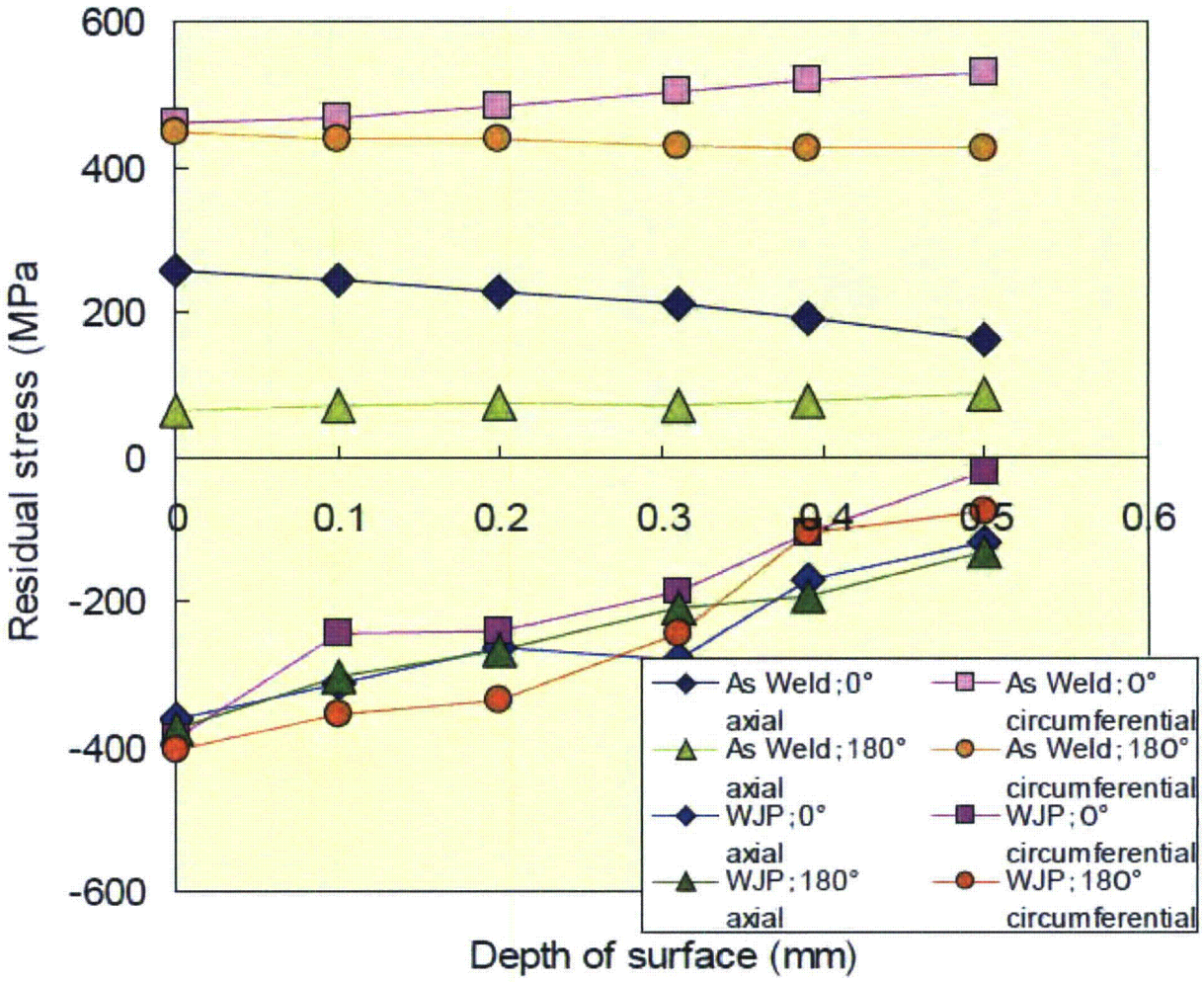

Figure A-59
Results of validation test for cross-section residual stress improvement effect on the BMN inner surface mockup, provided by Mitsubishi [67]

Surface integrity was evaluated on samples in this test group by visual and PT inspections. No surface distress or PT indications were found, as shown in Figure A-60. For these test samples, microstructural evaluations were also performed, at cross-section locations as shown in Figure A-61. A typical tube microstructure is illustrated in Figure A-62 and shows no grain distortion or evidence of excessive cold work at the surface.

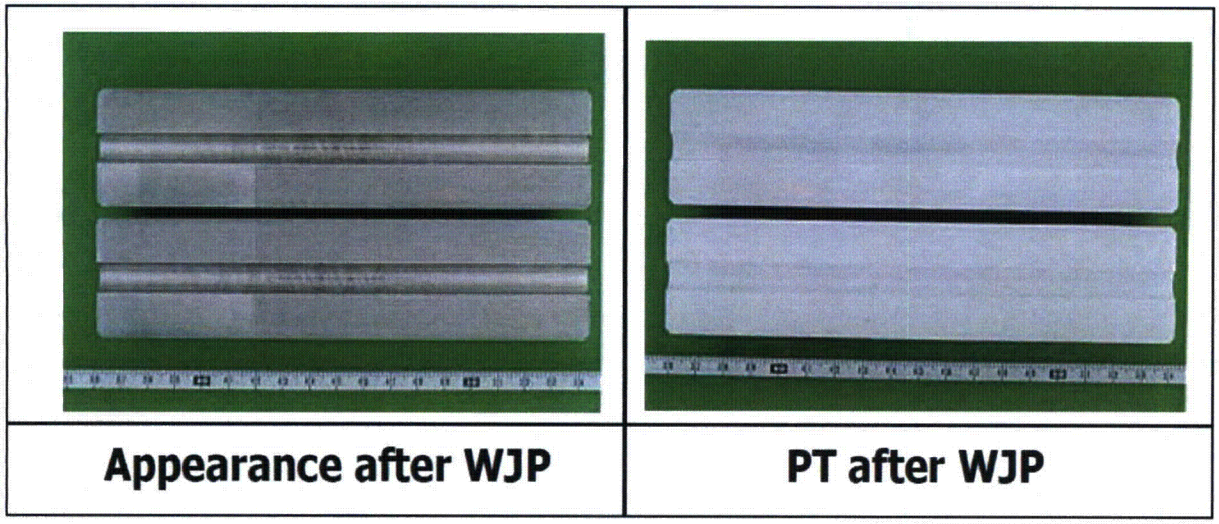

Figure A-60
Visual testing and penetrant testing after WJP on the BMN inner surface mockup, provided by Mitsubishi [67]

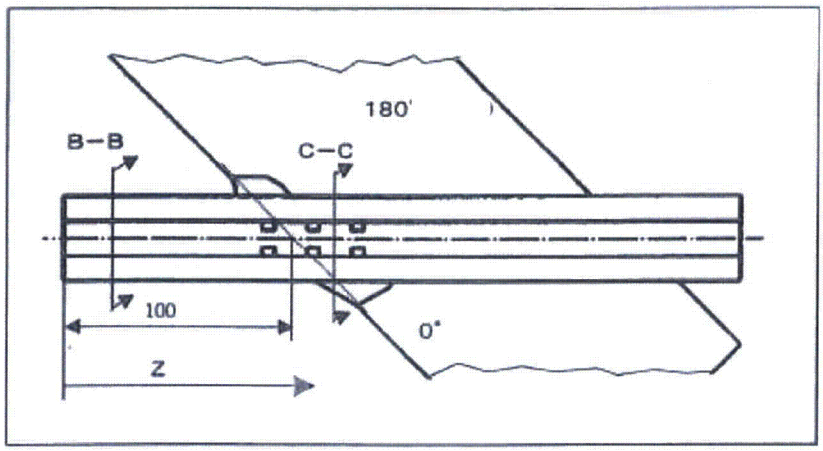

Figure A-61
Location of Microstructure Examinations, provided by Mitsubishi

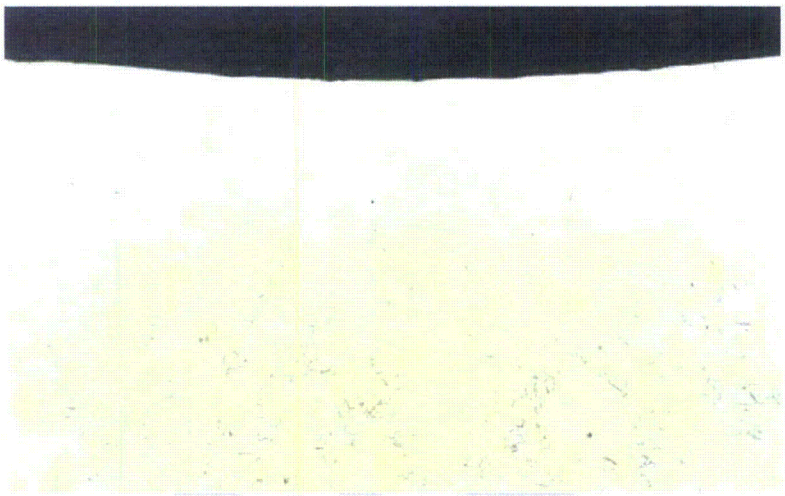

Figure A-62
Microstructure Examination for ID Configuration Mock-up Test – 9.5 mm ID C-C (100×), provided by Mitsubishi

A.1.5.3 Discussion of BMN ID Mock-up Testing

From the various data presented in the previous section the effect of the WJP treatment can clearly be seen. In the samples where the WJP treatment was not applied, substantial residual tensile stresses were present in the material. After the WJP treatment, all residual stresses of the treated areas were found to be compressive to a depth of at least 0.5 mm. Also, these tests proved that, under ideal application conditions, the WJP process is both effective and does not harm the material integrity nor cause any adverse effects to the materials which are treated. This was shown by the post treatment visual inspections, which showed the test blocks to be pristine and by the PT inspections which showed no recordable defects.

The evidence from the cross-sectional metallography is that the amount of cold work induced by WJP is relatively small, since no microstructural damage is observed at this level of examination.

This set of validation tests suggests that the parameters determined by laboratory testing are sufficient to produce the desired effect in a full scale validation test using mock-up test blocks without compromising material integrity or causing any adverse effect to the materials. These tests demonstrate that as long as the pre-mitigated components in the field are well represented by the samples used in this demonstration, the WJP process will be capable of inducing a layer of compressive residual stress at the surface of the components to a depth of 0.5 mm for the ID configuration of the WJP process.

A.1.6 Test Data on Peened OD/J-groove weld of a BMN Mock-up performed by Mitsubishi

A.1.6.1 Description of BMN OD/J-groove weld Mock-up Testing

A common configuration for components in a PWR is the situation where a tube penetrates a large radius surface. This occurs for components such as a BMN. The WJP process is well suited to be able to apply the treatment to such components on both the tube OD and the large-radius

surface. This requires that two configurations of the WJP equipment be used. This series of testing was conducted to ensure and verify that these components can be reliably treated. These tests were completed using process control parameters which would also be used in a production setting. The parameters selected represent the minimum settings which are still guaranteed to deliver the desired WJP effect on the materials. These parameters were previously determined from testing. These tests were carried out by first applying the tube OD configuration process to the tube surface, then using the large-radius configuration to treat the weld and large-radius surfaces.

The test coupon used in this testing is a mock-up of the BMN for a typical PWR. It is composed of a 38 mm OD Alloy 600 tube which penetrates and is welded to a plate of low alloy steel with 304 stainless steel cladding using an Alloy 132 weld. Figure A-63 shows the schematic of the test coupon. Figure A-64 and Figure A-65 show how the water jet peening process was applied to the test coupon.

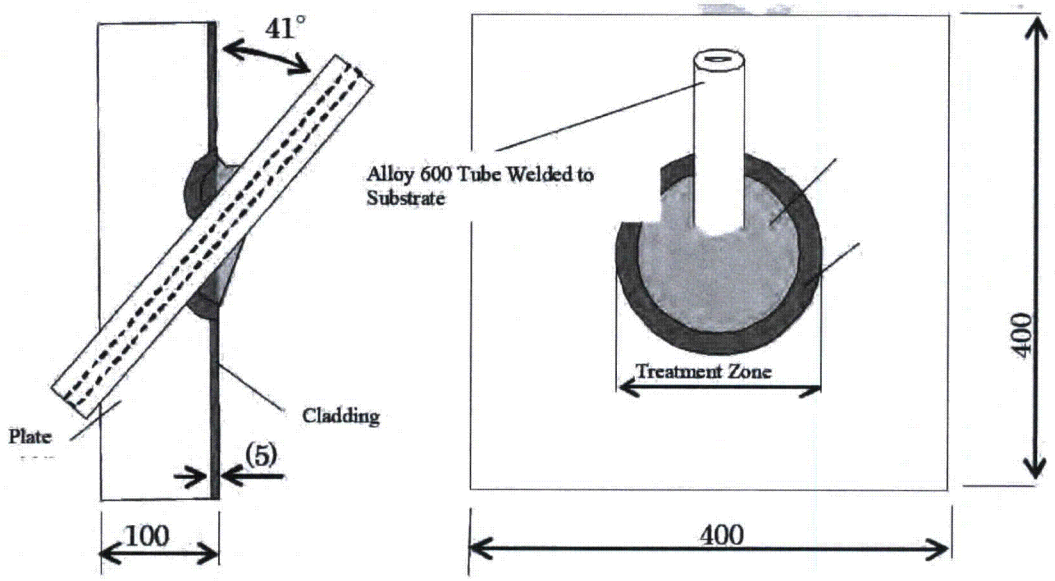

Figure A-63
Test Coupon Schematic for BMN Verification Testing, provided by Mitsubishi

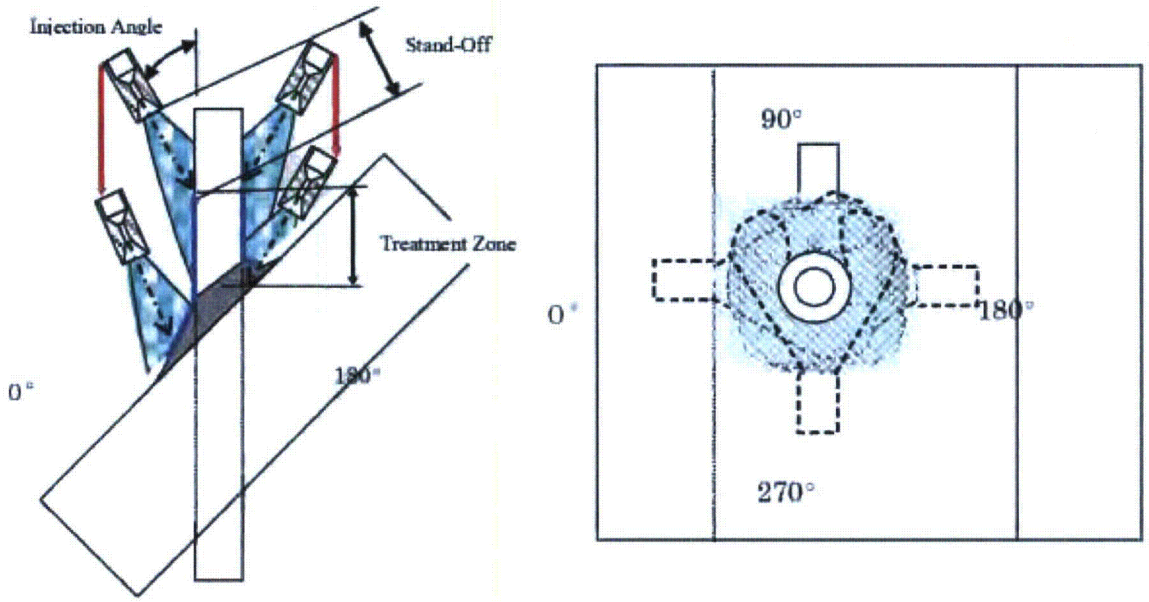

Figure A-64
WJP Application using the Tube OD Configuration, provided by Mitsubishi

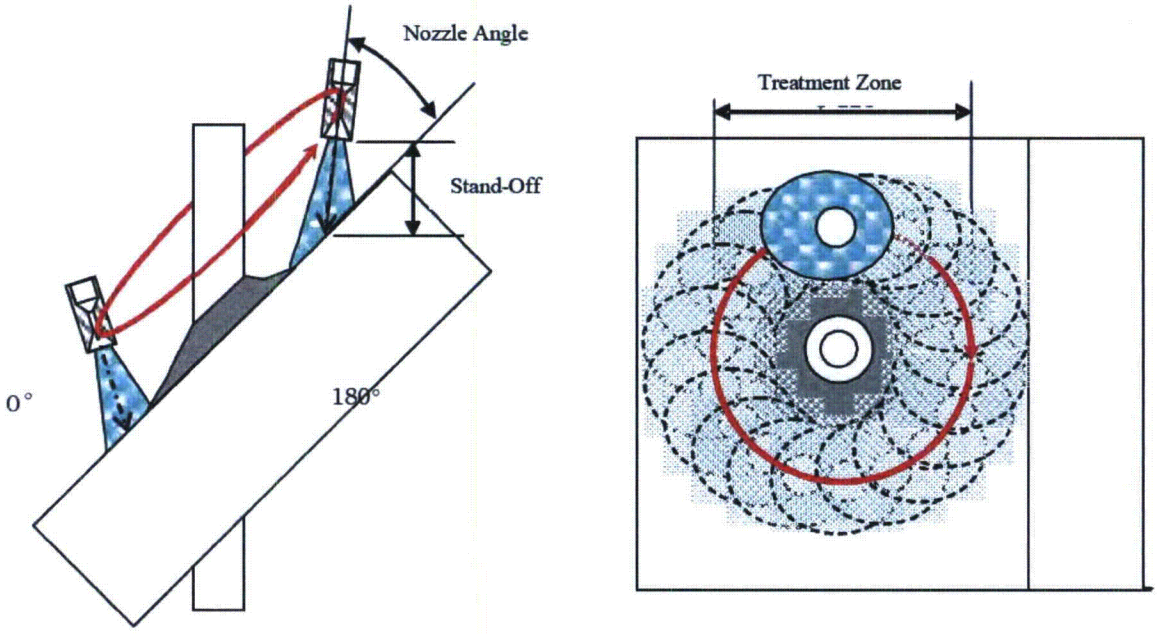

Figure A-65
WJP Application using the Large-Radius Surface Configuration, provided by Mitsubishi

Residual stress measurements were taken on both a sample that did not undergo the WJP process as well as a post-treatment sample to verify the effect of the WJP process. Measurements were

taken at 5 circumferential locations on the tube OD: 0°, 45°, 90°, 135°, and 180°. At each circumferential location, measurements were taken at 6 different depths. As well, residual stress measurements were taken on the surface of the J-groove weld at each circumferential location on the surface of the weld metal as well as the surrounding cladding on the base metal plate. Figure A-66 shows the locations of the residual stress measurements. Material surface integrity was verified by post-treatment visual and PT inspections. In addition to this normal suite of tests, stress corrosion tests were performed on a WJP-treated and a non-treated mock-up.

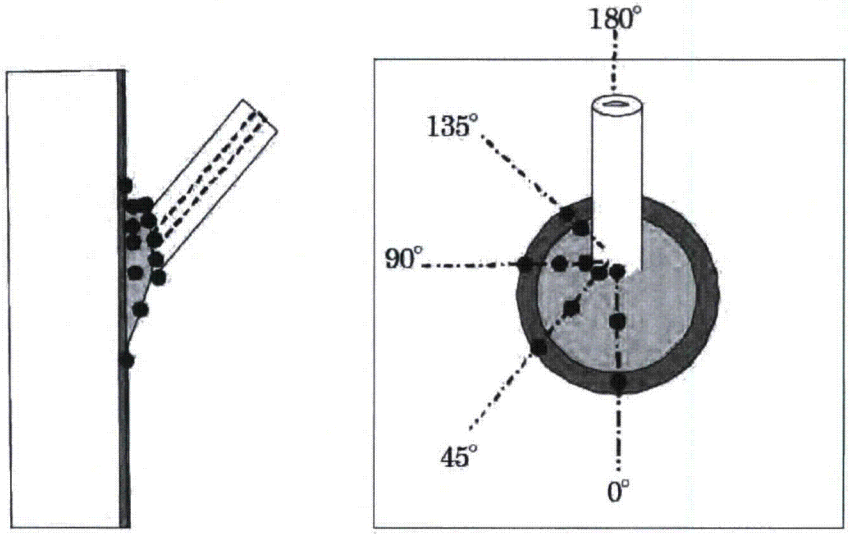

Figure A-66
Location of Residual Stress Measurements, provided by Mitsubishi

A.1.6.2 Results of BMN OD/J-groove weld Mock-up Testing

The residual stress measurements are tabulated for the OD of the tube, the J-groove weld surface, and the base metal cladding in Table A-7 and Table A-8. Representative depth profiles, Figure A-67 and Figure A-68, show that stress mitigation is achieved to a depth of at least 1 mm on the Tube OD. Surface residual stress measurements, Figure A-69 and Figure A-70, show that uniform mitigation is achieved in both the J-groove weld and base-metal cladding at all angular positions around the tube.

Table A-7
Residual Stresses for BMN Verification Testing – OD Tube Surface, provided by Mitsubishi

Coupon Config.	WJP process	Measurement Location		Residual Stress (MPa) X-ray Diffraction	
		Location	Depth (mm)	Axial	Hoop
BMN Mock-up	Peened (Minimum WJP Effect)	0°	0.00	-494	-354
			0.27	-381	-397
			0.51	-379	-335
			0.80	-327	-292
			1.02	-282	-247
			1.29	-273	-205
		45°	0.00	-459	-494
			0.22	-361	-389
			0.53	-346	-369
			0.78	-159	-305
			1.04	-158	-252
			1.28	-91	-151
		90°	0.00	-447	-415
			0.25	-372	-398
			0.52	-234	-262
			0.79	-144	-198
			1.03	-96	-77
			1.30	-44	0
		135°	0.00	-447	-396
			0.29	-340	-.69
			0.50	-300	-324
			0.79	-184	-202
			1.01	-72	-110
			1.28	-40	-35
		180°	0.00	-348	-215
			0.24	-281	-308
			0.54	-260	-276
			0.80	-158	-193
			1.03	-138	-180
			1.31	-52	-116

Table A-8
Residual Stresses for BMN Verification Testing – Large Radius Surfaces, provided by Mitsubishi

Coupon Config.	WJP process	Measurement Location		Residual Stress (MPa) X-ray Diffraction	
		Location	Circ. (°)	Axial	Hoop
BMN Mock-up	Peened (Minimum WJP Effect)	Surface of Weld	0	-526	-364
			45	-421	-329
			90	-469	-315
			135	-525	-384
			180	-483	-543
		Surface of Base Metal	0	-223	-319
			45	-278	-193
			90	-293	-253
			135	-247	-194
			180	-283	-271
BMN Mock-up	Non-Peened (Initial Material State)	Surface of Weld	0	337	145
			45	267	50
			90	206	65
		Surface of Base Metal	0	-61	126
			45	202	11
			90	408	46
			135	450	-

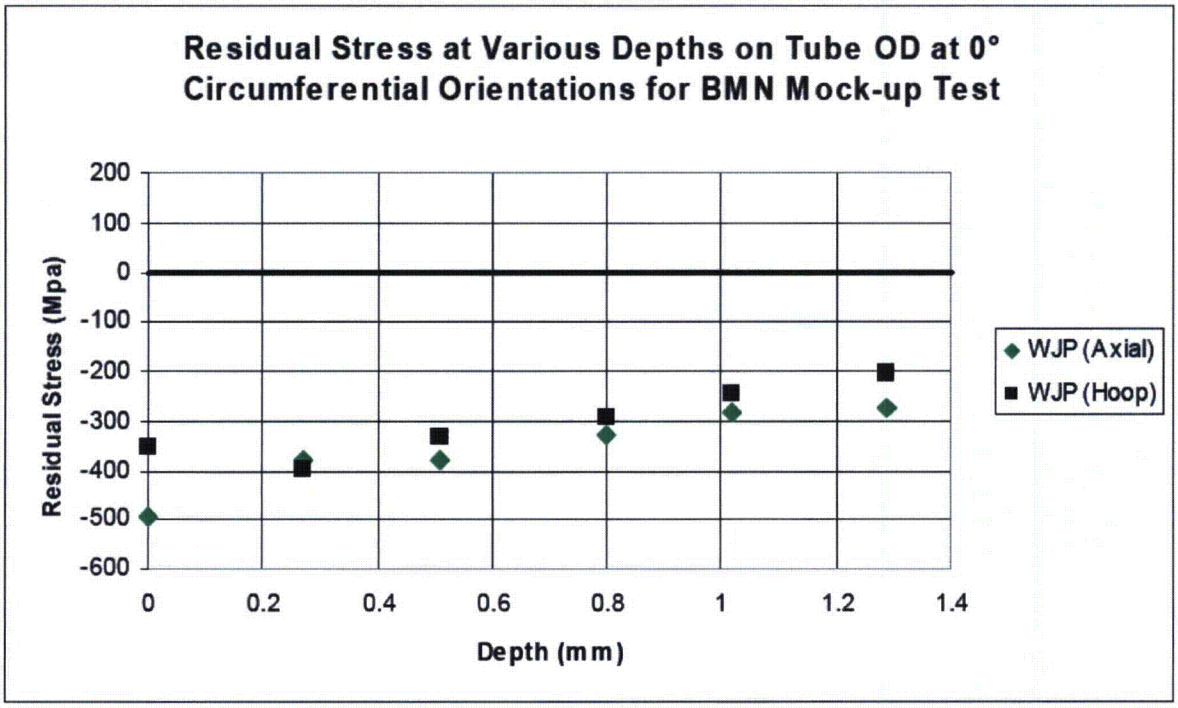

Figure A-67
Residual Stress Results for BMN Mock-Up Test – Tube OD at 0° Location, provided by Mitsubishi

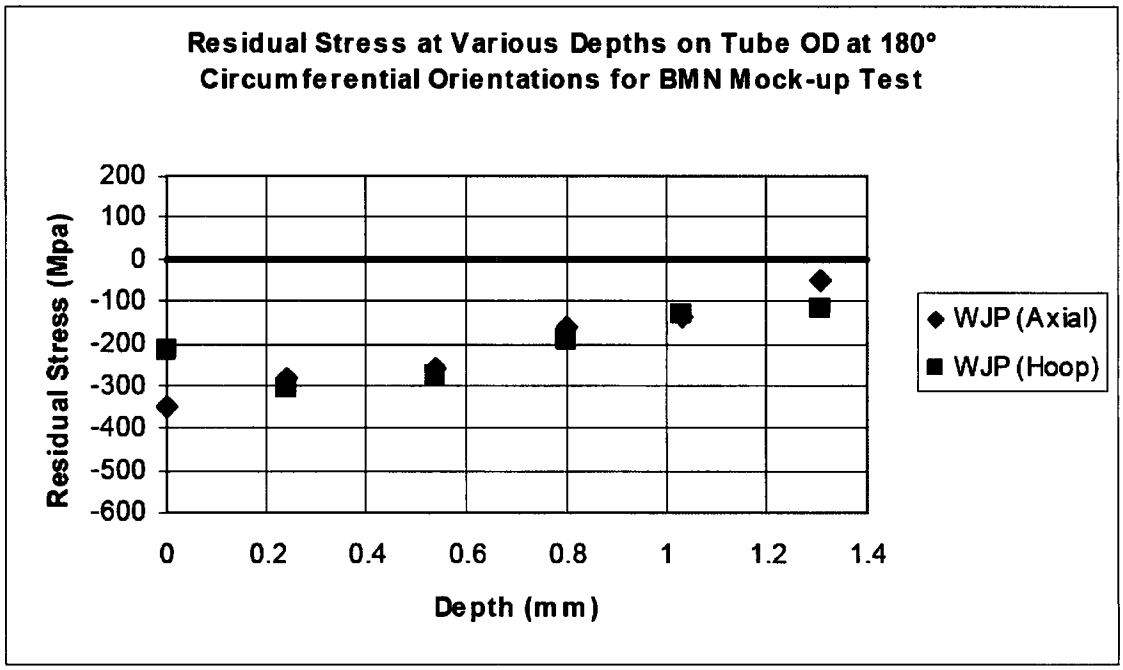

Figure A-68
Residual Stress Results for BMN Mock-Up Test – Tube OD at 180° Location, provided by Mitsubishi

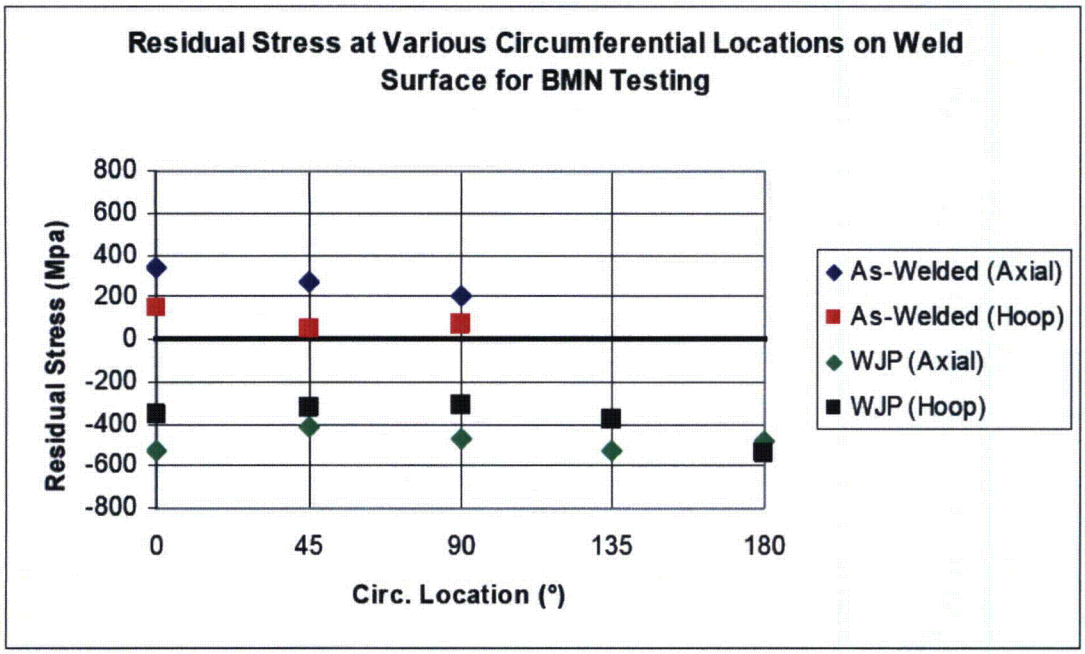

Figure A-69
Residual Stress Results for BMN Mock-Up Test – Surface of Weld, provided by Mitsubishi

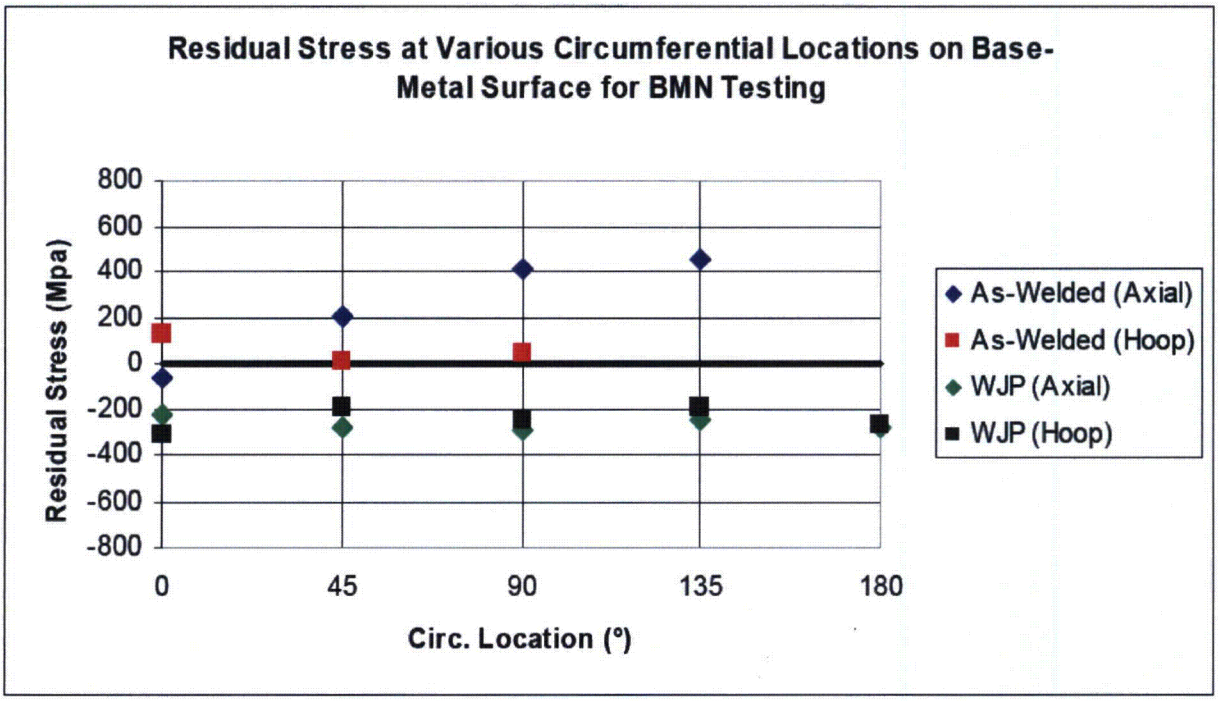

Figure A-70
Residual Stress Results for BMN Test-Surface of Base-Metal cladding, provided by Mitsubishi

Visual examination, Figure A-71, and PT inspection, Figure A-72, show the typical post-WJP surface condition of the various parts of the mock-up and demonstrate the absence of any surface distress. Near-surface microstructures were examined at various angular orientations around the mock-up. Typical microstructures for the three regions: tube, J-groove weld, and base metal cladding, are illustrated in Figure A-73 through Figure A-75. These micrographs show, at most, only slight distortion of grain features right at the surface. This effect, when present, is apparent to a depth of <25 μm. This is significant in that it is very much less than the depth of the compression effect of WJP, which is >1 mm.

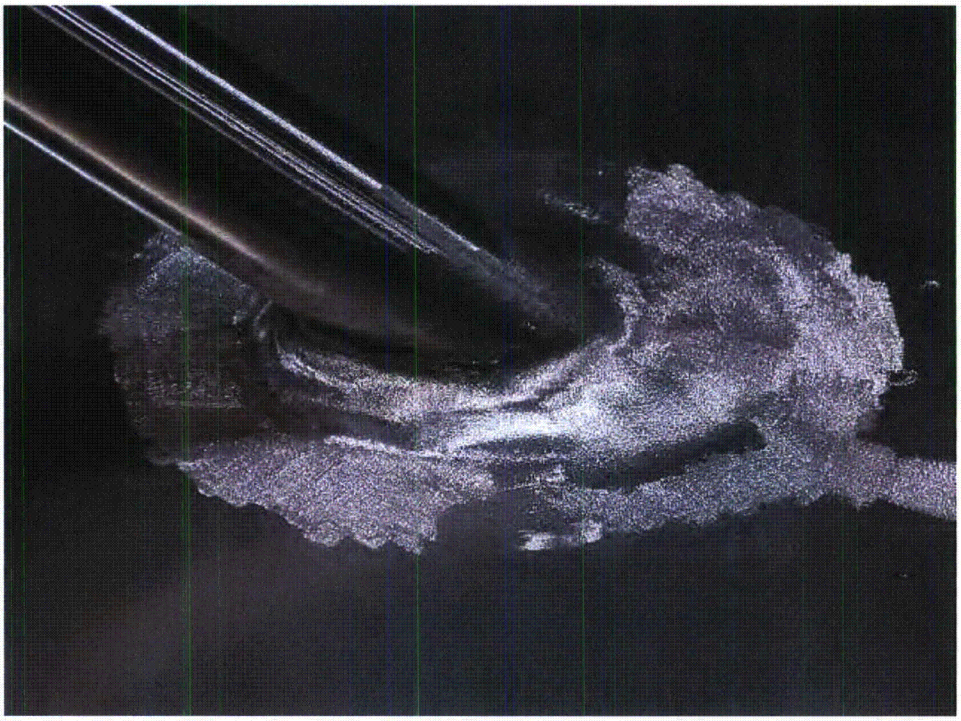

Figure A-71
Visual Inspection Results for BMN Mock-Up Test – 90° Location, provided by Mitsubishi

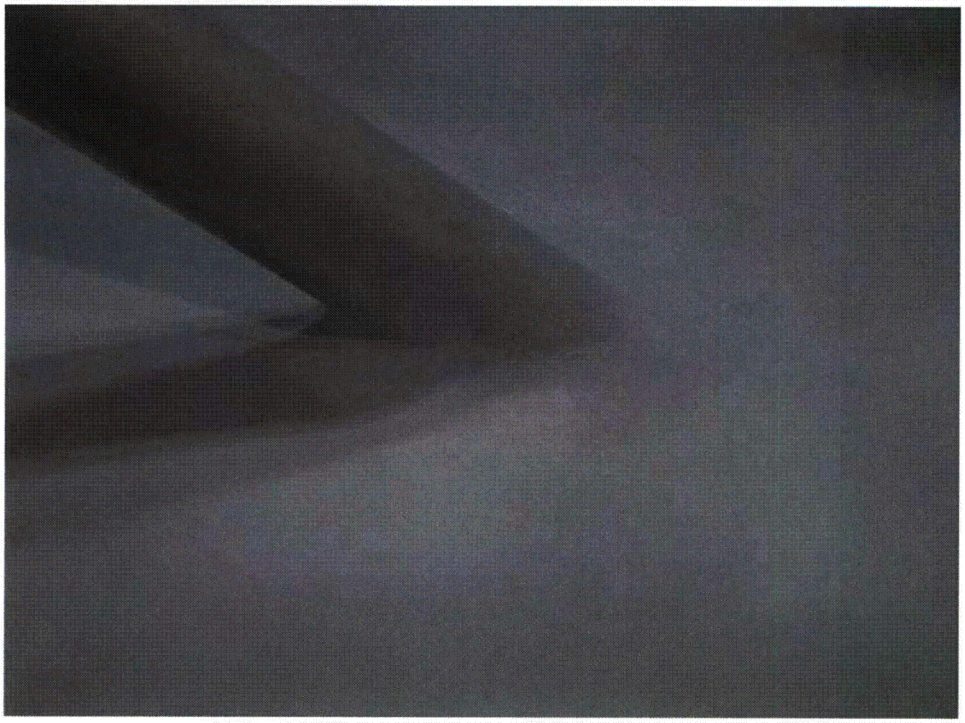

Figure A-72
PT Inspection Results for BMN Mock-Up Test – 90° Location, provided by Mitsubishi

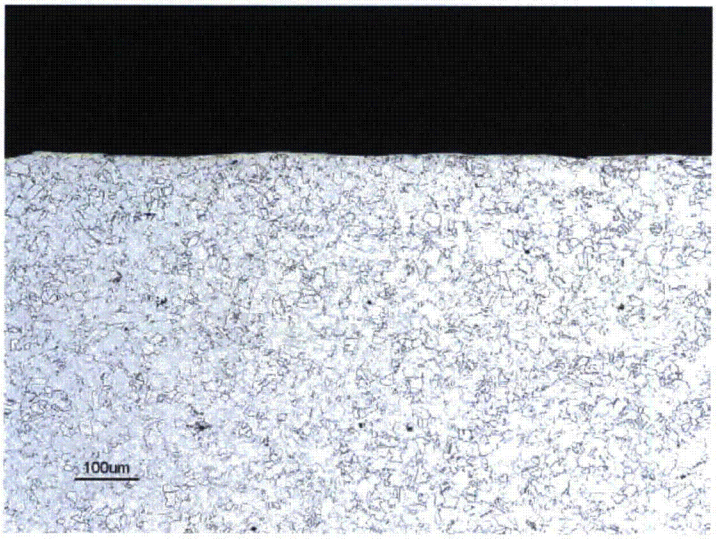

Figure A-73
Microstructure Results for BMN Mock-Up Test – Tube OD 0° Location, provided by Mitsubishi

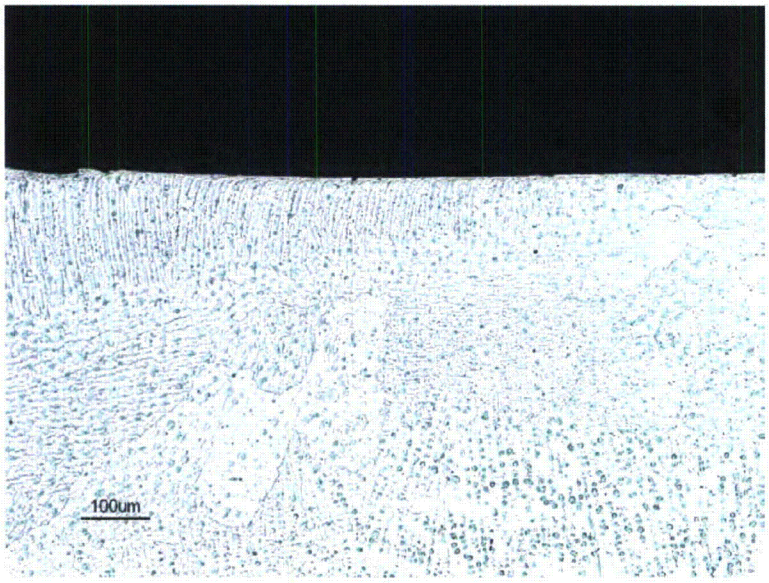

Figure A-74
Microstructure Results for BMN Mock-Up Test – J-Groove Weld Surface, provided by Mitsubishi

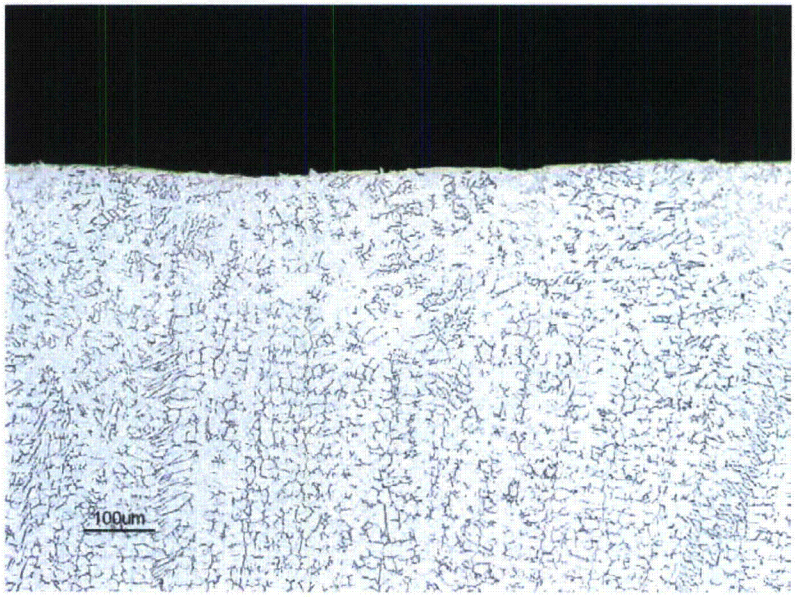

Figure A-75
Microstructure Results for BMN Test – Base-Metal Surface 0° Location, provided by Mitsubishi

A.1.6.3 Discussion of BMN OD/J-groove weld Mock-up Testing

This testing has verified that the WJP treatment process can deliver the desired mitigation effect by creating a surface layer of residual compressive stresses on complex geometries such as those of BMI nozzles. This verification test utilized both the tube OD configuration and large-radius

configuration to successfully treat the BMN mock-up block. The results of the residual stress measurements show that compressive stresses persisted to at least 1 mm into the surface of the components. Also, the post-treatment visual and PT inspections showed no recordable indications, thus the material integrity was not affected by the WJP treatment. Overall, this test represents the final verification for the WJP treatment. For this test, the process control parameters were set to nominal values as they would be in actual field execution.

The evidence from the cross-sectional metallography is that the amount of cold work induced by WJP is relatively small, since no microstructural damage is observed at this level of examination.

This testing has demonstrated that the process control parameters that were determined in previous testing phases produce the expected results in a full mock-up application. The system was capable of delivering the acceptable WJP effect to the components without causing any negative effects such as compromising material integrity. This test shows that the WJP process is qualified for use in actual plant configurations on components with complex geometry. In summary, it is concluded that the SCC mitigation effect of the WJP-induced compressive stress layer has been conclusively demonstrated.

A.1.7 Surface roughness measurements

If peening treatment causes a significant increase in surface roughness, corrosion inside the crevices caused by this roughness could be enhanced due to the difference of electrochemical potential between the free surface and the crevice during those limited periods when oxidizing conditions are present in the PWR reactor coolant system. To check this issue, flat plate specimens of 2" by 2" by 0.5" were prepared from Alloy 600 bar stock and stress relieved at 1650°F for two hours and air cooled, producing an oxidized surface film. The surface roughness of the Alloy 600 cavitation (water jet), underwater laser peened, and air laser peened specimens was measured over a one inch (25 mm) length using a Taylor-Hobson Surtronic 3 and is reported in Table A-9. The average surface roughness of untreated surfaces of the Alloy 600 test specimens was 3.05 μm, while the corresponding underwater laser peened specimens averaged 4.32 μm, cavitation (water jet) peened specimens 3.18 μm, and air laser peened specimens 3.38 μm.

The surface roughness of underwater laser peened Type 304 stainless steel was also measured by Toshiba and is shown in Figure A-76. The average roughness ranges from 1.2 to 1.3 μm, which corresponds to micro-cavities on the laser peened surface, and is smoother than usual surfaces of in-core components. Toshiba also performed surfaces roughness measurements on heat treated Alloy 600 plates treated with ULP, and the results are shown in Figure A-77. Similarly, roughness was increased compared to the plate in its ground state, but the roughness was still less than that of actual reactor internals. These data, coupled with the residual stress data discussed previously, indicate that laser peening should both enhance SCC resistance due to the compressive residual stress imparted on the surface and not have any detrimental effects on uniform surface corrosion resistance in high temperature water.

Hitachi-GE also measured surface roughness by height mapping three Type 316L stainless steel plates that were heavily ground, water jet peened, and shot peened respectively. The mapping is shown in Figure A-78 and the surface profile is shown in Figure A-79. Water jet peening was not found to increase the surface roughness significantly.

MIC treated a portion of an Alloy 600 plate with ALP parameters planned for reactor components (irradiance of 10 GW/cm^2 with a pulse duration of 18 ns and 3 layers of coverage, with no ablative layer). After peening, the surface roughness was measured in similar locations of the peened and unpeened sections for comparison. A Mitutoyo SJ-201 Surface Profiler was used to determine the R_a of the surfaces. The average roughness, R_a, in the peened area was 301.2 μin (7.65 μm) with a standard deviation of 37.8 μin (0.96 μm) compared to 298.9 μin (7.59 μm) with a standard deviation of 13.3 μin (0.34 μm) in the unpeened area. As a basis of comparison, peening a 300 μin (7.62 μm) surface has been nominally found to impart a 30 μin (0.76 μm) roughness, and root-mean-square roughness calculation that combines these two values yields 301 μin (7.65 μm), which agrees with the measured values. This suggests that the treatment adds very little to the existing surface roughness as predicted by the theoretical calculation.

Table A-9
Surface roughness of evaluated peening processes on Alloy 600 flat plates

Surface Treatment	Average Surface Roughness (μin)	Average Surface Roughness (μm)
Untreated	120	3.05
Underwater Laser Peened	170	4.32
Cavitation Peened	125	3.18
Air Laser Peened	133	3.38

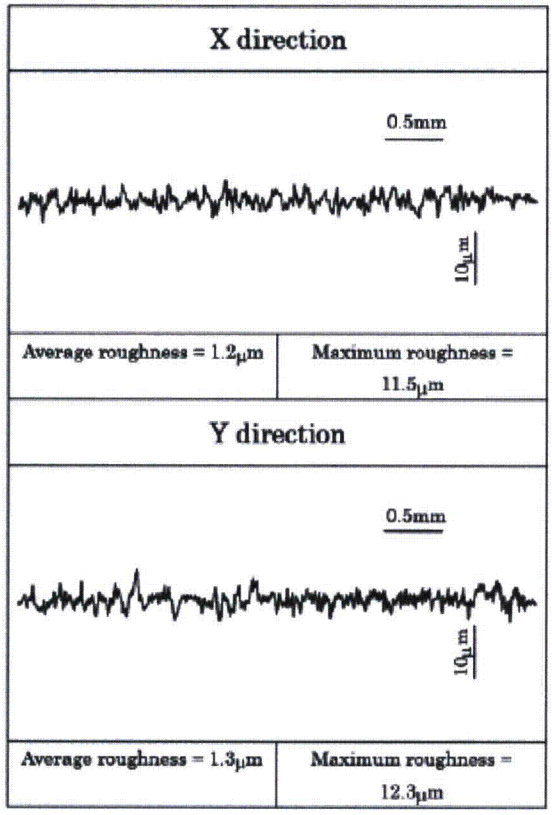

Figure A-76
Surface roughness of underwater laser peened surface 20% cold work Type 304 stainless steel – peened with spot diameter of 0.8 mm, pulse energy of 200 mJ, and 3600 pulses/cm^2, provided by Toshiba

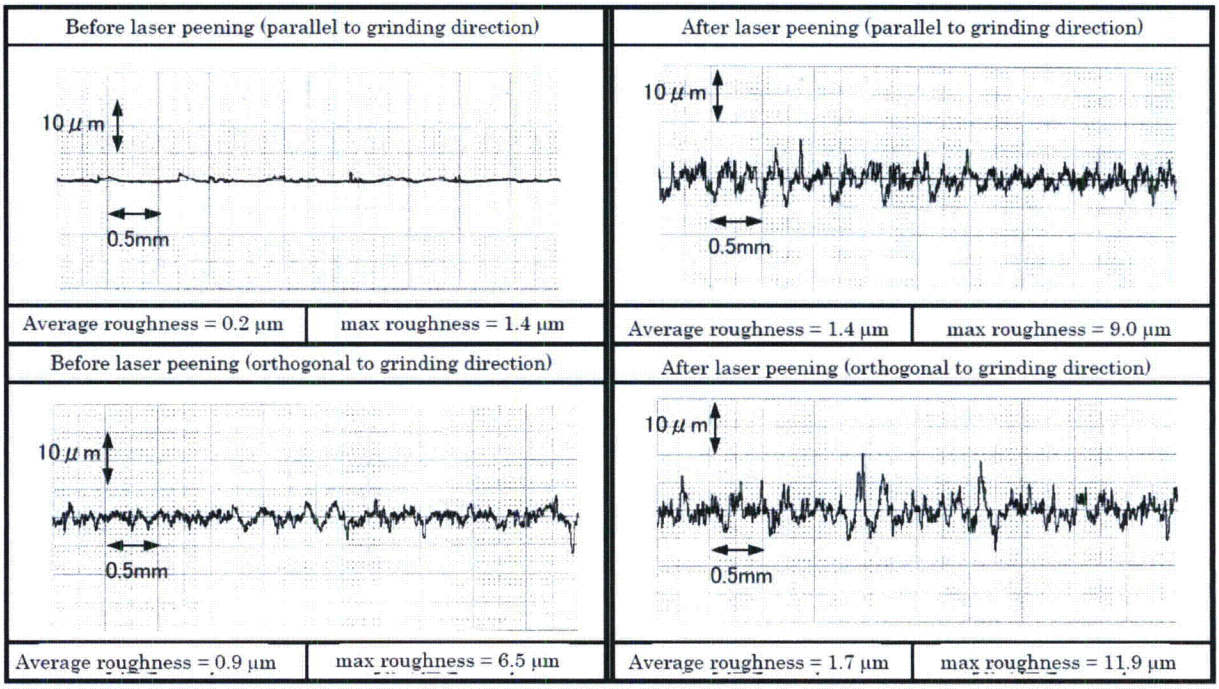

Figure A-77
Surface roughness measurement on heat-treated Alloy 600 before and after ULP

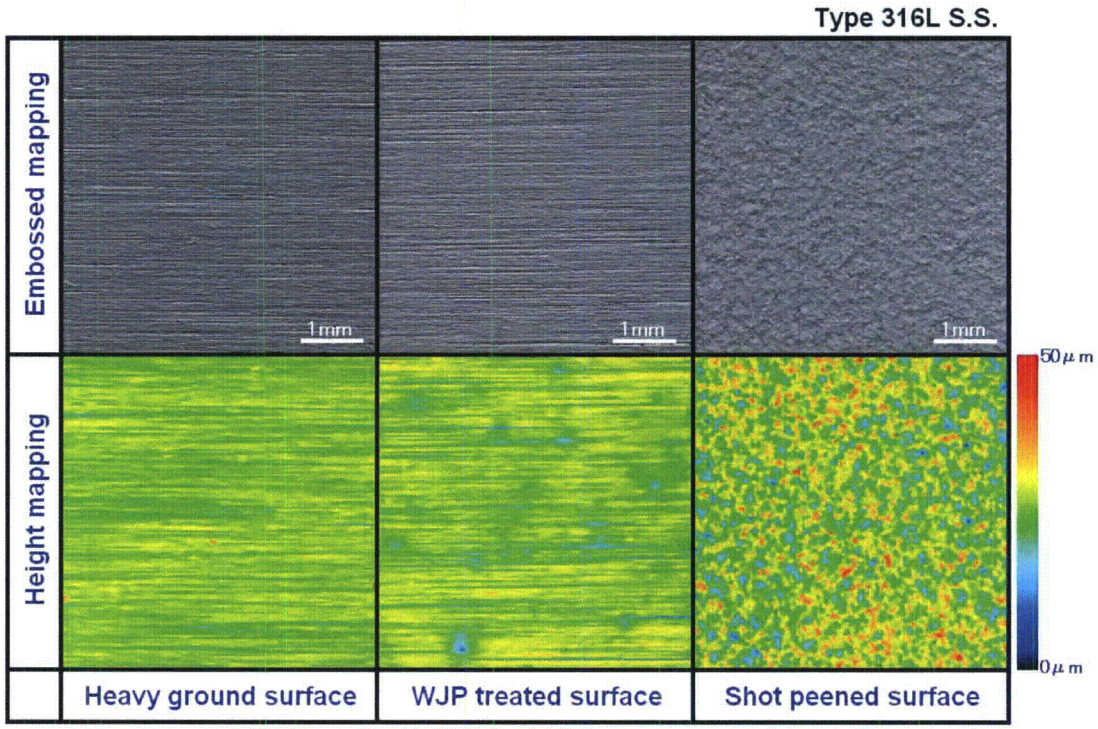

Figure A-78
Surface roughness with 3D measurement method on Type 316L SS after peening, provided by Hitachi-GE

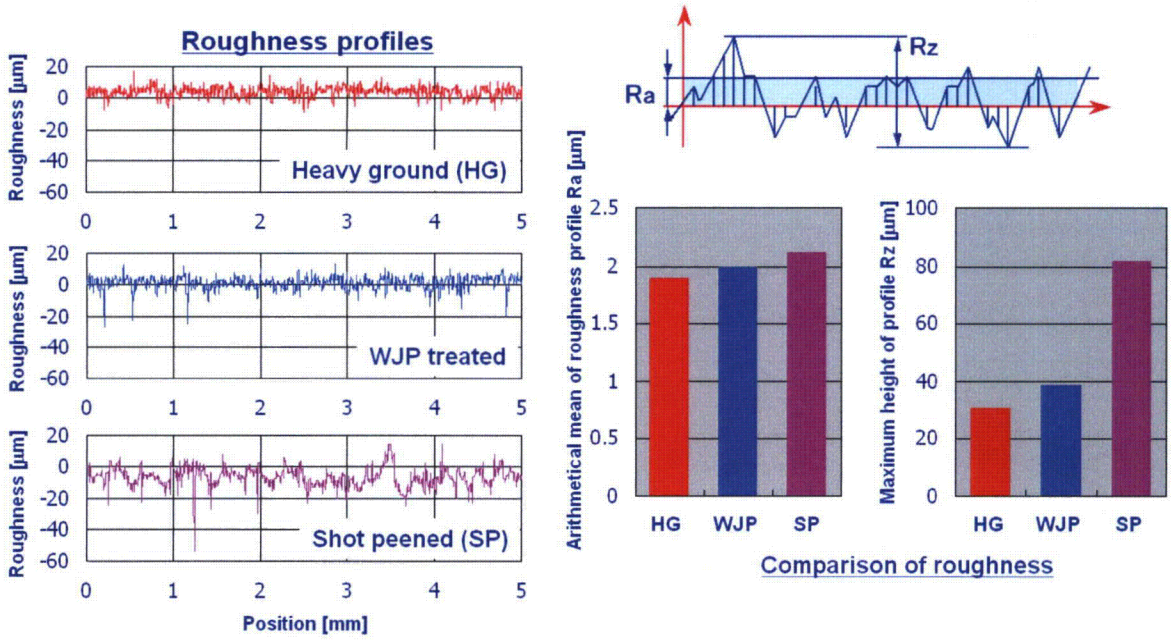

Figure A-79
Surface roughness profile on Type 316L SS after peening, provided by Hitachi-GE

A.1.8 Hardness measurements

A picture of a underwater laser peened specimen cross section shows where microhardness measurements were performed along the cross section (Figure A-80, left). One can note that some of the grains are larger beneath the surface than in other locations of the cross section of this underwater laser peened specimen. However, another picture of an untreated cross section C-008 also shows larger grains beneath the surface (Figure A-80, right). This confirms that these larger grains are due to the heat treatment of the flat plates and are not induced by the surface treatment. This nonuniformity of the grain size on the cross sections of the specimens probably creates some scatter in the microhardness measurements.

The microhardness results for the underwater laser peened specimens are shown in Figure A-81. The underwater laser peened specimens all show a higher microhardness close to the treated surface compared to untreated specimens, except for specimen T-004. This difference in microhardness is significant until a depth of about 0.4 mm. The specimens treated with the following parameters, 2.3 GW/cm^2 irradiance, 8 ns pulse width, 4500 pulses/cm^2, with no ablative layer, show the highest hardness magnitude difference between treated and untreated conditions and a depth of almost 0.5 mm. The corresponding depth of the compressive residual stress field is around 1 mm for specimens that were laser peened with these parameters.

The microhardness results for the air laser peened specimens are shown in Figure A-82. The air laser peened specimens all show higher microhardness values close to the treated surface compared to untreated specimens. This difference in microhardness is significant until a depth of about 2 mm. The specimens treated with the following parameters, 10 GW/cm^2 irradiance, 18 ns pulse width, 5 layers of peening, with an ablative layer, show the largest difference in hardness magnitude between treated and untreated conditions up to a depth similar to the other specimens.

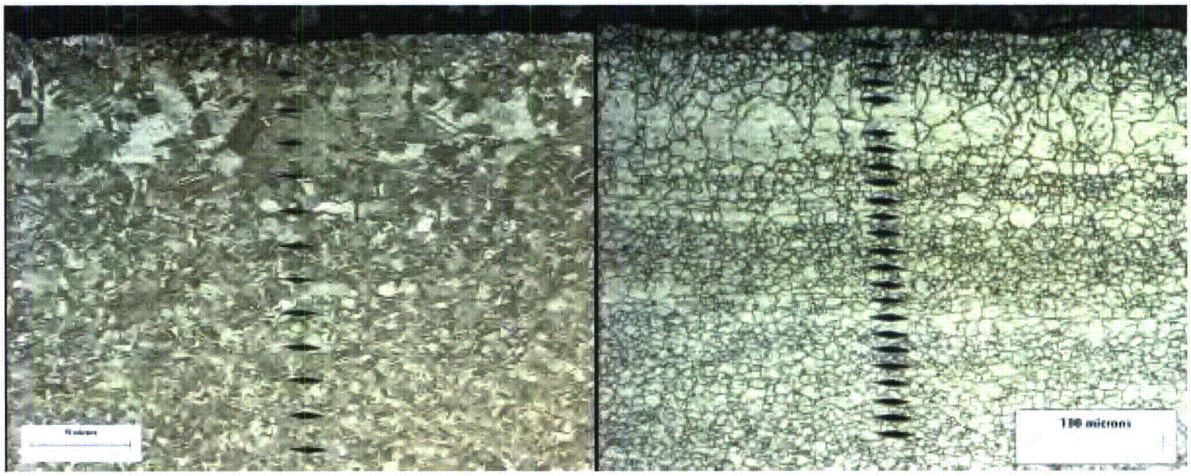

Figure A-80
Microhardness measurements as a function of depth on the cross section of untreated specimen C-008 (right) and on the cross section of flat plate specimen T-009, underwater laser peened with 2.3 GW/cm^2 irradiance, 8 ns pulse width, 4500 pulses/cm^2 coverage, and no ablative layer (left) (x100)

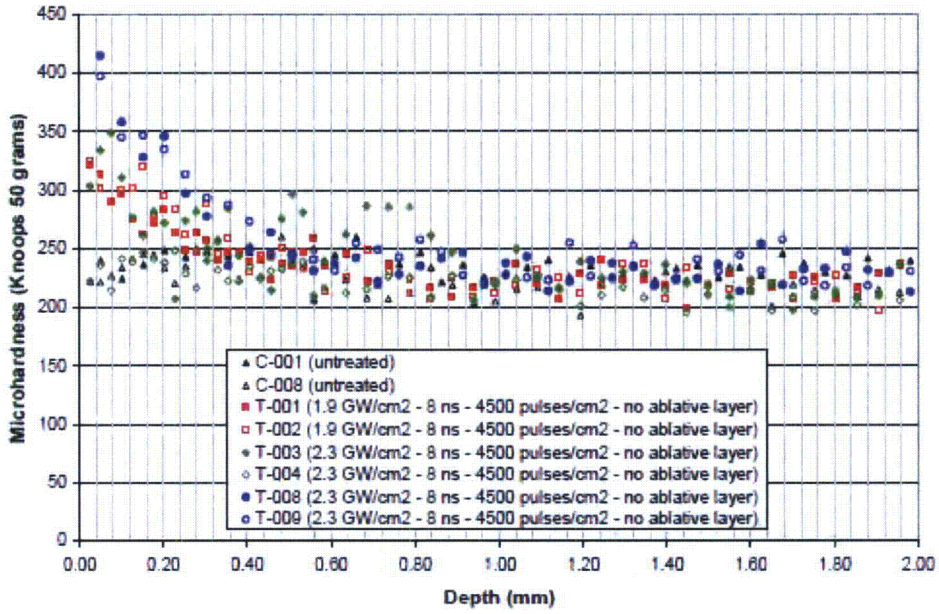

Figure A-81
Microhardness measurements results for underwater laser peened specimens (treated by Toshiba)

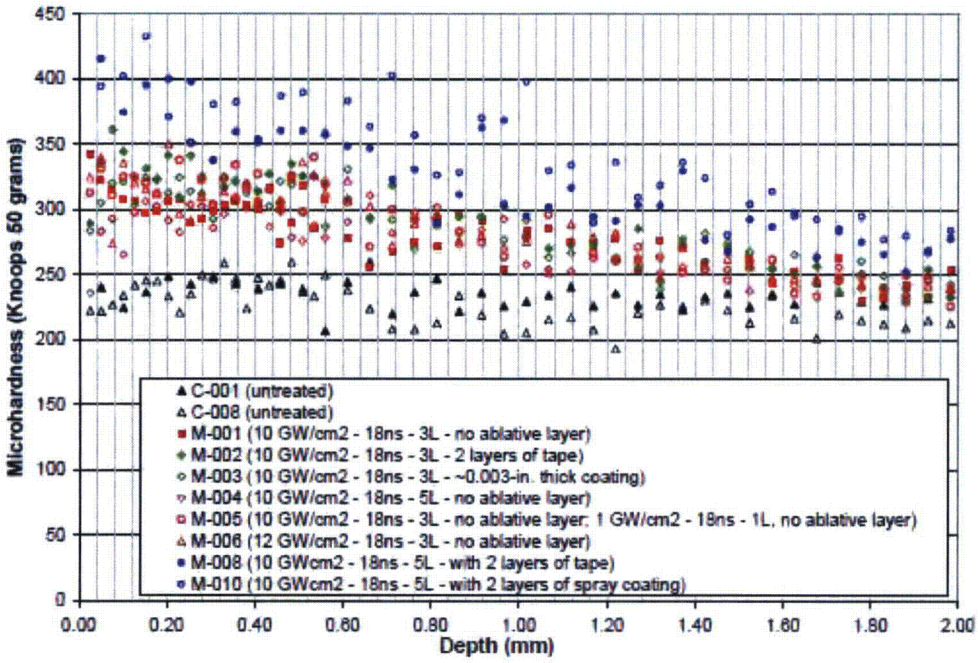

Figure A-82
Microhardness measurements results for air laser peened specimens (treated by MIC)

Mitsubishi measured Vickers hardness in the BMN ID mock-up and in the BMN OD/J-groove weld every 0.1 mm to a depth of 1.5 mm. In the BMN ID, comparing hardness profiles before and after WJP revealed that only slight hardness was produced to a depth of 0.5 mm. This trend was observed at the J-groove weld and far away from the J-groove weld. The hardness profile at the J-groove weld is shown in Figure A-83. In the BMN OD/J-groove weld mock-up, measurements were taken at five equally spaced angular locations between 0° and 180° in the Alloy 600 tube, in the Alloy 132 J-groove weld, and in the stainless steel base metal cladding. All near-surface hardness values were below 300 Hv. The hardness profiles at 45° in the tube outer diameter, in the J-groove weld, and in the base metal cladding are shown in Figure A-84.

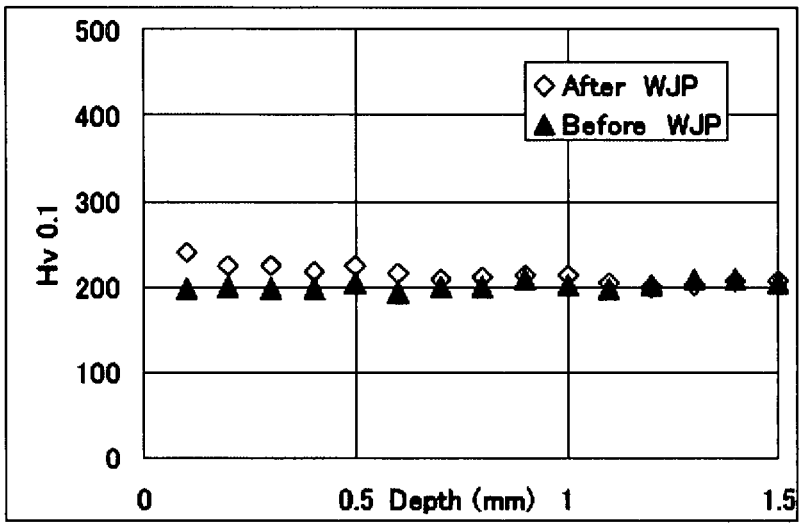

Figure A-83
Hardness depth profile on BMN ID mock-up, 9.5 mm ID tube, at the J-groove weld, 0° orientation, provided by Mitsubishi

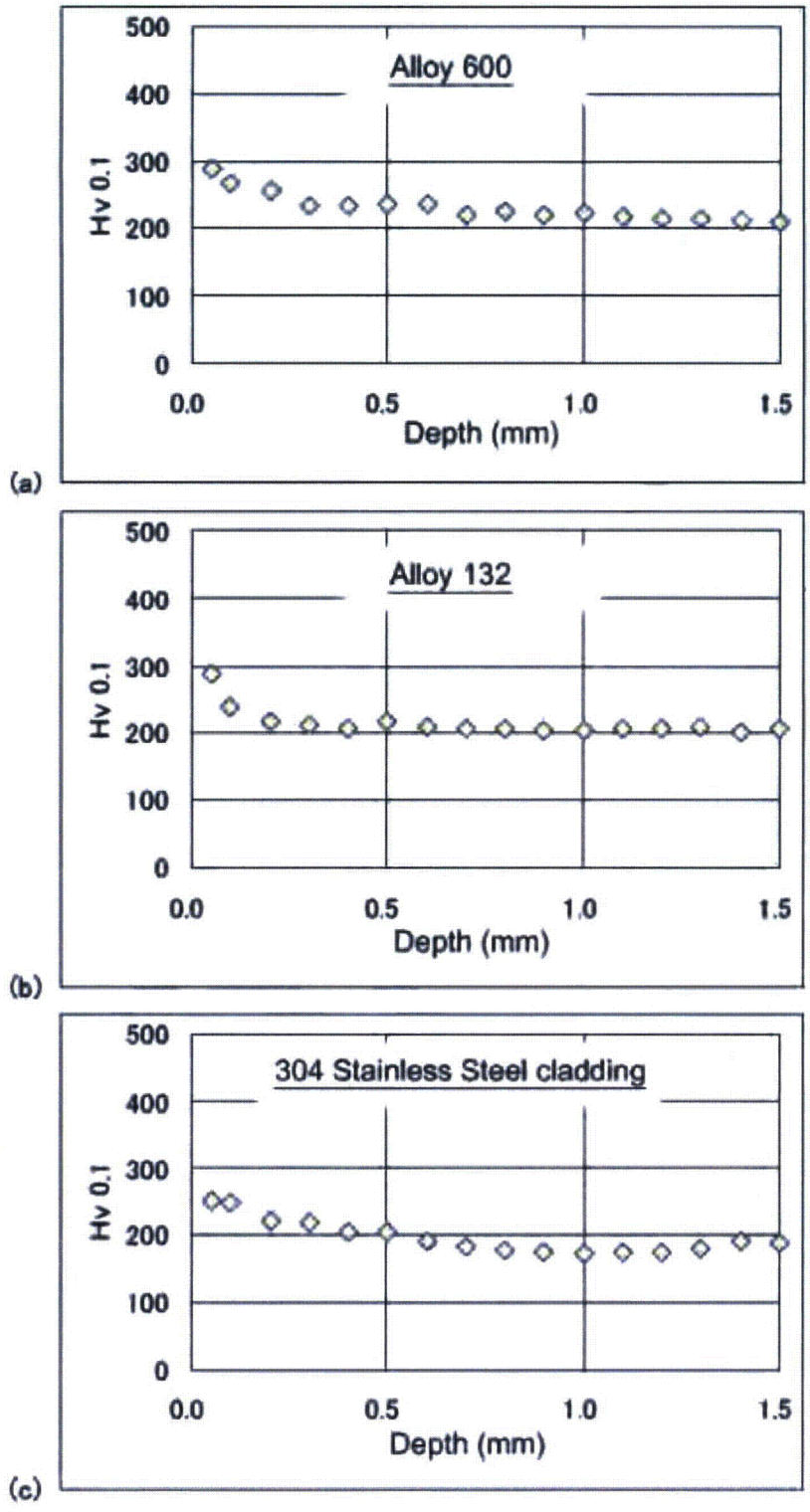

Figure A-84
Hardness depth profiles on BMN OD and J-groove weld mock-up at 45° location (a) tube OD, (b) J-groove weld, and (c) base-metal cladding, provided by Mitsubishi

Hitachi-GE measured hardness values in flat plates of Alloy 600 and Alloy 182 to a depth of 1.0 mm. All flat plates were polished and electro-polished and the Alloy 600 plates were solution heat treated and stress relief heat treated prior to polishing. To compare hardness induced by different peening techniques, flat plates were subjected to three different surface treatments: one set was water jet peened, one set of plates was shot peened, and one set was not peened. While each data of the shot peened specimen shows strong hardening from the surface to a depth of approximately 200 μm, data of the WJP treated specimen shows weak or negligible hardening comparing to the shot peened specimen as shown in Figure A-85. From this result, WJP was found to be one of the best mitigation methods from a viewpoint of avoiding cold work addition on materials. These results show that WJP has no adverse effect from the view point of hardening and deformation, potential factors affecting SCC susceptibility.

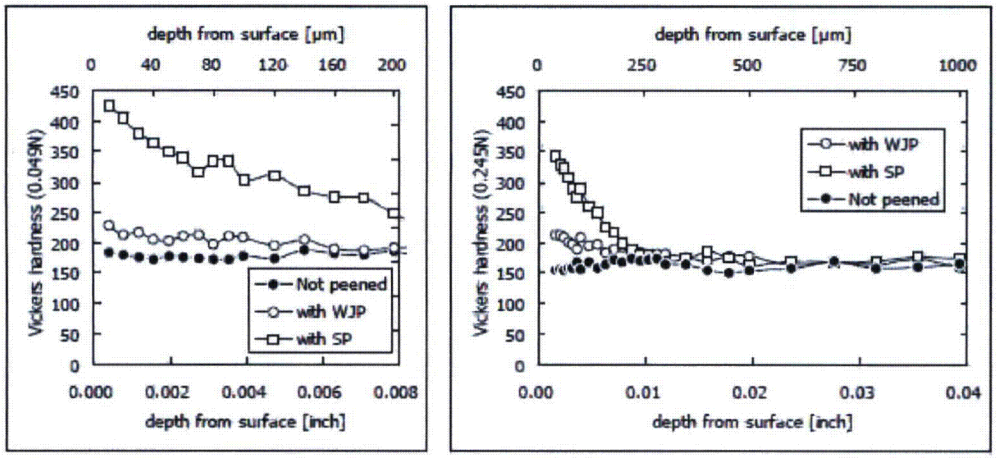

a) Alloy 600 [17]

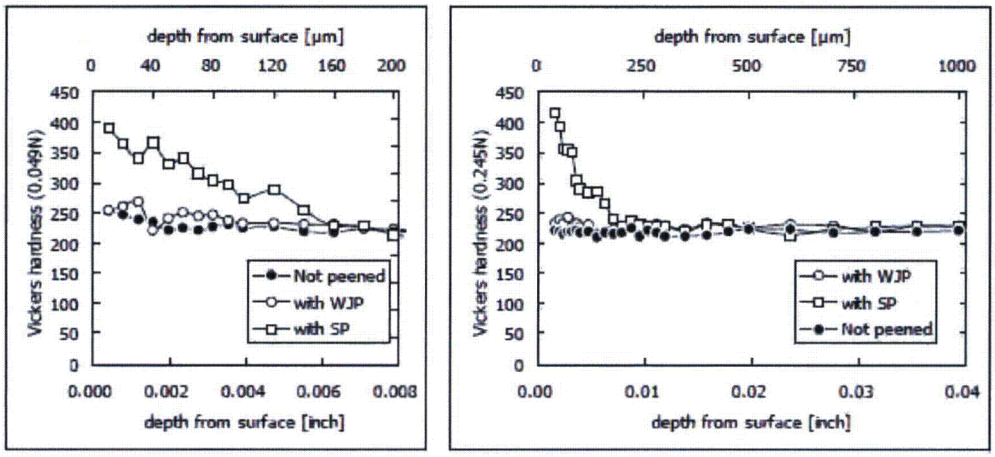

b) Alloy 182 [17]

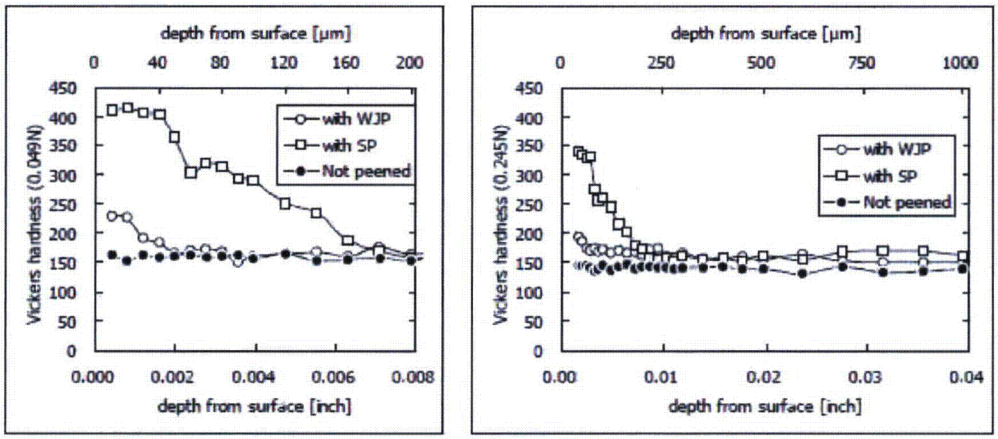

c) Type 316L S.S. [10]

Figure A-85
Cross-sectional hardness profile with WJP and SP (Shot Peening), provided by Hitachi-GE

A.1.9 Peening at extreme parameter values

Mitsubishi performed experiments where specimens of various geometries were peened at extreme conditions. This was done to define an appropriate upper limit for control parameters such that there would be no adverse effects on the component. Control parameters investigated include water flow rate, application time, offset distance and nozzle diameter at levels that would correspond to a worst case scenario from a material integrity standpoint. For example, if the peening nozzle became immobilized and a component was peened for longer than intended, it must be verified that material integrity would not be compromised. Experiments were performed on 9.5 mm ID Alloy 600 Tubing, Alloy 600 and stainless steel flat plates welded together using Alloy 132 weld metal, and a 38 mm OD alloy 600 tube welded to a plate of low alloy steel with 304 stainless steel cladding using Alloy 132 weld metal. All tests were carried out in a pressurized chamber to simulate the effect of being submerged under meters of water. Visual Tests (VTs) and PT were performed to ensure that there were no adverse surface effects, and the results are shown in Figure A-86 to Figure A-89. In all three experimental setups, no adverse surface effects were observed.

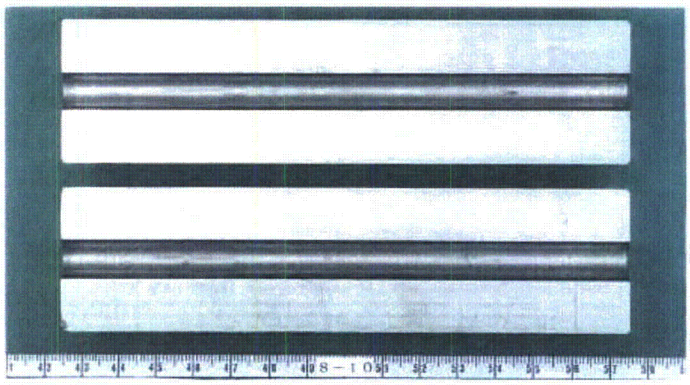

Figure A-86
Visual Inspection Results for ID Configuration Testing – Stuck Nozzle Test, provided by Mitsubishi

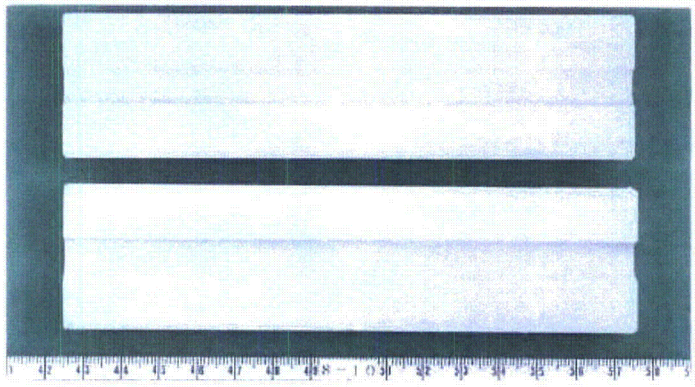

Figure A-87
PT Inspection Results for ID Configuration Testing – Stuck Nozzle Test, provided by Mitsubishi

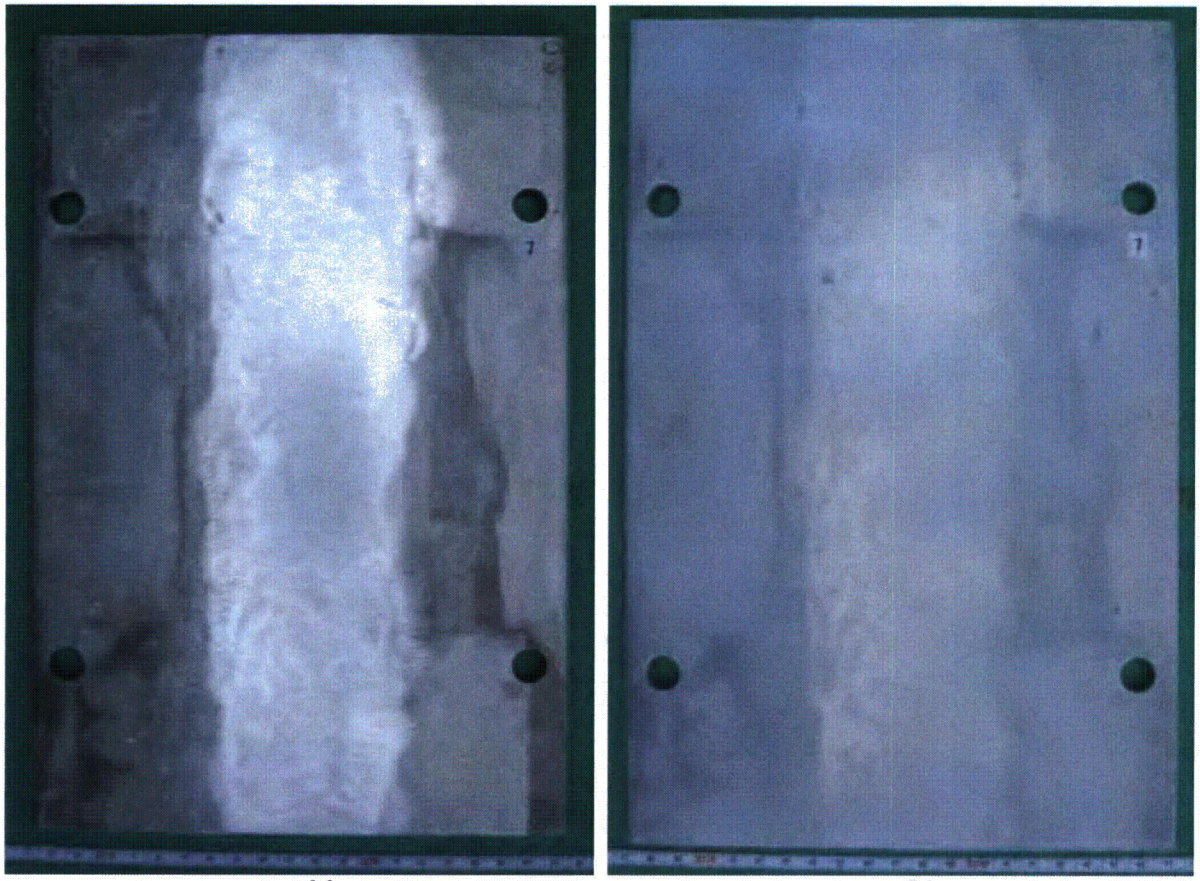

Figure A-88
Results of (a) Visual Inspections and (b) PT examination for Extreme Conditions on welded flat plate configuration testing, provided by Mitsubishi

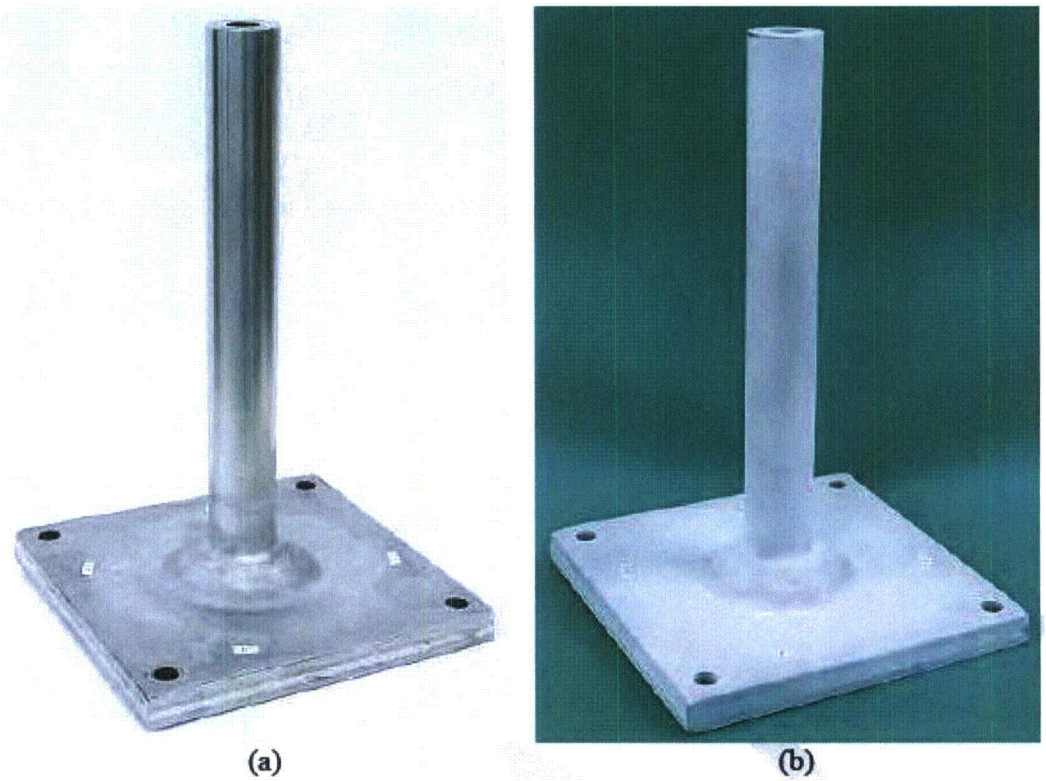

Figure A-89
Visual (a) and PT (b) Inspection Results of Tube OD Configuration Verification Test at 0° Location, provided by Mitsubishi

A.2 SCC test data from vendors

Vendors have performed SCC tests to verify the effect of peening on improving resistance to SCC initiation and propagation. This section summarizes these test results in two parts: a) effects of surface peening on SCC in specimens with no pre-existing cracks, and b) effects of peening on SCC in specimens with pre-existing flaws.

A.2.1 SCC initiation test on specimens with no pre-existing flaws

To demonstrate the effectiveness of underwater laser peening (ULP) in mitigating SCC cracking, Toshiba performed a CBB test on Type 304 stainless steel to confirm the effectiveness of ULP in SCC mitigation. A high carbon (0.06 wt%) Type 304 stainless steel was first sensitized at 620°C for 240 hours, and then cold worked up to 20%. The CBB coupons were machined from this sensitized and cold worked 304SS. After each CBB coupon was fixed in a CBB test jig with 1% strain, ULP treatment was applied to 5 CBB specimens and no ULP was applied to the other 5 CBB specimens.

These 10 CBB specimens were exposed to high purity water at 288°C for 500 hours. With no ULP treatment to the surface in 5 CBB specimens, all suffered SCC cracking. With ULP treatment of the other 5 CBB specimens, all showed no SCC cracking after 500 hours of exposure in the test environment, Figure A-90.

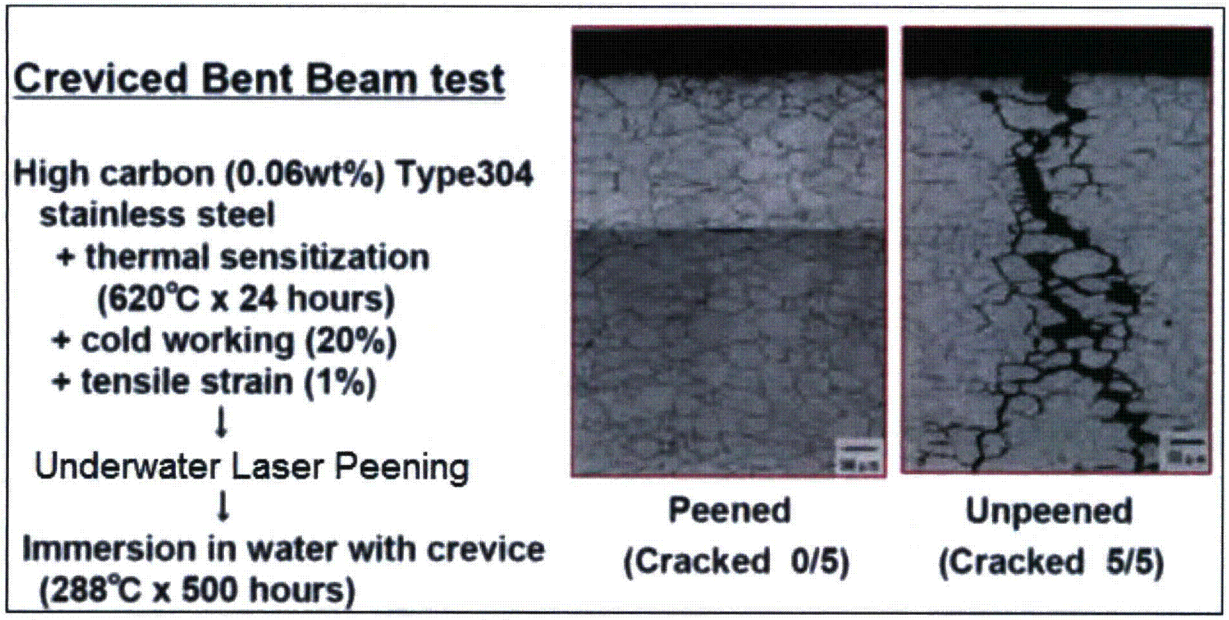

Figure A-90
The CBB test result in 304SS with and without ULP treatment (by Toshiba)

Toshiba also performed a peening and SCC test on Alloy 132 weld metal. Alloy 132 has similar characteristics and properties to Alloy 182, and is widely used for DMWs in Japanese nuclear plants. In this test, a thin Alloy 132 plate was first bent into half-pipe shape, and then tensile specimens were fabricated by machining this half-pipe. Each tensile specimen was subjected to a 20% tensile strain and then formed into a reverse U-bend sample. The specimen fabrication process is illustrated in Figure A-91. Twenty-one reverse U-bend specimens were treated with ULP on the out-facing surfaces, and they were divided into three groups based on the three laser peening processing conditions. Another 7 U-bend specimens received no ULP treatment and were used as the control samples. All 28 U-bend specimens were placed in a simulated PWR environment for SCC testing.

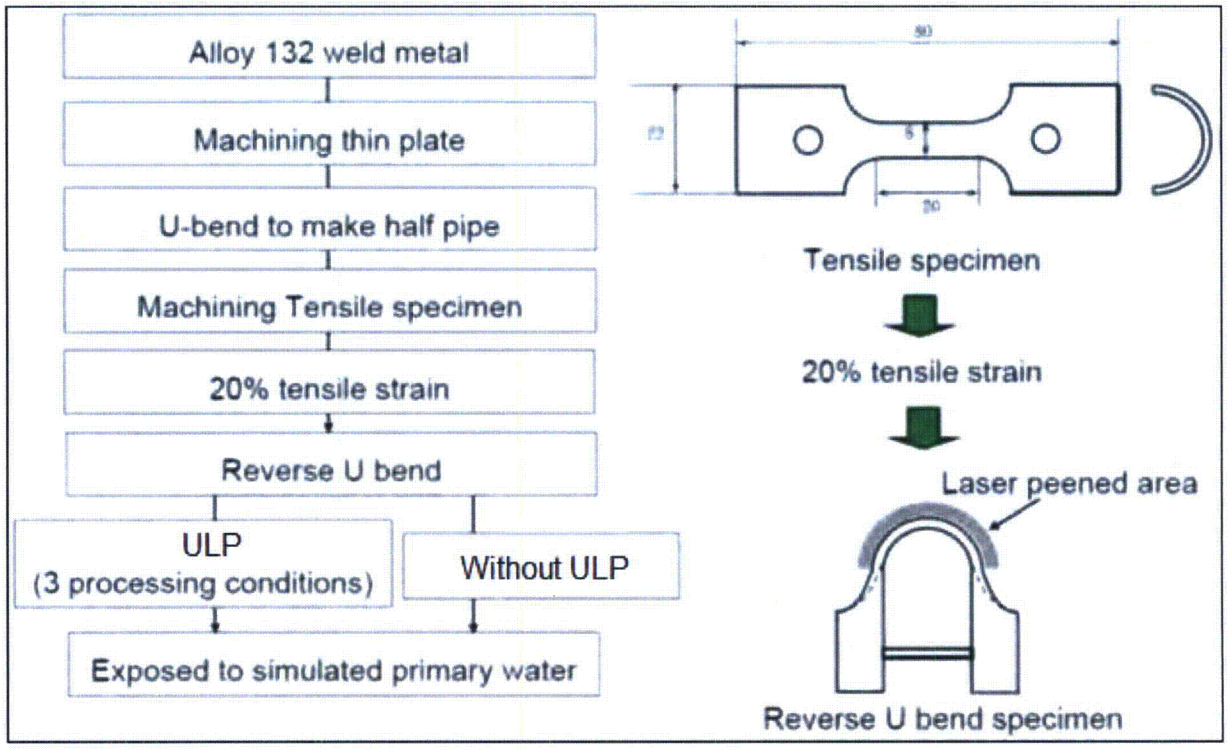

Figure A-91
Experiment procedure of PWSCC test on Alloy 132 with and without ULP treatment

The SCC test was performed at 360°C in simulated PWR water with 500 ppm B, 2 ppm Li, and 30 cc H_2/kg H_2O. The test duration was 1000 hours. For control specimens with no ULP treatment, the specimens were checked for SCC cracking after 500 hours of immersion. If no SCC cracking was observed on a specimen then it was put back to test for the remaining 500 hours. The post immersion examination was first performed by VT, and then enhanced by PT.

Among all 21 ULP treated U-bend specimens, no crack was found after 1000 hours in simulated PWR environment at 360°C. By comparison, SCC cracking was observed after 500 hours of immersion in 3 of 7 control specimens with no ULP treatment, and in 5 out of 7 after 1000 hours. The summary of this PWSCC test is illustrated in Figure A-92. This PWSCC result has again demonstrated that surface peening is effective to mitigate the initiation of SCC. This result also shows that ULP is effective at developing protective residual stresses in highly cold worked Alloy 600 type weld metal since the U-bends had a 20% pre-strain and were then bent using a fairly tight bend radius, adding additional strain (estimated to be about 10% based on the dimensions shown in the figure), before they were peened.

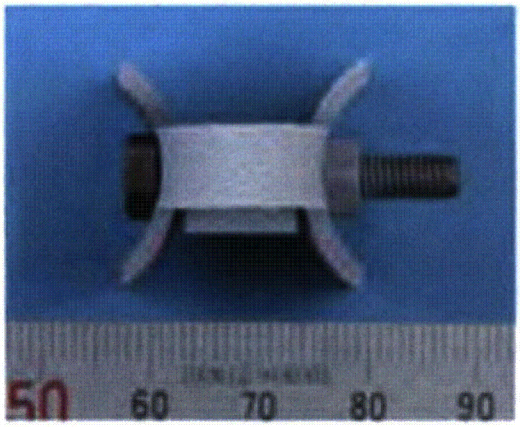

Underwater laser peening / condition 3

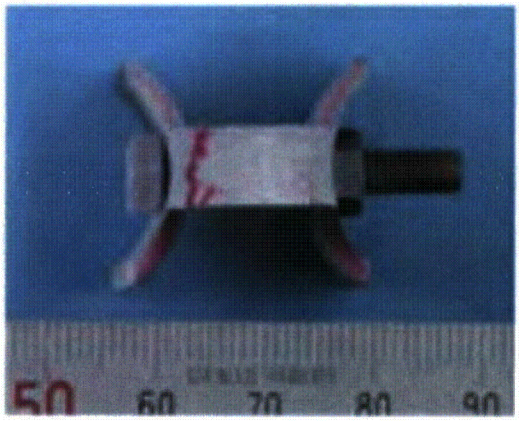

Without underwater laser peening

Summary of PWSCC test

	ULP conditions	Cracked specimens /total specimens	
		500h	1000h
ULP	1	0/7	
	2	0/7	
	3	0/7	
Without ULP	-	3/7	5/7

Figure A-92
Summary of PWSCC test

To verify the effectiveness of WJP to mitigate SCC, Hitachi-GE had performed a CBB test on a non-cracked specimen in a boiling 42% $MgCl_2$ solution. Two Type 304 stainless steel plates were welded at the centerline by SMAW, and one half of the welded plate was masked to shield the as-welded surface from the WJP process. After the WJP treatment, the test piece was immersed in boiling 42% $MgCl_2$ solution. While SCC was generated on the as-welded surface, no SCC was found on the WJP treated surface (Figure A-93). In this test, cracking occurs at the as-weld surface due to the weld residual stress; however the WJP treatment was able to improve the surface stress condition and to prevent SCC cracking.

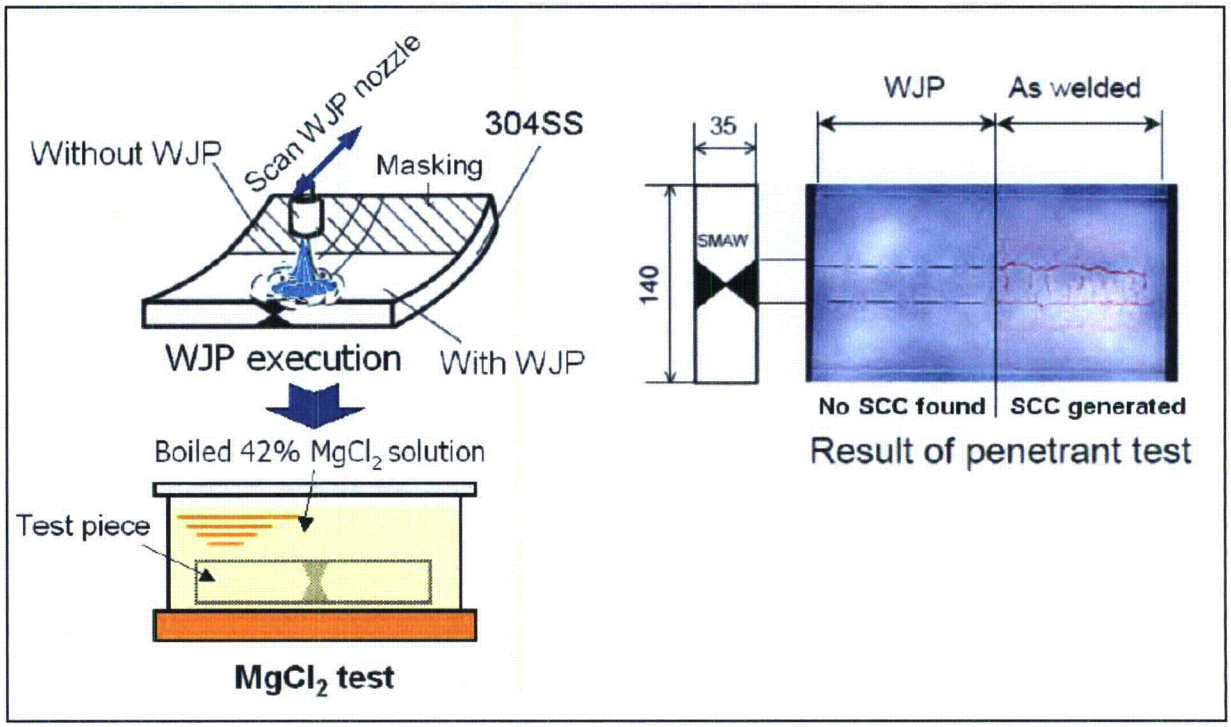

Figure A-93
SCC test of Type 304 stainless steel with and without WJP treatment in boiling 42% $MgCl_2$ solution, provided by Hitachi-GE

In another CBB test, Hitachi-GE had applied WJP treatment to sensitized 304SS coupons, and performed the SCC tests in a BWR environment (high purity water with 8 ppm dissolved oxygen at 288°C). In this test, several levels of strain were applied to the CBB specimen. For the coupons with no WJP treatment, SCC cracking was observed when a strain of 0.1% was applied. No crack was found on the coupons that received WJP treatment with a slower raster speed of 30 min/m (46 s/in), up to strain of 0.3%. No crack was observed either on coupons that received WJP treatment with a faster raster speed of 10 min/m (15 s/in), up to strain of 0.15%, see Figure A-94. A slower raster speed allows longer treatment time and generally a thicker layer of compressive stress on the surface. This result also confirms that WJP treatment is effective in mitigating SCC initiation.

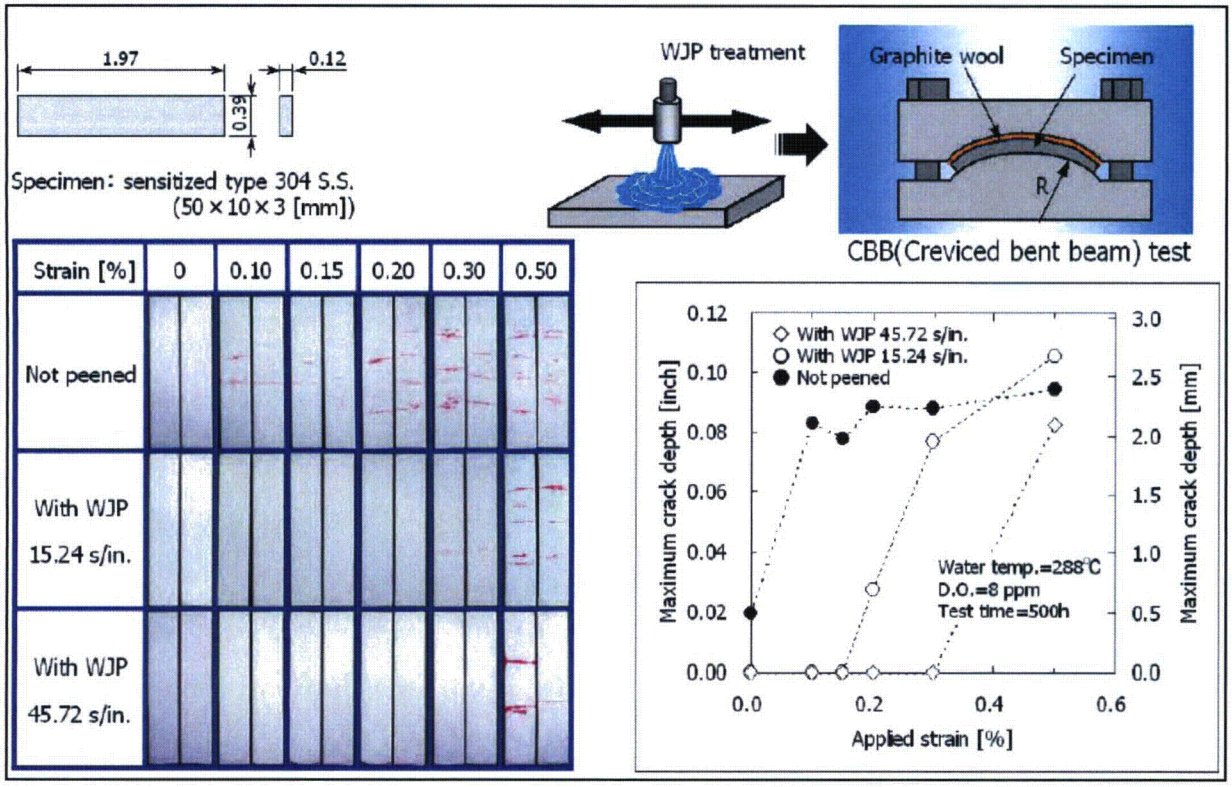

Figure A-94
CBB test of 304SS with and without WJP treatment to verify the effectiveness of WJP to mitigate SCC susceptibility, provided by Hitachi-GE

Hitachi-GE has also investigated the effect of WJP treatment on the SCC susceptibility of Ni-base alloys. Weld metal Alloy 182 was welded onto an Alloy 600 plate, and CBB specimens were fabricated from the A600/182 plate, Figure A-95. The CBB test specimen was 3 mm in thickness and all CBB test coupons were heavily ground. Each CBB specimen was then fixed into a CBB jig, and a 1% strain was applied. The CBB test jig was designed so that surface treatment could be done after the specimen had been fixed in the jig. With a total of 7 CBB specimens, 2 were treated with WJP and 5 were not treated (There were other specimens with various surface treatments, but they are not included in this report). The SCC test was performed in 288°C pure water containing 16 ppm oxygen and the conductivity was 0.1 μS/cm and lower. After immersion testing for up to 1600 h, each specimen was examined for SCC cracking.

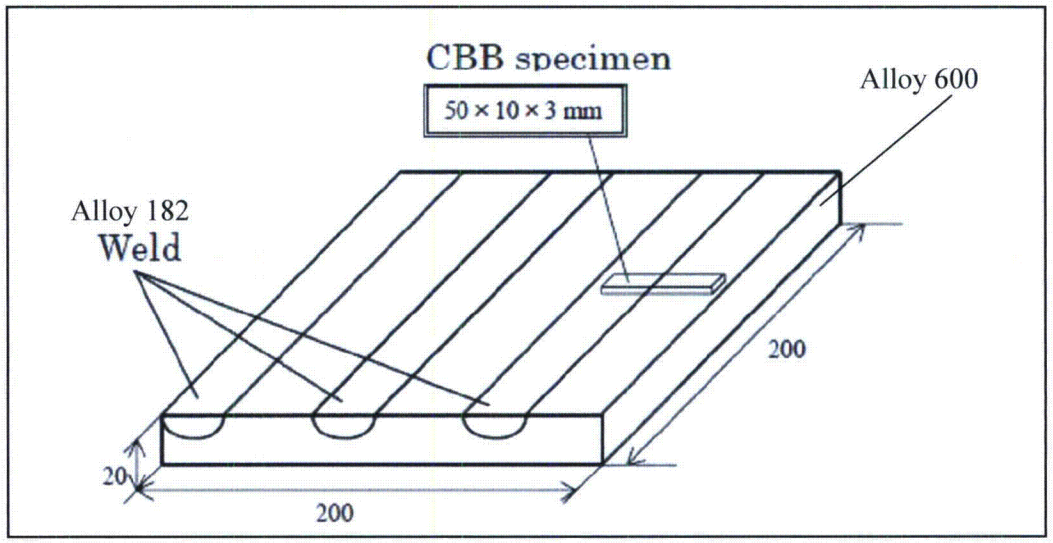

Figure A-95
The schematic of weld and CBB specimen fabrication—The CBB test specimen was 3 mm in thickness and all CBB test coupons were heavily ground

Cracks were observed in all 5 grinding-only specimens that received no WJP treatment. However, no crack was observed in the 2 specimens that were treated with WJP, Figure A-96. The test result indicated that WJP effectively reduced the SCC susceptibility of nickel-base alloys.

In a SCC test performed by MHI, two mock-up blocks were fabricated each with a 316L stainless steel tube that penetrated and was welded to a 304 stainless steel plate using an Alloy 316 weld. The mock-ups had the similar geometry and configuration of BMN and J-groove weld. One mock-up was treated with WJP treatment, and the other with no WJP treatment. The results of the residual stress measurements show that compressive stresses were present on the surface with WJP treatment, and to a depth of at least 1 mm into the surface of the components. Additionally, the post-treatment visual and PT inspections showed no recordable indications, thus the material integrity was not affected by the WJP treatment. The BMN mock-up block was WJP treated by utilizing the WJP procedure developed for both the tube OD configuration and large-radius configuration. The WJP process had been qualified for use in actual plant configurations on components with complex geometry.

The two mock-up blocks discussed in Section A.1.6 were then immersed in boiling 42% $MgCl_2$ solution for 120 hours. Post-test examinations were carried out by visual test (VT) and by penetration test (PT). The SCC tests in $MgCl_2$ clearly demonstrate the mitigation effects of peening on SCC initiation: cracking was observed only in the mock-up with no WJP treatment (Figure A-97), while no SCC cracking was observed in the mock-up with WJP treatment (Figure A-98). This has verified that WJP induces a compressive stress layer that effectively mitigates SCC cracking on parts with complex geometries such as BMNs. From these results, MHI confirmed that the desired levels of compressive stress were developed and that at the weld fusion line, SCC was inhibited.

Result of SCC cracking after CBB tests:

Materials	Surface Condition	
	Grinding (no WJP)	Grinding + WJP
Alloy 600/182	5 / 5	0 / 2

SCC test parameters:
Materials: Alloy 600/182 weld
Environment: Pure water with 16 ppm DO
Temperature: 288°C
Strain: 1%
Test duration: up to 1600 h

SCC cracks observed in CBB specimens with no WJP treatment

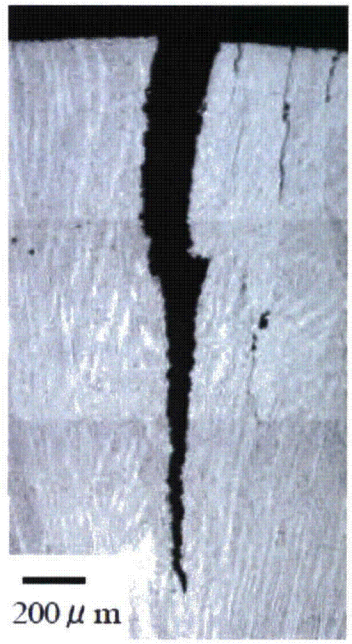

Figure A-96
Summary of SCC test results—The CBB test exposed Alloy 600/182 weld coupon in pure water with 16 ppm DO at 288°C, with 1% strain to the coupon, provided by Hitachi-GE

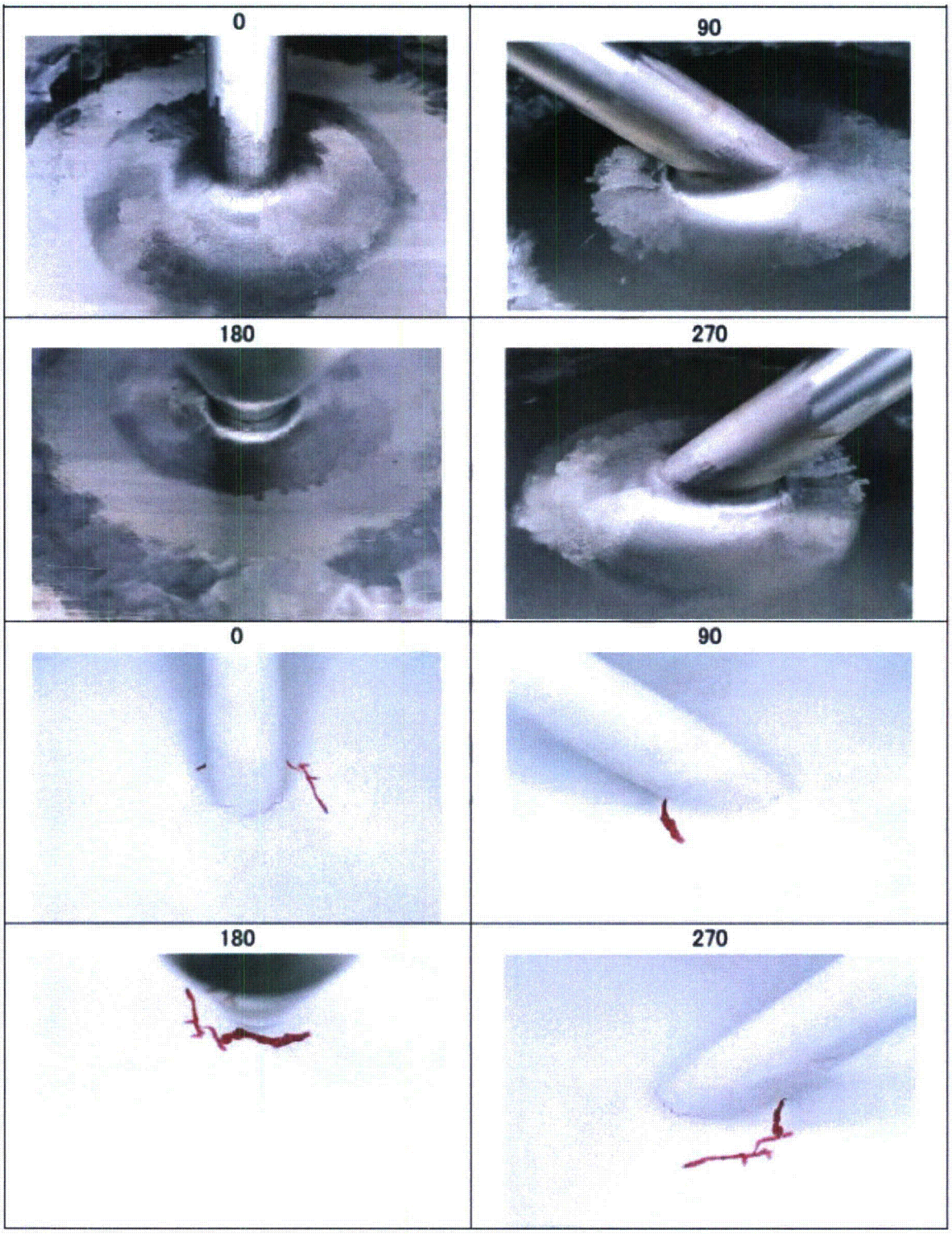

Figure A-97
Visual (upper photograph) and PT (lower photograph) Results for $MgCl_2$ Solution Test on an untreated mock-up, provided by Mitsubishi

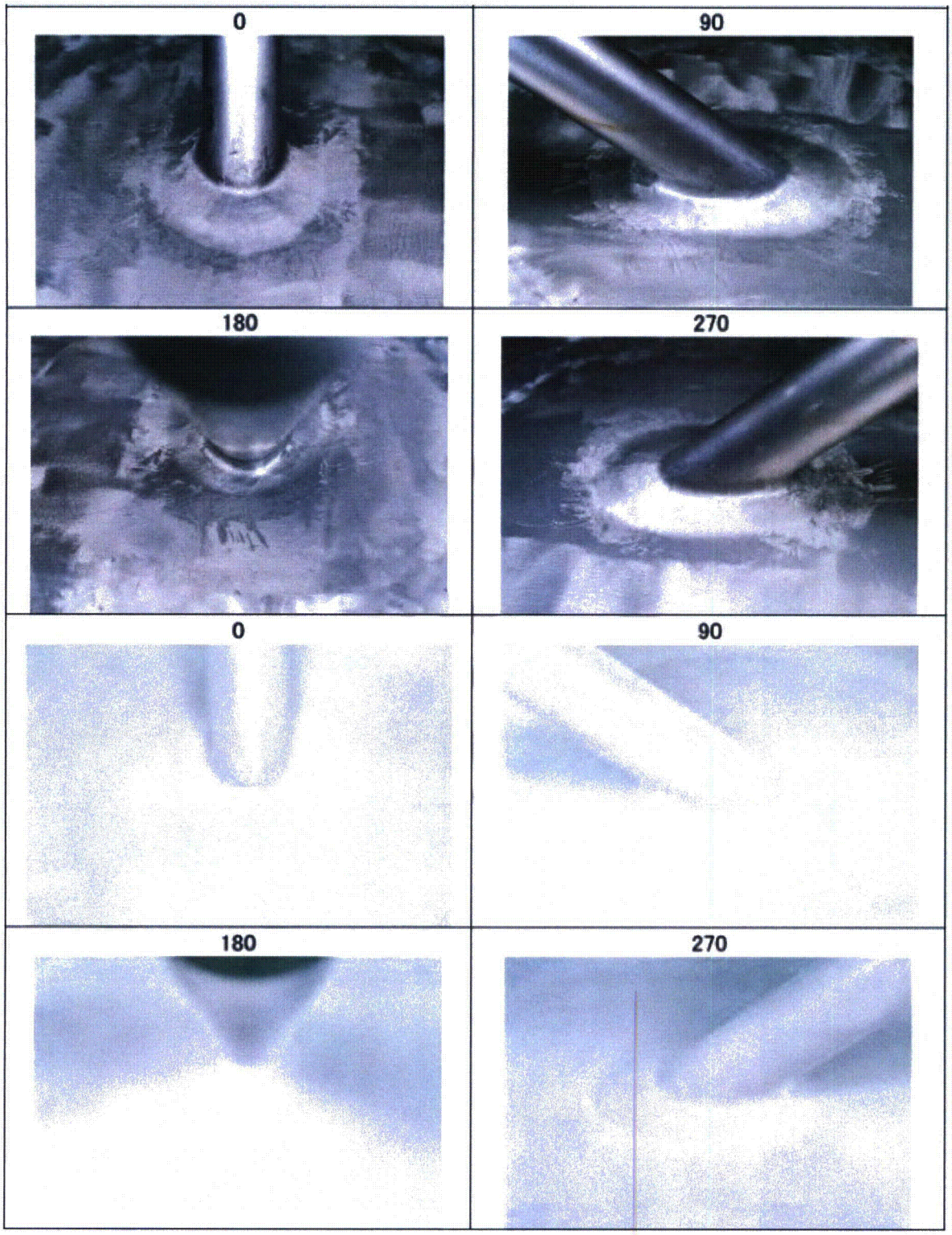

Figure A-98
Visual (upper photographs) and PT (lower photographs) Results for $MgCl_2$ Solution Test Mock-Up treated with WJP, provided by Mitsubishi